Hans-Otto Carmesin

The Elementary Charge Explained by Quantum Gravity

Book, Book chapter as: published version (Version of Record)

DOI of this document*(secondary publication): https://doi.org/10.26092/elib/2668

Publication date of this document: 12/01/2024

* for better findability or for reliable citation

Recommended Citation (primary publication/Version of Record) incl. DOI:

The Elementary Charge

Explained by Quantum Gravity

This text has also been published in the form of a printed book and is available in book trading companies or book stores since October 2021.

author: Hans-Otto Carmesin

title: The Elementary Charge Explained by Quantum Gravity

ISBN: 978-3-96831-023-7

ISSN: 2629 1525

Please cite this text as follows:

Carmesin, Hans-Otto (October 2021): The Elementary Charge Explained by Quantum Gravity. Verlag Dr. Köster, Berlin.

Hans-Otto Carmesin

November 3, 2021

b

Question

Our observable universe ranges from the light horizon at a distance of $4.1 \cdot 10^{26}$ m towards the Planck scale at lengths of $1.6 \cdot 10^{-35}$ m. Corresponding bodies are galaxy clusters, our home region of galaxies Laniakea, our Milky Way, our Solar System, Earth, cities, villages, houses, ourselves and elementary particles. How do these different bodies interact? The heavenly bodies mainly interact by gravity. In contrast, most forces among bodies of everyday life are based on the electric interaction. Gravity and the electric interaction are regarded as two fundamental interactions. However, are these two interactions really fundamentally different?

Discovery

We discover the formation of the elementary charge based on quantum gravity. Hereby the difference between theory and experiment amounts to five millionth of a percent. Of course, we use no fit parameters. We show how classical electrodynamics and quantum electrodynamics are both based on our finding.

Perspective

I derived a new theory of quantum gravity. It describes physics ranging from the Planck scale towards the light horizon. With it, I discovered results in cosmology, general relativity and particle physics: In the standard model of cosmology, there are six parameters. One is independent, as it describes the time after the Big Bang. I derived the other parameters from quantum gravity, using no fit. The standard model of elementary particles essentially describes masses of particles and three fundamental interactions: electric, weak and strong interaction. Using quantum gravity, I derived the mass of the Higgs boson, which in turn causes the masses of the other particles, except neutrinos. For these, I derived the cosmological constant of neutrino masses. In this book, we apply the above findings in order to derive the formation of the elementary charge and electric interaction. So the electric charge and electric interaction are not fundamental. It will be interesting and challenging to use a theory ranging from the Planck scale towards the light horizon, in order to investigate other properties of elementary particles.

Comprehensive Explanation

In this book we derive all findings in a systematic, clear and smooth manner. We summarize our results by many definitions, propositions and theorems. We are classes from grade 10 or higher, courses, research clubs, enthusiasts, observers, experimentalists, mathematicians, natural scientists, researchers etc.

The Elementary Charge

Explained by Quantum Gravity

This text has also been published in the form of a printed book and is available in book trading companies or book stores since October 2021.

author: Hans-Otto Carmesin

title: The Elementary Charge Explained by Quantum Gravity

ISBN: 978-3-96831-023-7

ISSN: 2629 1525

Please cite this text as follows:

Carmesin, Hans-Otto (October 2021): The Elementary Charge Explained by Quantum Gravity. Verlag Dr. Köster, Berlin.

Hans-Otto Carmesin

November 3, 2021

Contents

Chapter 1

Basic Concepts

1.1 Introduction

1.1.1 Five great concepts

Physical theories are based on five great fundamental concepts:

Ubiquitous discrete objects: Leukippos (fifth century BC) and his student Democritos (460-370 BC) proposed that objects are constituted by smallest indivisible particles, see e. g. Tsoucalas et al. (2013), Oldershaw (1998), Wußing and Brentjes (1987). They proposed an essential argument: These particles constitute the phase gas, the phase fluid and the phase solid including the corresponding phase transitions. Dalton (1808) established the modern concept of the atom. Constituents of atoms are investigated in the current field of elementary particle physics, see e. g. Tanabashi et al. (2018). Boltzmann (1877) developed statistical physics, **SP**, including the universal constant k_B, while van der Waals (1873) applied that theory in order to model phase transitions, describing the reorganization of discrete objects.

Heavenly objects move in space according to the law of gravity: In the geocentric concept, Earth formed the center, and nearby, there were some heavenly bodies. Aristarchos discovered the he-

liocentric concept, described by Archimedes (287-212 BC), see e. g. (Archimedes, 1897, Chap. The Sand-Reckoner). In the heliocentric concept, there was a very huge space. In that space, the planets move around the sun, and the stars are very far away. Using that concept, Brahe (1588) and Kepler (1627) developed the basic observation and analysis (Kepler (1619)) of gravity, while Newton (1686) developed the law of gravity including the universal constant G, measured by Cavendish (1798), see also Carmesin et al. (2021).

Discrete objects form according to the law of quantum physics: Planck (1900) discovered the quantization of objects in nature, introduced quantum physics, **QP**, including the universal constant h, **zero-point oscillations, ZPOs**, and the corresponding **zero-point energy, ZPE** (Planck (1911)).

Space and time evolve according to general relativity: Einstein (1905) applied the invariance of the velocity of light, the universal constant c, in order to derive the special relativity theory, **SRT**. Moreover, Einstein (1915) discovered the curvature of spacetime, leading to his proposal of general relativity, **GR**, including a theory for gravity and SRT. Using GR, we can explain the continuous expansion of space since the Big Bang (see continuous line in Fig. 1.1, Einstein (1917), Wirtz (1922), Hubble (1929), Carmesin (2021d)).

The essential source of electromagnetism: Coulomb (1785) discovered the law of electric force, it shows that the electric charge is the essential source of electromagnetism. Oersted (1820) discovered electromagnetism. Faraday (1852) introduced the concept of fields that transfer that force from one location to another, moreover he discovered electromagnetic induction.

Maxwell (1865) unified the results about electromagnetic fields, and using these, he derived the concept of electromag-

netic waves. Millikan (1911) measured the essential quantum of electricity: the **elementary charge** e. That charge essentially corresponds to the coupling constant of electrodynamics. Indeed, Feynman (1985) wrote that the corresponding **coupling constant of electrodynamics** *'... has been a mystery ever since it was discovered ...'*. In fact, in this book, we derive the elementary charge and the coupling constant of electrodynamics from quantum gravity!

1.1.2 Interesting problems

Scientific progress is often achieved by identifying and solving problems, see e. g. Popper (1974). Thereby scientific explanations can be achieved and tested Ruben (1990).

Hierarchy problem: In nature there occur objects at very different energy scales. For instance, the neutrinos have rest energies in the meV-scale, the electron, muon, tauon and quarks have rest energies ranging from 511 keV (electron) or 2.15 MeV (up-quark) to 173 GeV (top-quark), see Tanabashi et al. (2018), while the Planck energy is $1.22 \cdot 10^{19}\, GeV$. These different energy-scales cannot be explained by the **standard model of elementary particles, SMEP**, Peskin (2015). That problem is called hierarchy problem, see e. g. Shaposhnikov and Shkerin (2018).

Indeed, the new theory of **quantum gravity, QG**, represents a well-founded theory that ranges from the Planck scale towards the light horizon, see e. g. Carmesin (2021d). Moreover, that theory has been tested in detail by essentially explaining the **standard model of cosmology, SMC**, see e. g. Carmesin (2021c) or (Carmesin, 2021a, Chap. 14). Accordingly, in this book, we apply that theory of QG to the problem of understanding particles and its electric charge.

Mass problem: Aad et al. (2012) and Chatrchyan et al. (2012) discovered the Higgs boson. In the standard model of elementary particles, that particle can basically explain the masses of the W bosons, W^+, W^- and W^0 (also called Z), the quarks, the electron, the muon and the tauon, see e. g. (Peskin, 2015, 9-10). Indeed, the mass of the Higgs boson as well as the masses of the neutrinos have been explained by the new theory of quantum gravity (Carmesin, 2021a, Chapters 7-9), see also Fig. (1.1). Accordingly, in this book, we apply that explanation of the Higgs boson, in order to analyze the internal dynamics of such a particle.

Fundamental interactions: In the standard model of elementary particles, SMEP, there are four fundamental interactions: the electromagnetic interaction (Tanabashi et al., 2018, Sect. 7), the strong interaction (Tanabashi et al., 2018, Sect. 9), the weak interaction (Tanabashi et al., 2018, Sect. 10) and gravity (Tanabashi et al., 2018, Sect. 20). Thereby, the electromagnetic interaction and the weak interaction can be combined at sufficiently high energy. However, is the electromagnetic interaction really fundamental, or can it be explained by another fundamental interaction?

Electric charge: In SMEP, the electric charge is a fundamental property of elementary particles (Tanabashi et al., 2018, p. 33-127). However, is the electric charge really fundamental, or can it be explained by another fundamental property?

Elementary charge: In SMEP (Tanabashi et al., 2018, p. 127) as well as in quantum electrodynamics (Feynman, 1985, p. 127), the elementary charge is a fundamental quantity that cannot be derived with help of a fundamental theory from the essential universal constants: gravitational constant G, velocity of light c, Boltzmann constant k_B and Planck constant h. However, is

it really impossible to derive the elementary charge e with help of a fundamental theory from the essential universal constants G, c, k_B and h?

Magnetic monopoles: In the SMEP (Tanabashi et al., 2018, Sect. 116), as well as in electromagnetism, see e. g. Maxwell (1865), Landau and Lifschitz (1971), Jackson (1975), the following question arises: Are there magnetic monopoles in analogy to electric monopoles or electric charges? However, are magnetic monopoles really analogous to electric monopoles?

1.1.3 Unification

In this book we derive the electromagnetic interaction and the elementary charge. Thereby, all results are in precise accordance with observation and have been derived from quantum gravity only. In particular, the only numerical inputs are the universal constants G, c, k_B and h. Thus, in this book, we present a unification of gravity and electromagnetic interaction.

1.1.4 Aims and organization of the book

In this book we aim to explain electromagnetism and the elementary charge by quantum gravity.

In order to achieve our advanced and innovative aim in a scientific and clear manner, we present our method first:

In chapter 1, we elaborate basic concepts in cosmology, universal constants and the standard model of elementary particles.

In chapter 2, we combine GR[1] and quantum physics. So we summarize the new theory of QG. Hereby, we introduce the quanta of spacetime, QST. These include the dark energy, the corresponding vacuum (including its time evolution, see Fig 1.1) and the possible excitation states of the vacuum. These

[1]It is also describing gravity.

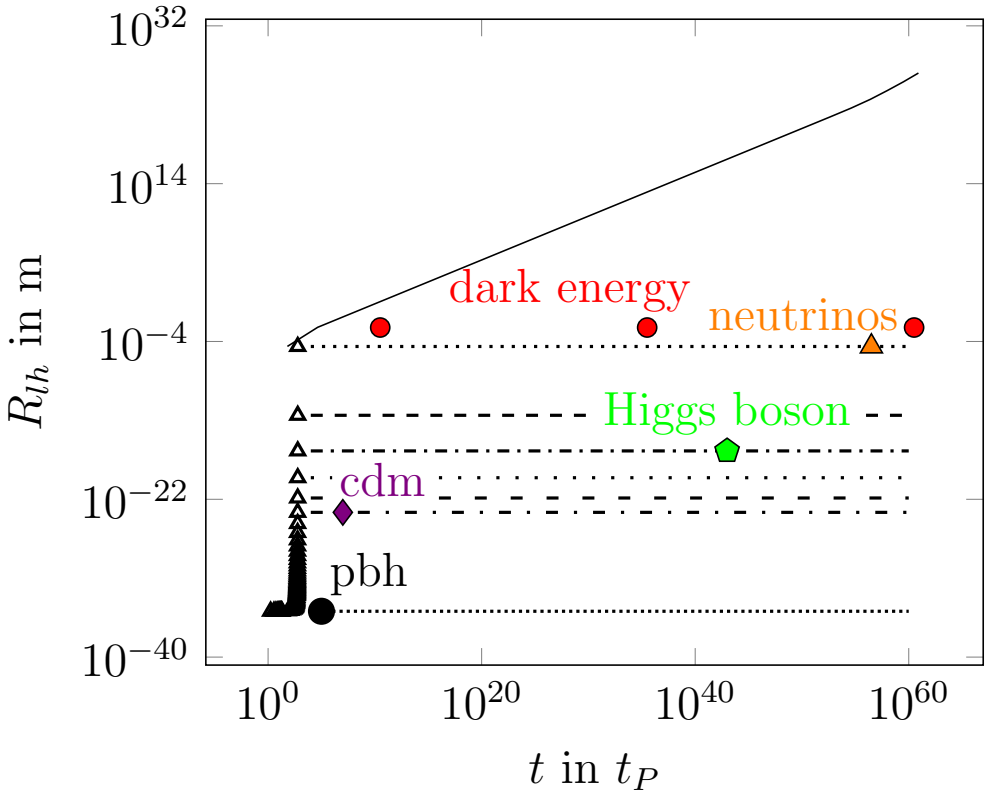

Figure 1.1: Time evolution of the light horizon including dimensional phase transitions (solid line and open Δ). These take place at critical densities, see Carmesin (2021d). Some quanta of spacetime of early phases (other lines). Elementary particles: neutrinos ν (full Δ) Higgs boson (pentagon), quanta of dark energy at $D = 3$ (upper $\circ$), cold dark matter, cdm ($\diamond$) and primordial black holes, pbh (lower $\circ$), see Carmesin (2020b).

excitation states form the elementary particles[2].

Among the elementary particles, the Higgs boson is prototypical, as the mass of most elementary particles is caused by the Higgs boson via the Higgs mechanism. Accordingly, we analyze the Higgs boson in particular: it is formed by three QST.

In chapter 3, we analyze the physics, time evolution and dynamics of the three QST within the Higgs boson and within elementary particles caused by the Higgs mechanism: As a result of that dynamics, such a particle emits particular QST. These QST can be identified with the quanta of the electric interaction. Moreover, the dynamic structure emitting these QST can be identified with the elementary charge. In this chapter, we derive the basic process, and we achieve a difference between theory and observation of 0.36 %. In chapter 6, we analyze the simultaneous emission of several such QST, and we analyze screening and corrections according to QED. Thereby, we achieve a relative difference between theory and observation of $5.4 \cdot 10^{-8}$. So our result is within the errors of measurement. Thus our finding is in precise accordance with observation.

In chapter 4, we show that the above described QST of the electric interaction exhibit the correct symmetries of the electromagnetic interaction.

Based on the above described QST of the electric interaction, we derive the theory of electromagnetism, and we show how the QED can be derived. Hereby, we discuss the additional physical structure achieved by these QST.

In chapter 7, we present a discussion of our results, including the following essential insight: Electromagnetism is not a fundamental interaction, as it is derived from quantum gravity. The elementary charge is not a fundamental constant of nature, since it can be derived with help of quantum gravity from the universal constants G, c, k_B and h.

[2]Historically, Einstein (1917) introduced a cosmological constant Λ, in order to represent a possible homogeneous energy or density of the vacuum.

The precise derivation of the elementary charge and of electromagnetism provides a clear evidence of our theory.

Altogether, we show that quantum gravity explains very different phenomena: For instance, quantum gravity explains the standard model of cosmology, SMC, including its cosmological parameters, see Carmesin (2021a). Quantum gravity shows its enormous integrative capability by also explaining essential parts of the SMEP, e. g. QG provides a solution of the hierarchy problem and explains the formation of mass, see Carmesin (2021a), as well as the formation of the elementary charge and electromagnetism shown here[3].

1.2 Standard model of elementary particles

In this section we present a short description of the standard model of elementary particles (Tanabashi et al. (2018), Bethge and Schröder (1991), Kobel et al. (2017)), so that the results obtained below can be related to that model. The model is essentially constituted by three generations, see e. g. Kobel et al. (2017). These are basically understood by the beta decay.

1.2.1 β-decay

In the beta decay, a neutron, n, decays into a proton, p, an electron, e^- and an electronic antineutrino, $\bar{\nu}_e$:

$$n \to p + \bar{\nu}_e + e^- \tag{1.1}$$

On the level of quarks, the beta decay can be modeled by the decay of a down quark, d, into an up quark, u, an electron, e^- and an electronic antineutrino, $\bar{\nu}_e$:

$$d \to u + \bar{\nu}_e + e^- \tag{1.2}$$

[3]I derived the present theory progressively. The publication started in 2017 in books, papers and my book series. See e. g. Carmesin (2017b), Carmesin (2018g), Carmesin (2018f), Carmesin (2018e), Carmesin (2018a), Carmesin (2019c), Carmesin (2017b), Carmesin (2019a), Carmesin (2019e), Carmesin (2020b), Carmesin (2020a), Carmesin (2021d), Carmesin (2021a), Carmesin (2021c), Carmesin (2021b), Carmesin (2021e).

1.2.2 Isospin - pairs

In the above reaction Eq. (1.2), we transfer the antineutrino from the products to the educts by changing it to a neutrino:

$$d + \nu_e \rightarrow u + e^- \tag{1.3}$$

This is interpreted by a transformation of a down quark into an up quark combined with a transformation of an electronic neutrino into an electron. Correspondingly, the down quark and the up quark are interpreted as two states such as two spin states. Accordingly, a new isospin has been introduced, and the down quark has isospin $I_z = -1/2$, while the up quark has isospin $I_z = 1/2$. So these two quarks form a pair:

$$\begin{pmatrix} u \\ d \end{pmatrix} \tag{1.4}$$

Similarly, and the electronic neutrino has the isospin $I_z = 1/2$, while the electron has the isospin $I_z = -1/2$, see Eq. (1.7). Thus, these two leptons constitute another isospin pair:

$$\begin{pmatrix} \nu_e \\ e^- \end{pmatrix} \tag{1.5}$$

As these two isospin pairs are combined in the beta decay, they are combined to the following quadruple:

$$\begin{pmatrix} \begin{pmatrix} u \\ d \end{pmatrix} \\ \begin{pmatrix} \nu_e \\ e^- \end{pmatrix} \end{pmatrix} \tag{1.6}$$

1.2.3 Isospin - symmetry

The usual spin states are related to rotations, and these are represented by the special (with determinant one) orthogonal group in three dimensions, the $SO(3)$. Similarly, the isospin states are related to transformations, and these are again represented by a group, the special unitary group in two dimensions, $SU(2)$.

1.2.4 Generations

The quadruple in Eq. (1.6) is a first quadruple that had been developed in several steps: Pauli proposed the existence of the neutrino as a part of the beta decay in 1930. That neutrino has been directly observed since 1953. The quark model has been proposed around 1960.

Later, two similar quadruples have been discovered. Thereby the top quark was discovered in 1993 and completed these three quadruples. The numbers of these three quadruples are called generations, see Eq. (1.8). The particles of the second and third generation in Eq. (1.8) are the charm quark, c, strange quark, s, top quark, t, bottom quark, b, muon, μ, tauon, τ as well as corresponding neutrinos ν_μ and ν_τ.

$$\begin{pmatrix} gen.1 \\ \begin{pmatrix} u \\ d \end{pmatrix} \\ \begin{pmatrix} \nu_e \\ e^- \end{pmatrix} \end{pmatrix} \rightarrow \begin{pmatrix} I_z \\ \begin{pmatrix} \frac{1}{2} \\ -\frac{1}{2} \end{pmatrix} \\ \begin{pmatrix} \frac{1}{2} \\ -\frac{1}{2} \end{pmatrix} \end{pmatrix} \rightarrow \begin{pmatrix} q \\ \begin{pmatrix} \frac{2}{3} \\ -\frac{1}{3} \end{pmatrix} \\ \begin{pmatrix} 0 \\ -1 \end{pmatrix} \end{pmatrix} \tag{1.7}$$

$$\begin{pmatrix} gen.1 \\ \begin{pmatrix} u \\ d \end{pmatrix} \\ \begin{pmatrix} \nu_e \\ e^- \end{pmatrix} \end{pmatrix} \rightarrow \begin{pmatrix} gen.2 \\ \begin{pmatrix} c \\ s \end{pmatrix} \\ \begin{pmatrix} \nu_\mu \\ \mu \end{pmatrix} \end{pmatrix} \rightarrow \begin{pmatrix} gen.3 \\ \begin{pmatrix} t \\ b \end{pmatrix} \\ \begin{pmatrix} \nu_\tau \\ \tau \end{pmatrix} \end{pmatrix} \tag{1.8}$$

In addition to these particles, the standard model contains bosons that transmit interactions:

The weak interaction is transmitted by W bosons, W^+, W^- and W^0 (also called Z-boson, Z represents zero). The electromagnetic interaction is transmitted by virtual photons. The strong interaction is transmitted by gluons. Beyond the standard model is the hypothetical graviton, see Blokhintsev and

Galperin (1934), Carmesin (2021d). The masses of most particles of the standard model are based on the Higgs boson, see e. g. (Peskin, 2015, p. 9-10) or Tanabashi et al. (2018).

1.2.5 Two additional symmetries

We remind that the isospin states form pairs and are related to transformations that represent a group, the special unitary group in two dimensions, the $SU(2)$. Similarly, the quarks u, d and s form a triplet and are related to transformations that represent a group, the special unitary group in three dimensions, the $SU(3)$. That group can explain several elementary particles that are formed from the quarks u, d and s.

An additional symmetry is related to the electromagnetic interaction. An effect of that interaction can be modeled by a change of a phase of a complex number. As numbers represent one dimension, the corresponding group is the special unitary group in one dimension, the $SU(1)$. Altogether, symmetries inherent to elementary particle physics are described by using the groups $SU(1)$, $SU(2)$ and $SU(3)$ including their combinations. Possible relations to higher dimensional groups are being investigated since many decades.

1.2.6 Mixing

The system of elementary particles (Eq. 1.8) has been developed according to reactions such as the beta decay and according to symmetries of $SU(1)$, $SU(2)$ and $SU(3)$. However, the neutrinos of the three generations ν_e, ν_μ and ν_τ can periodically transform into each other, that phenomenon is called neutrino oscillation, see e. g. Tanabashi et al. (2018). Correspondingly, these neutrinos ν_e, ν_μ and ν_τ are modeled as linear combinations of underlying neutrinos ν_1, ν_2 and ν_3. That linear combination is called neutrino mixing and it is described by a mixing matrix U, see e. g. (Tanabashi et al., 2018, S. 14).

Similarly, the masses of the six quarks of the three generations (see Eq. 1.8) are derived on the basis of a mixing matrix, called V_{CKM}, see e. g. (Tanabashi et al., 2018, S. 12).

1.2.7 Gauge theory

Each symmetry inherent to elementary particle physics can be described by an operator $\hat{S}$. Each such operator $\hat{S}$ can be expressed in terms of a set of infinitesimal generators $\hat{G}_j$ and by corresponding generalized angles α_j as follows:

$$\hat{S} = \exp[\Sigma_{j=1}^{n} \alpha_j \cdot \hat{G}_j] \tag{1.9}$$

Each local change of such symmetry can thus be expressed by local changes of these angles:

$$\alpha_j(\vec{x}) \tag{1.10}$$

In each local theory, such a local angle $\alpha_j(\vec{x})$ cannot propagate faster than the velocity of light. Thus, each global theory must be invariant with respect to such local angles $\alpha_j(\vec{x})$. This statement constitutes the principle of gauge invariance, it can be applied to each local theory, and it has been used in order to derive several theories in elementary particle physics. In the present book series, locality is appropriately generalized to higher dimension.

1.2.8 Open question: formation of charge

The formation of the electric charge of particles presented in Eq. (1.8) has neither been explained in the SMEP, see Tanabashi et al. (2018), nor in classical electrodynamics, see for instance Maxwell (1865), Jackson (1975), nor in quantum electrodynamics, see Feynman (1985), Landau and Lifschitz (1982).

Chapter 2

Quantization of Gravity

In this chapter, we summarize parts of the new theory of quantum gravity, see Carmesin (2021d). That theory describes the **quanta of spacetime, QST**.

2.1 Results based on QST

In this section, we summarize some essential structures that are formed by the QST.

1. These QST are the bosons that form the space in which we live.

2. These QST are the elementary quanta that have been forming and still form the time evolution of space since the Big Bang.

3. These QST range from the Planck scale towards the macroscopic scale. So these QST include the smallest and most elementary quanta that are possible in nature.

4. These QST are the bosons of the gravitational interaction, the gravitons.

5. These QST are the elementary quanta that form the curvature of spacetime at a mesoscopic level.

6. These QST are the elementary quanta that form the gravitational field $\vec{G}^*$ at a mesoscopic level[1].

7. The QST form the neutrinos as well as the Higgs particle, and so they cause the masses of all elementary particles, see Carmesin (2019c).

8. In this book we show that QST are the elementary quanta that form the electric charge too. As a consequence, QST form the bosons of the electromagnetic interaction, so they represent the elementary basis of classical electrodynamics, see e. g. Maxwell (1865), Landau and Lifschitz (1971), Jackson (1975), and of quantum electrodynamics, QED, see e. g. Schwinger (1948), Landau and Lifschitz (1982), Feynman (1985).

9. These QST have been tested by many different methods (Carmesin, 2021d, Sect. 8.9). Thereby, the results are in precise accordance with observation. In particular, these QST explain the time evolution of spacetime, including the H_0-tension (Fig. 2.14), see Carmesin (2021c).

2.2 Smallest length achieved by QST

In this section, we show how the QST represent objects that can range from the smallest length, the Planck length L_P, towards the largest observable length, the light horizon R_{lh}.

2.2.1 Smallest observable length

As a consequence of gravity and quantum physics, there is a smallest observable length Δx, it is the smallest observable uncertainty or smallest observable standard deviation. That fact

[1]The gravitational field is marked by a G with a star.

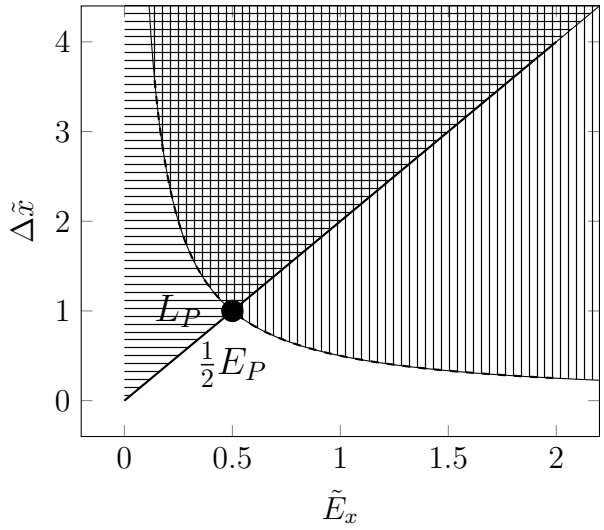

Figure 2.1: Shortest observable uncertainty (dot): Observable states outside the event horizon of a possible black hole (horizontal lines). Sufficient uncertainty according to the Heisenberg uncertainty relation (vertical lines). Observable and sufficient uncertainty (intersection).

has been proven (Carmesin, 2021a, PROP 4), and it is illustrated in Fig. (2.1). Hereby and in the following, we mark a quantity by a tilde, if it is expressed in terms of the Planck units, see table (8.3).

In essence, that fact can be understood directly as follows: A single observation of a length requires a quantum object. The observed length is at least equal to the Heisenberg uncertainty Δx of that quantum object. The shortest possible uncertainty Δx is a function of the energy E of that object, see area with vertical lines in Fig. (2.1). The shortest observable structure of that energy E of the quantum object is set by the Schwarzschild radius of the black hole of that energy, see area with horizontal lines in Fig. (2.1). Observable states correspond to the intersection of the areas with vertical and horizontal lines in Fig. (2.1). That intersection exhibits a smallest observable length, the Planck length, hereby G is the gravitational constant, see table (8.1):

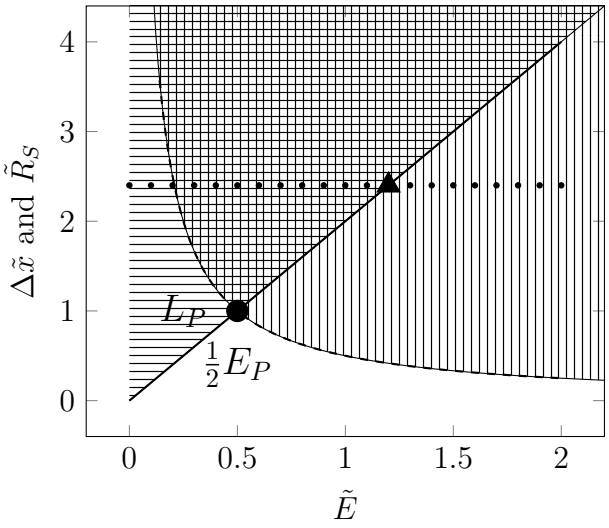

Figure 2.2: An upper bound for the density: Observable states (horizontal lines). Sufficient uncertainty (vertical lines). Observable and sufficient uncertainty (intersection). Dots show states at an uncertainty $\Delta\tilde{x}$, among these states, the observable state with the largest energy is marked by the triangle. Among these triangle states at the straight line, the state at the dot has the largest density.

$$\Delta x = L_P = \sqrt{\frac{\hbar \cdot G}{c^3}} = 1.616 \cdot 10^{-35}\,\mathrm{m} \tag{2.1}$$

2.2.2 Highest possible density

As a consequence of the smallest observable length L_P, there occurs a highest possible density $\rho_{highest}$:

$$\rho_{highest} = \frac{1}{2} \cdot \frac{3}{4\pi} \cdot \frac{c^2}{G \cdot L_P^2} \tag{2.2}$$

Hereby, the last fraction is called **Planck density**:

$$\rho_P = \frac{c^2}{G \cdot L_P^2} = \frac{c^5}{G^2 \cdot \hbar} \tag{2.3}$$

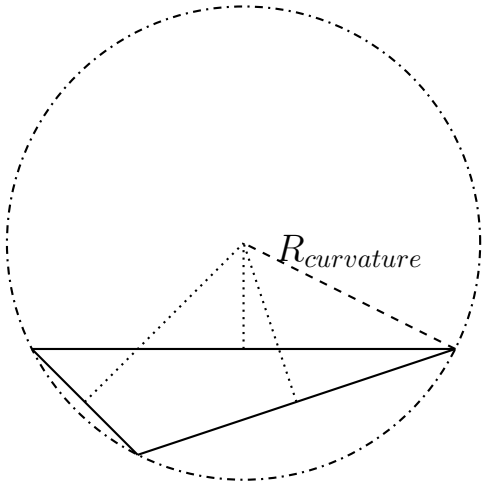

Figure 2.3: Three locations form a triangle (solid lines). Line orthogonal to a side of the triangle and through the middle of that side (dotted). Dotted lines intersect at the center of the circle (dashdotted) through the three locations. Each of the three locations has the distance $R_{curvature}$ to the center. In that manner, a radius of curvature can be measured by using three locations.

Moreover, we identify $\frac{3}{4\pi} \cdot \rho_P$ by the Planck density of a ball, $\bar{\rho}_P$, see table (8.3):

$$\rho_{highest} \frac{1}{2} \cdot \bar{\rho}_P \tag{2.4}$$

Alternatively, we apply the scaled density $\tilde{\rho} = \rho / \bar{\rho}_P$, see table (8.3):

$$\tilde{\rho} \leq \frac{1}{2} \tag{2.5}$$

That fact has been proven (Carmesin, 2021a, PROP 5), and it is illustrated in Fig. (2.2).

2.2.3 Planck scale

The smallest observable length L_P and the highest possible density are two examples for quantities at the Planck scale. Note that the quantities of the Planck scale have been elaborated for each dimension $D \geq 3$ of space, see e. g. Carmesin (2019c).

2.2.4 Curvature and GR are mesoscopic concepts

Einstein (1915) described the theory of general relativity, GR, in terms of the curvature of spacetime. However, the concept of the curvature requires at least three observable locations of the corresponding space or spacetime, see e. g. Landau and Lifschitz (1971), Lee (1997).

How can this curvature be measured geometrically? For it we present a straightforward, intuitive and well known method: In the case of an anisotropic space or spacetime, the curvature can be described by several radii of curvature $R_{curvature}$, see e. g. Lee (1997). Hereby, these radii correspond to respective circles that can be defined in an appropriate space. The radius of curvature $R_{curvature}$ of such a circle can be measured by using at least three locations, see e. g. Fig. (2.3). In particular, these three locations form a triangle, and the center of the circle is the intersection of the three orthogonal lines through the middle of the three sides of the triangle.

In GR, curvature is often defined by using four dots forming a loop, see e. g. Landau and Lifschitz (1971), Straumann (2013), Carmesin (1996), Stephani (1980), Moore (2013). In general, at least three locations are required for a geometric measurement of the curvature of a space or a spacetime. Correspondingly, GR is a mesoscopic theory, as the essential concept of curvature requires several locations.

2.2.5 QST range from L_P towards R_{lh}

The quanta of spacetime, QST, describe the physical states ranging from the Planck length, L_P towards the light horizon, R_{lh}, see e. g. Carmesin (2021d).

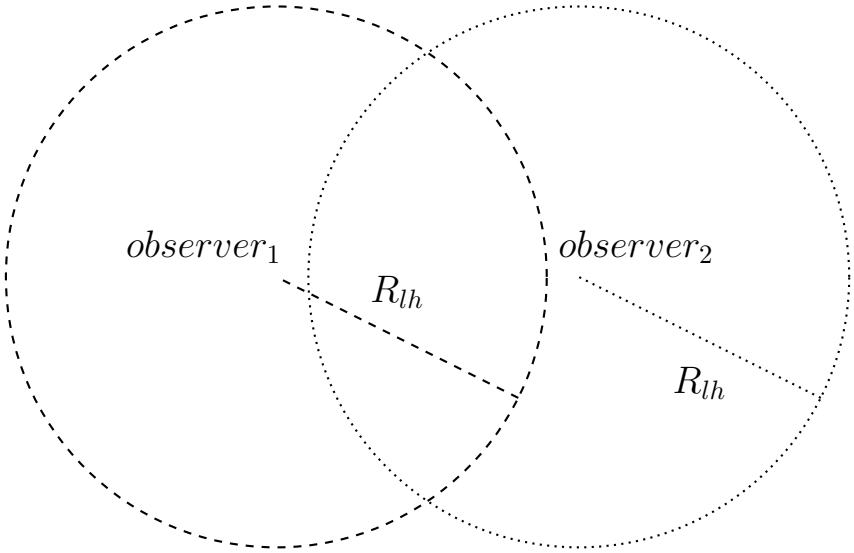

Figure 2.4: Each observer is influenced by objects within the ball with the center at the observer and the radius R_{lh}. Corresponding to translation invariance, the laws of physics hold in the respective balls of two observers, even if there is no causal influence among the two observers.

So the QST establish the ultimately microscopic theory of space and time. Moreover, if several observers with their respective observable balls are considered, and if the principle of translation invariance is used, then the QST describe space beyond the light horizon, in addition, see Fig. (2.4).

2.3 QST unify concepts in Hilbert space

How can the detailed structure of spacetime be represented, if we use regions of the size L_P, without any substructure? The essential structures are as follows:

(1) Local additional volumes describe the expansion of space.

(2) More generally, local deformations ε_{ij} describe the symmetries and polarization modes of space. These modes are elaborated in Sect. (2.4).

(3a) (Carmesin, 2021d, Chapters 1-5) showed that gravitational

fields G_i^* and corresponding tensors G_{ij}^* form at a mesoscopic scale by additional quanta of space[2].

(3b) (Carmesin, 2021d, Chapters 1-5) showed that these fields can be used in order to describe the rate of formation of additional quanta, including deformations, of space.

(3c) (Carmesin, 2021d, Chapters 1-5) showed that masses, energies or dynamical masses can also be used in order to describe the rate of formation of additional quanta, including deformations, of space.

(4) (Carmesin, 2021d, Chapters 1-5) showed that the curvature of spacetime forms at a mesoscopic scale by additional quanta of space.

(5) Accordingly, the quanta of the above described additional volumes or deformations of space, including the related variations of time, are called **quanta of spacetime, QST**. How can these complex structures be described at the fully microscopic level of the Planck length?

(6) According to the concept of quantum physics, complex objects can be described at a completely local and microscopic level by using the description in an additional abstract space, Hilbert space, see e. g. Landau and Lifschitz (1965). This concept has been applied in the new theory of quantum gravity, (Carmesin, 2021d, Chapters 1-6).

Using Hilbert space: The QST are quanta. So they can be described in Hilbert space, see e. g. Landau and Lifschitz (1965). States in Hilbert space can be described by functions of space and time or by Fourier transforms of these, namely functions of wavelength and frequency, or by other complete systems of functions, including distributions, if necessary. In order to develop the appropriate functions in Hilbert space for the case

[2]Moreover, in the following, we develop a microscopic concept of G_i^* and G_{ij}^*.

of quantum gravity, Carmesin (2021d) derived fields, symmetries, differential equations or wave equations and functions describing quantum gravity. The quantization of these functions provides the QST (Carmesin, 2021d, C. 6).

These QST exhibit wavelengths λ and periodic times T, thus they have the potential to constitute spacetime at a microscopic, at a mesoscopic and at a macroscopic level. Indeed, these QST constitute spacetime in precise accordance with observation (Carmesin, 2021d, sections 6.6, 7.5, 8.5, 8.6). Carmesin (2021c) illustrated the accordance of the QST with observation in an especially accurate manner by explaining the H_0-tension, whereby the small local underdensity of Laniakea has been included additionally, see e. g. Tully et al. (2014), Dupuy et al. (2019), Böhringer et al. (2015). In particular, the dynamics of the QST describes the evolution of spacetime since the Big Bang, see Carmesin (2021d).

Moreover, QST provide the curvature of spacetime by averaging the QST appropriately (Carmesin, 2021d, section 8.8). Correspondingly, the QST transfer the gravitational interaction and include the hypothetic graviton (Carmesin, 2021d, THM 34).

Additionally, the quanta of spacetime, QST, describe the various constituents of the vacuum, including the excitation states of these constituents, the elementary particles, both in precise accordance with observation, see Carmesin (2021a).

2.3.1 Why GR fails to reach the Planck scale

GR is based on the concept of curvature, whereby the geometric description of curvature requires at least three locations, so GR cannot describe objects at the Planck length in sufficient geometric detail.

Furthermore, GR cannot describe the evolution of the universe from the present light horizon R_{lh} backwards towards the

Planck length. The reason is that GR can describe that time evolution only until the highest possible density $\rho_{highest} \approx \rho_P$ is reached. At that density, the present-day light horizon represents a length of approximately 0.003 mm (Carmesin, 2020b, Fig. 5.7), see also Fig. (2.5) and Carmesin (2021b).

Altogether, we realize that neither space, nor spacetime, nor the continuity of space, nor the dimensions of space are fixed or constant. Instead, space, spacetime, the continuity of space and the dimension of space evolve, and this evolution is described by the QST. As a consequence, the QST range from the Planck scale towards the horizon of objects that can have a causal influence upon us, the light horizon.

2.3.2 Why QST reach the Planck scale

The quanta of spacetime can transform to higher dimensions of space, see Carmesin (2018f), Carmesin (2018e), Carmesin (2019c), Carmesin (2021d). Thus they describe dimensional phase transitions. These dimensional phase transitions constitute the rapid change of distance in the early universe, see e. g. Carmesin (2017b), Carmesin (2021d). The increase of the distance as a consequence of the decrease of the dimension is illustrated in Fig. (2.6).

A quantitative analysis of that rapid increase provides the time evolution in the early universe (see triangles in Fig. 2.5) in precise accordance with observation (Carmesin, 2021d, chapter 8).

2.4 Modes of polarization of QST

In this section, we work out the modes of polarization characterizing space, see e. g. Carmesin (2021d).

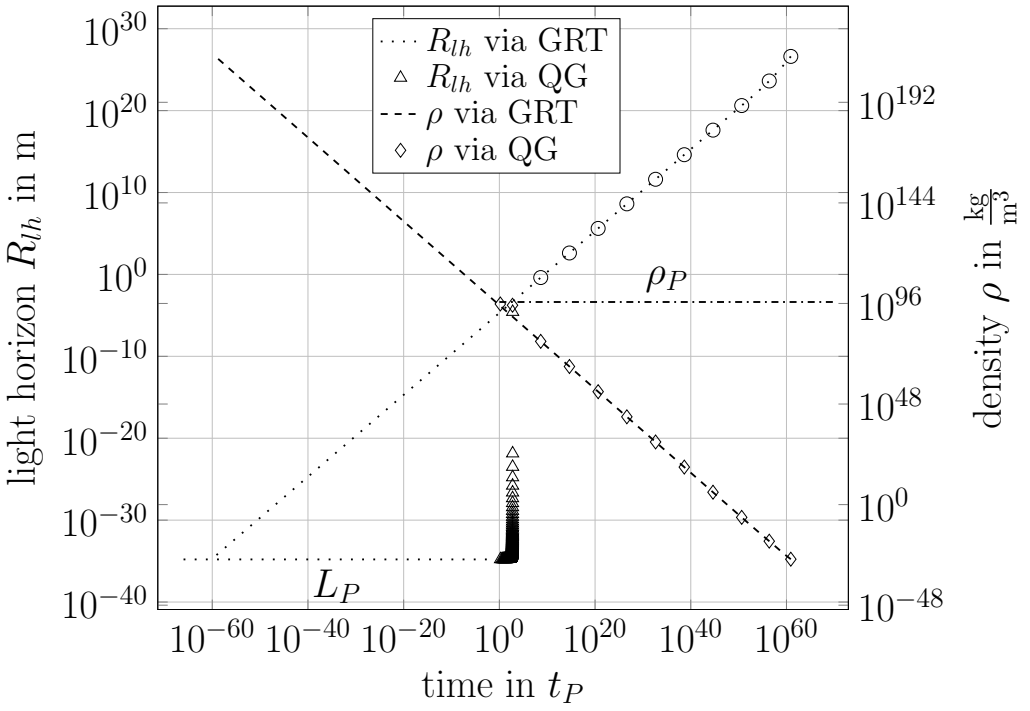

Figure 2.5: Density limit of expansion of space: The time evolution of R_{lh} according to the GR ($\circ$) ranges from the present-day value $4.14 \cdot 10^{26}$ m backwards to 0.003 mm, as at this point the density ($\diamond$) achieves the Planck density $\rho_P = 5.155 \cdot 10^{96} \frac{\text{kg}}{\text{m}^3}$ (dashdotted), and no higher density is physically possible.
However, the physically possible lengths can be as short as the Planck length L_P (loosely dotted). Hence the time evolution of the GR is **incomplete**.
In contrast, we derive the **complete time evolution** of $R_{lh}(t)$, ranging from the current value $4.14 \cdot 10^{26}$ m backwards to L_P. For it we apply GR ($\circ$) combined with dimensional phase transitions ($\triangle$) derived by quantum gravity. Thereby, the phase transitions cause the **extremely rapid distance enlargement in the early universe**

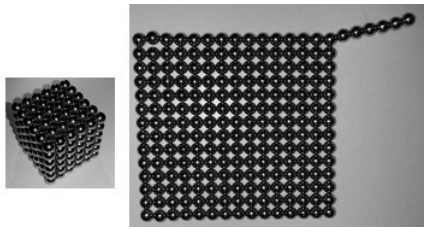

Figure 2.6: 216 magnetic balls model local objects or observable regions at high density and illustrate the relation between the distance and the dimension D: If the dimension increases from two (right) to three (left), then the largest distance decreases. More generally and conversely, a decrease of the dimension D implies an increase of the largest distance.

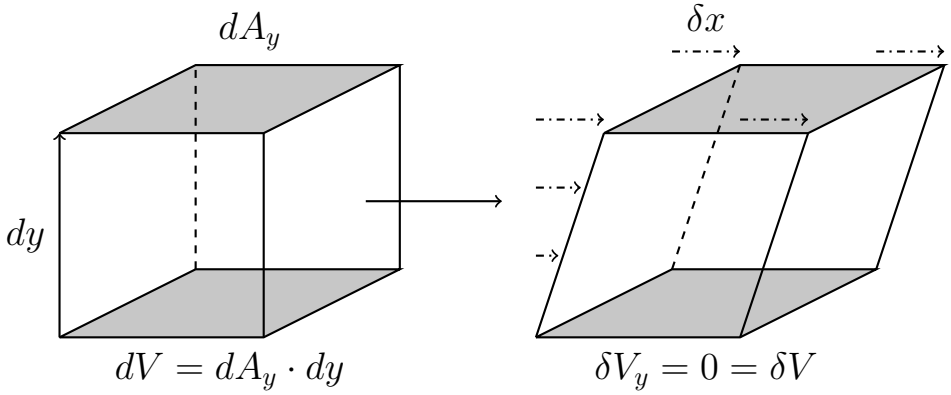

Figure 2.7: Deformation: A cube with a cross section dA_y. At each height δy, the cross section is shifted according to a factor $\varepsilon_{x,y}$ by $\delta x = \varepsilon_{x,y} \cdot \delta y$.

2.4.1 Modes of Modifications of space

In this section, we characterize the possible modifications of space. For it, we explicate the linear modifications of space. Hereby, these can be extended to general modifications by linear combination and by forming Taylor series or similar systems of functions.

Description by figures and tensors: We describe linear modifications by figures showing the modification (see e. g. Fig. 2.7) and by corresponding tensors, see e. g. Sommerfeld (1978), Landau and Lifschitz (1975). For it we use an infinitesimal cube with a constant cross section dA_y orthogonal to the y-direction and with a height dy, see Fig. (2.7).

Non diagonal deformation: First, we describe a shift of each cross section dA_y: At each height δy, the cross section is shifted according to a factor $\varepsilon_{x,y}$ by $\delta x = \varepsilon_{x,y} \cdot \delta y$, see Fig. (2.7). Hereby the factor $\varepsilon_{x,y}$ is an element of the deformation tensor, see e. g. (Sommerfeld, 1978, p. 3). The volume is invariant in a non-diagonal deformation.

Diagonal deformation or elongation: Secondly, we describe a shift of the cross section dA_y in the direction orthogonal to dA_y: At each height δy, the cross section is shifted according to a factor $\varepsilon_{y,y}$ by $\delta y = \varepsilon_{y,y} \cdot \delta y$, see Fig. (2.8). Hereby the factor $\varepsilon_{y,y}$ is a diagonal element of the deformation tensor, see e. g. (Sommerfeld, 1978, p. 3). In a diagonal deformation, the volume changes as follows:

$$\delta V_y = dA_y \cdot \delta y \tag{2.6}$$

Linear deformation: The above two deformations are linear. We obtain a general linear deformation from the above two particular cases by allowing all coordinate directions. Thus, a general

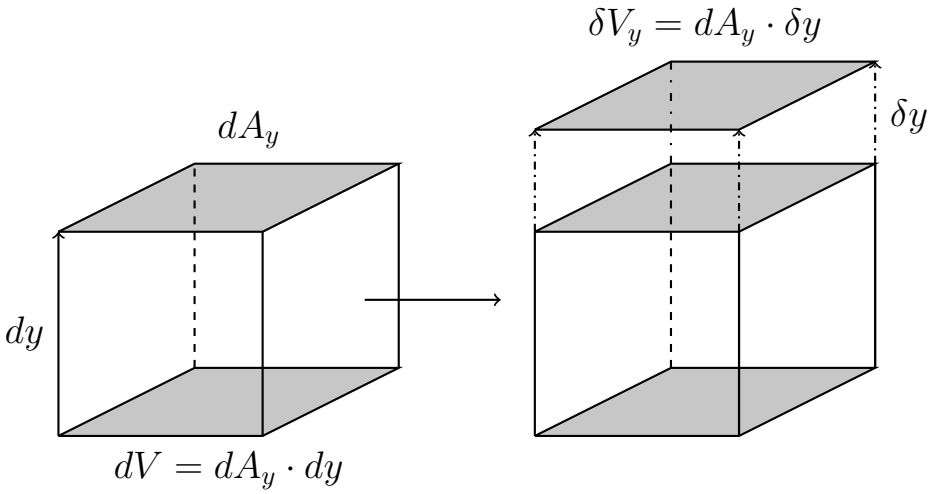

Figure 2.8: Elongation: A cube with a cross section dA_y is elongated by an increment δy.

linear deformation is described by the following tensor:

$$\hat{\varepsilon}_{i,j} = \frac{\partial r_i}{\partial r_j} \tag{2.7}$$

So the following shift of a cross section dA_j is achieved:

$$\delta r_i = \hat{\varepsilon}_{i,j} \cdot \delta r_j = \frac{\partial r_i}{\partial r_j} \cdot \delta r_j \tag{2.8}$$

The non-diagonal deformations, the diagonal deformations and the combinations thereof form the possible **modes of modification**.

2.4.2 Rate of change of a modification

In this section, we summarize the possible rates of change of modifications.

Discovery of the dynamics: Of course, there are many possibilities to discover the dynamics of the QST. Here we proceed as follows. (Carmesin, 2021d, CHAP. 1-5) analyzed the symmetry of the gravitational objects of the microscopic and of the

macroscopic dynamics. As a result, I obtained a rate equation, a DEQ. The solutions are either waves, describing the propagation of the QST, including dark energy and the graviton. Or the solutions are monotonically increasing or decreasing functions of time. These describe the increase or decrease of the number of QST, which in turn describe the Big Bang and the dynamically conceivable Big Crunch, see Goodstein (1997), the latter has not been observed, however.

Completely microscopic rate of change of volume: (Carmesin, 2021d, THM 6) showed that the rates of change of the volume $\dot{\varepsilon}$ are as follows:

$$\dot{\varepsilon}^2 = \left(\frac{\delta V}{\delta t \cdot dV}\right)^2 = 24\pi \cdot G \cdot \rho \text{ for isotropic expansion of space} \tag{2.9}$$

$$\left(\frac{\delta V}{\delta t \cdot dV}\right)^2 = 8\pi \cdot G \cdot \rho \text{ for unidirectional vacuum formation} \tag{2.10}$$

These equations are completely microscopic, as the density can be expressed in terms of delta distributions.

Completely microscopic concept of the field: (Carmesin, 2021d, Chapters 1, 2) showed that in the rates of change of the volume $\dot{\varepsilon}$,

$$\dot{\varepsilon}^2 = 8\pi \cdot G \cdot \rho, \tag{2.11}$$

the density can be expressed in terms of the field:

$$\rho = \frac{G^{*2}}{8\pi \cdot G \cdot c^2} \tag{2.12}$$

So the field can be expressed as a root of the density:

$$G^* = \sqrt{\rho \cdot 8\pi \cdot G \cdot c^2} \tag{2.13}$$

Thus the concept of the field is completely microscopic, at the Planck scale, as the density can be expressed in terms of delta distributions.

Completely microscopic concept of the DEQ: Using the above relations, (Carmesin, 2021d, THM 7) showed that the rate of change can be expressed at a completely microscopic scale of L_P and in a Lorentz invariant manner. Thereby, the **rate gravity scalar, RGS**, is zero:

$$\dot{\varepsilon}^2 = \frac{G^{*2}}{c^2} \quad \text{or} \quad \dot{\varepsilon}^2 - \frac{G^{*2}}{c^2} = 0 \tag{2.14}$$

Hereby, the corresponding **rate gravity four-vector, RGV** is as follows:

$$RGV_i = \begin{pmatrix} \dot{\varepsilon} \\ G^*_x/c \\ G^*_y/c \\ G^*_z/c \end{pmatrix} \tag{2.15}$$

.

Completely microscopic concept for general deformations: Using the above relations, (Carmesin, 2021d, Sect. 2.4) showed that the rate of change can be expressed at a completely microscopic scale of L_P and in a Lorentz invariant manner, also for the case of general deformations. This is summarized next.

For it, we analyze the time derivatives of the corresponding tensors $\hat{\varepsilon}_{i,j}$:

$$\dot{\hat{\varepsilon}}_{ij} = \frac{\delta}{\delta t}\frac{\partial r_i}{\partial r_j} \tag{2.16}$$

Rate of change of volume: Similar to Eq. (2.6), the increase of volume is as follows:

$$\delta V_j = dA_j \cdot \delta r_j \tag{2.17}$$

We divide by the volume $dV = dA_j \cdot dr_j$ of the infinitesimal cube. So we derive the following relative change of volume:

$$\frac{\delta V_j}{dV} = \frac{\delta r_j}{dr_j} \tag{2.18}$$

Thus, a linear deformation with the tensor $\hat{\varepsilon}_{i,j}$ causes the following change of the volume:

$$\frac{\delta V}{dV} = \Sigma_{j=1}^{j=D} \frac{\delta V_j}{dV} = \Sigma_{j=1}^{j=D} \frac{\delta r_j}{dr_j} = \text{Trace}(\hat{\varepsilon}_{ij}) \tag{2.19}$$

Consequently, the rate of formed volume $\dot{\hat{\varepsilon}}$ is analogous to the time derivative of the deformation tensor as follows:

$$\frac{\delta V}{dV \cdot \delta t} = \dot{\hat{\varepsilon}} = \text{Trace}(\dot{\hat{\varepsilon}}_{ij}) \tag{2.20}$$

We name the above tensor $\dot{\hat{\varepsilon}}_{ij}$ the **generalized rate tensor**.

2.4.3 Gravity tensor

In this section, we introduce a tensor of gravity by the following product (Carmesin, 2021d, Eq. 2.67):

$$\hat{G}_{ij} = G_i^* \cdot G_j^* \tag{2.21}$$

2.4.4 A basic DEQ of spacetime

In order to derive the above structures formed by the QST, Carmesin derived a DEQ describing the time evolution of spacetime (Carmesin, 2021d, THM 8(3)):

$$\boxed{[Trace(\dot{\varepsilon}_{ij})]^2 = \frac{Trace(\hat{G}_{ij})}{c^2}} \tag{2.22}$$

Next we illustrate the applicability of that DEQ by using it for several examples, while the corresponding theory is presented in Carmesin (2021d).

2.4.5 Single mode

If there is only one nonzero component of $\dot{\varepsilon}_{ij}$, then the trace in the above equation can be neglected. So we derive:

$$\boxed{[\dot{\varepsilon}_{ij}]^2 = \frac{\hat{G}_{ij}}{c^2}} \tag{2.23}$$

2.4.6 General deformations

The deformations ε_{ij} describe small modifications of space in a linear manner. Such small deformations can be combined to general modifications of space, including nonlinear deformations, by using linear and nonlinear combinations of these ε_{ij}. This can be achieved systematically by using series of deformations. Naturally, the range of convergence can be finite, a corresponding divergence usually represents a phase transition. Indeed, the theory of QST includes phase transitions.

Alternatively, nonlinear functions can be achieved in the framework of Fourier transforms (Carmesin, 2021d, Chapters 5, 6).

2.4.7 From quanta to space, an example

The QST that establish the present-day three dimensional space and that propagate in the z-direction, for instance, are described by the following two tensors ε_{ij}, describing two possible directions of polarization (Carmesin, 2021d, DEF 7):

$$\varepsilon_{i,j} = \begin{pmatrix} 1 & 0 & 0 \\ 0 & -1 & 0 \\ 0 & 0 & 0 \end{pmatrix} \tag{2.24}$$

$$\varepsilon_{i,j} = \begin{pmatrix} 0 & 1 & 0 \\ -1 & 0 & 0 \\ 0 & 0 & 0 \end{pmatrix} \tag{2.25}$$

These QST are illustrated in Fig. (2.9). Each such QST represents an amount of volume of space. In this manner, the QST form the space.

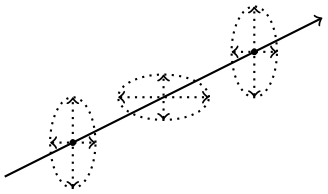

Figure 2.9: Quanta of spacetime of this type extend in three dimensions and establish the space in which we live. Thereby, these QST propagate at the velocity c, so they provide relativity of spacetime as a consequence.

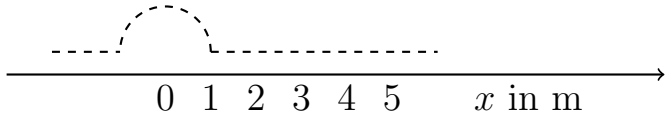

Figure 2.10: Quanta of spacetime (dashed) form a one dimensional space, for instance.
For $|x| > 1$, the QST form one meter of $1D$-space per one meter of the coordinate axis, on a mesoscopic and macroscopic level.
For $|x| < 1$, they form π meter of $1D$-space per one meter of the coordinate axis. So there occurs a curvature with the radius of curvature $R = 1$ meter at a mesoscopic level.
This illustrates, how additional QST at $|x| < 1$ form additional space and curvature of space at a mesoscopic and macroscopic level.

2.4.8 From additional quanta to curvature

If there are additional QST in a local region, then this may cause a curvature of space. Such additional QST are illustrated by an example of a one dimensional space in Fig. (2.10).

2.4.9 From energy or mass to additional quanta

As a further example, we apply the above Eq. (2.22) for the case in which the trace $Trace(G_{ij})$ is equal to a gravitational field $\sum_{i=1}^{i=3} G^*_{ii} = G^*$. In this case, Eq. (2.22) takes the following form:

$$[Trace(\dot{\varepsilon}_{ij})]^2 = \frac{G^{*2}}{c^2} \tag{2.26}$$

The above square of the field corresponds to an energy density u. So that energy density causes a change $\dot{\varepsilon}_{ij}$ of QST, usually corresponding to additional QST. These in turn cause a curvature. In this manner, energy or a mass cause additional QST on the elementary level and a curvature of space on the mesoscopic level. For details see Carmesin (2021d).

Single mode: In the particular case of a single mode i, the above equation is as follows:

$$[\dot{\varepsilon}_{ii}]^2 = \frac{G_i^{*2}}{c^2} \tag{2.27}$$

We apply the root to the above equation:

$$\dot{\varepsilon}_{ii} = \pm\frac{G_i^*}{c} \tag{2.28}$$

This equation is an example for a QST that can be described by a linear equation.

2.4.10 A longitudinal mode of spacetime

The above Eq. can be applied to a single Cartesian direction x_j. The respective deformation is $\varepsilon_{jj} = \frac{\delta x_j}{dx_j}$, describing an elongation δx_j per distance dx_j. The corresponding component of the gravitational field is $G_j^* = G_{jj}$. That component is described by a gravitational potential:

$$G_j^* = -\frac{\partial}{\partial x_j}\Phi(\vec{r}) \tag{2.29}$$

The resulting DEQ is as follows:

$$c^2 \cdot \left(\frac{\partial}{\partial t}\,\varepsilon_{jj}\right)^2 - \left(\frac{\partial}{\partial x_j}\,\Phi(\vec{r})\right)^2 = 0 \tag{2.30}$$

Solutions of that wave equation are planar waves (Carmesin, 2021d, THM 16). Such waves represent an especially simple

Figure 2.11: Longitudinal rate gravity wave of QST, illustrated at a mesoscopic level. The direction of elongation is equal to the direction of propagation, as the QST has a longitudinal polarization.

form of rate gravity waves, RGWs. Algebraically, such a mode can be represented by a tensor, multiplied by a function of time $b(t)$:

$$\varepsilon_{i,j} = \begin{pmatrix} 1 & 0 & 0 \\ 0 & 0 & 0 \\ 0 & 0 & 0 \end{pmatrix} \cdot b(t) \tag{2.31}$$

Geometrically and mesoscopically, such a mode represents a linear chain of volumes propagating in the direction of the line, whereby the volumes change periodically in the direction of the chain. For an illustration see Fig. (2.11).

2.4.11 The modes of spacetime

The DEQ (2.22) describes many situations and systems, while the above examples are just particular cases. That means, in addition to the above planar mode of a RGW, Carmesin analyzed all possible modes of the RGWs (Carmesin, 2021d, THM 15(2)): A mode is represented by a tensor ε_{ij} in Eq. (2.22). The number of linearly independent modes is equal to the dimension of the space of the tensors ε_{ij}. Consequently, in the case of a D dimensional space, the number of linearly independent modes is equal to D^2.

2.4.12 General RGWs or states spacetime

In order to obtain a generally applicable and most useful theory, Carmesin (2021d) elaborated the general case, in which the above modes of space form a linear superposition. That superposition may include a finite or infinite number of modes or an

integral over modes of RGWs. Hence a general RGW of spacetime is such a superposition. A corresponding description of these general RGWs has been worked out, including a transformation to generalized coordinates of RGWs (Carmesin, 2021d, THM 18).

2.4.13 Quanta of spacetime

In order to derive a full quantum theory, Carmesin (2021d) quantized the above RGWs. Thereby, he derived the quantum theory in various representations, so that the most appropriate representation can be used in each particular application:

(1) A representation with a generalized Hamiltonian has been derived.

(2) In that representation, a quantization has been derived in a unique manner.

(3) Using that quantization, corresponding ladder operators $\hat{a}^+$ and $\hat{a}$, number operators $\hat{n}$ as well as the corresponding eigenvalues n have been derived (Carmesin, 2021d, THM 19).

(4) That theory applies to general systems of orthonormal functions as well as to all tensors ε_{ij} of deformation.

2.5 QST of the vacuum

Since the Big Bang, there exist QST. They form the vacuum. In this section, we summarize the possible states of the vacuum including the excitation states.

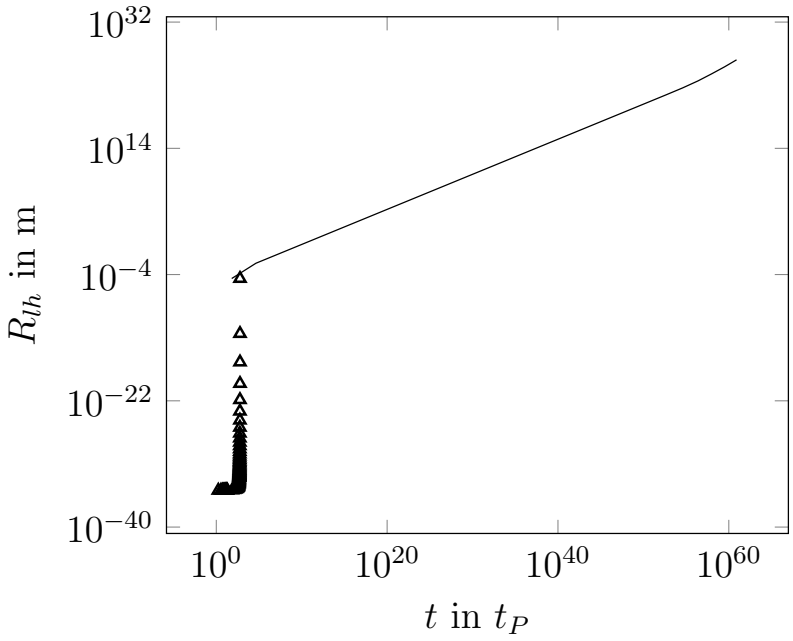

Figure 2.12: Time evolution of the light horizon including dimensional phase transitions.

2.5.1 QST of the present-day vacuum

Using the above QST, (Carmesin, 2021a, theorem 6) derived the **time evolution of the vacuum** ranging from the Big Bang towards the present-day[3]. Thereby, the present-day vacuum is represented by three dimensional states $\Psi_{D=3}$, while former states are represented by higher dimensional states $\Psi_{D\geq 4}$.

2.5.2 Time evolution of the vacuum

Only objects within the light horizon exhibit any influence upon us, so only these objects can be observed by us. Accordingly, the light horizon is a **causal horizon**, most generally. In the early universe, the space was folded (see Figs. 2.6 and 2.12). At each dimensional transition, the folding corresponds to a redshift. That redshift does not apply to light, as light propagates in

[3]These results have already been derived earlier, see Carmesin (2018f), Carmesin (2018e), Carmesin (2019c), Carmesin (2021d).

space. However, that redshift applies to the QST, as these form the space.

Going backwards in time, the space within the present-day light horizon was in a smaller light horizon. Also the space within the present-day Hubble radius $R_H = c/H_0$ was in a smaller radius at earlier times. In the very early universe, that space was folded to higher dimensions. Hereby, the largest possible dimension of that space is called dimensional horizon $D_{horizon}$. At $D_{horizon}$, the QST were at the Planck scale. Thereby, $D_{horizon} \approx 301$, see e. g. Carmesin (2017b), Carmesin (2021d), Carmesin (2021a).

Starting at that state at $D_{horizon} \approx 301$ and going forwards in time, the QST experienced a series of phase transitions, whereby the dimension decreased. That process is called **cosmic unfolding** (see Figs. 2.6 and 2.12). The states of the QST of the cosmic unfolding are the possible states of the vacuum, as these states represent the possible folding states that are inside our causal horizon.

Altogether, the present-day vacuum is constituted by the present-day QST. Moreover, the possible folding states of the QST within the causal horizon are possible excitation states of the present-day vacuum.

2.5.3 Excitation states of the present-day vacuum

In this section, we explicate the states of the vacuum in more detail. The states (QST) of the time evolution of the vacuum exhibit a higher energy than the states (QST) of the present-day vacuum. Consequently, the states $\Psi_{D\geq 4}$ of that time evolution are possible excitation states of the present-day vacuum.

As a consequence of the above tensor modes or modes of modification of the QST, the QST of the vacuum form additional excitation states by changing from a low energy tensor mode $\Psi_{D,q}$ to a high energy tensor mode $\Psi_{D,q'}$. Hereby, we

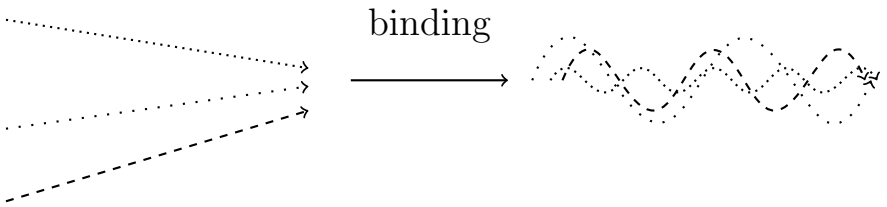

Figure 2.13: Illustration of the binding of three longitudinal QST to a Higgs particle.
Before the binding, the three longitudinal QST propagate freely, at straight paths.
After the binding, the three longitudinal QST form a superposition. Thereby, a common direction of propagation occurs. For each QST, the component parallel to that common direction propagates freely, whereas the component orthogonal to that common direction is bound and does not propagate freely. In a semiclassical description, that effect is illustrated by three wiggly lines.

mark a mode by a subscript q (Carmesin, 2021a, chapter 7).

Moreover, each mode $\Psi_{D,q'}$ provides excitation states as a consequence of the quantization, namely the states achieved by the ladder operators. This implies excitation states numerated by the eigenvalues n of the number operator $\hat{n}$, $\Psi_{D,q',n}$. In particular, a zero-point oscillation, ZPO, has the eigenvalue $n = 0$, so it is a state $\Psi_{D,q',n=0}$ (Carmesin, 2021a, chapter 7).

For instance, a state with a polarization mode q of the dark energy represents a state of the vacuum, and it can be excited to another state with another polarization mode q'.

2.6 QST form elementary particles

In this section, we summarize the formation of elementary particles from the above QST.

The elementary particles can be generated from energy. For instance, this can be achieved in accelerators such as the large hadron collider, LHC. Thereby, many elementary particles have been found and organized in the SMEP, see Chap. (1).

Carmesin (2021a) showed how the excitation states of the vacuum form elementary particles, for a summary see section (2.5.3).

Hereby, the most elementary modes are most likely to form, these are longitudinal modes described by longitudinal tensors, see (Carmesin, 2021a, DEF 6). Moreover, three such modes can constitute a three dimensional object, see (Carmesin, 2021a, THM 6(e)). Hereby, the binding energy has been modeled, derived and calculated, see (Carmesin, 2021a, Sect. 9.4 and THM 9).

In fact, (Carmesin, 2021a, theorems 6-9) showed that such bound triples of the most elementary QST can form elementary particles, whereby the triples of lowest energy exhibit masses that are in precise accordance with observation.

2.7 QST explain the Hubble tension

In this section, we apply the QST to the time evolution of space. With it we analyze, how the observed values of the Hubble constant H_0 depend on the time or redshift, at which the probe had been emitted, that is used in that observation. As a result, we derive the observed values $H_{0,obs}$ as a function of the redshift z. That function $H_{0,obs}(z)$ derived by quantum gravity is in precise accordance with observation, see Carmesin (2021c) and Fig. (2.14). For details see e. g. Carmesin (2021c) or Carmesin (2021a), Carmesin (2021d), Carmesin (2018e). Fig. (2.14) illustrates that the QST describe the cosmological time evolution and the dark energy in an especially precise manner.

2.8 QST explain cosmological parameters

The QST explain five of the six parameters of the standard model of cosmology. The remaining parameter essentially represents the present-day time after the Big Bang. So that param-

eter cannot be explained further, it is an independent parameter of its own. We emphasize that these five cosmological parameters as well as the theoretical $H_0(z)$-values in Fig. (2.14) have been derived from the QST (that means from quantum gravity) without using any fit parameter. So the only numerical input are the four universal constants G, c, k_B and h. All parameters and H_0-results are in precise accordance with observation (that means within the errors of observation), see Carmesin (2021a).

So the QST have been tested in the field of cosmology in a very robust and precise and integrating manner, and these QST present the quanta and modes of excitation of the vacuum. So these QST are an ideal basis for an explanation of elementary particles. Indeed, the formation of masses has already been explained, see Carmesin (2021a).

Accordingly, in this book, we analyze how the QST forming an elementary particle interact within that particle and how they form the electromagnetic interaction as an effective interaction based on gravity.

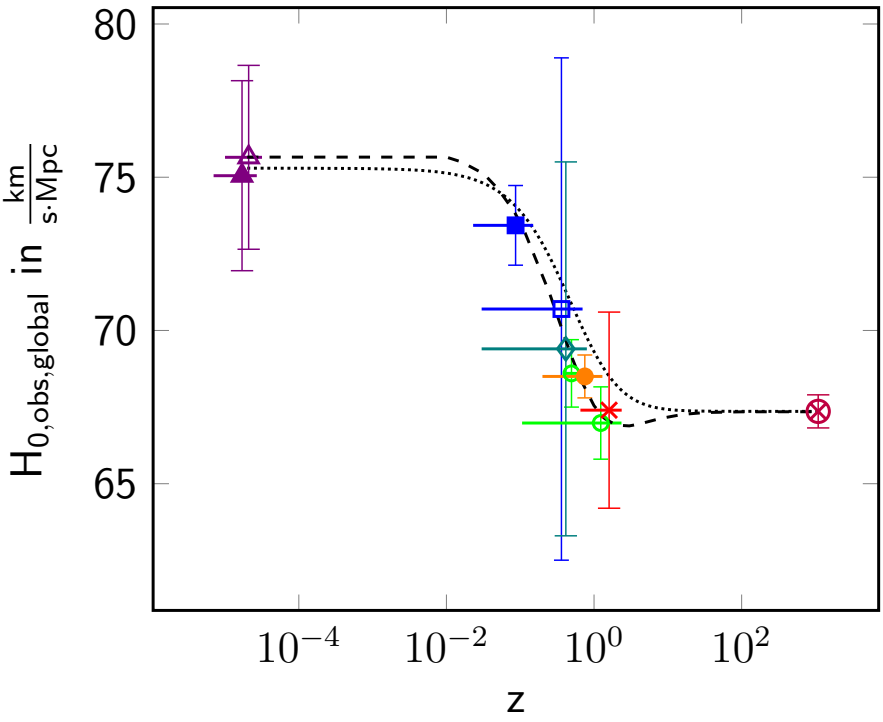

Figure 2.14: Observed global Hubble constant $H_{0,obs,global}$ as a function of the redshift z of the probe.
Probes:
△, megamaser, Pesce et al. (2020).
▲, surface brightness, Blakeslee et al. (2021).
■, distance ladder at small z, Riess et al. (2021).
□, distance ladder at large z, Suzuki et al. (2011).
◇, gravitational wave, Escamilla-Rivera and Najera (2021).
○, baryonic acoustic oscillations, BAO , Philcox et al. (2020), Addison et al. (2018)).
●, weak gravitational lensing and galaxy clustering, Abbott et al. (2020)).
×, strong gravitational lensing, Birrer et al. (2020).
⊗, CMB, Planck-Collaboration (2020).
Theories:
both without any fit
· · · · · · · · · Semiclassical dark energy theory, Carmesin (2021d).
– – – – – quantum theory of dark energy.
under-densities of the local universe (see Tully et al. (2014), Dupuy et al. (2019), Böhringer et al. (2015)) have been applied to probes at $z < 0.04$, for details see Carmesin (2021c).

Chapter 3

QST Form Electric Charge

In this chapter, we elaborate the formation of electric charge and electromagnetic interaction from the quanta of spacetime, QST. Thereby, we derive the fine-structure constant α and the elementary charge e from the QST. We work out the basic process of the formation of electric charge. In chapter (4), we analyze the symmetries of that charge, as these are essential and very useful, see Tanabashi et al. (2018). In a following chapter (5), we use the charge obtained by QST in order to derive electrodynamics and to show how quantum electrodynamics, QED, can be obtained on that basis.

The QST generate fields G^* that are again represented by QST. We analyze the effect of such second order QST in terms of corrections, and we elaborate these in chapter (6). Altogether, our concept provides a relative difference between the theoretical elementary charge and the observed charge of the electron of $5.4 \cdot 10^{-8}$, this difference is within the errors of observation.

3.1 Derivation of the electric field constant

The electric field constant ε_0 is equal to one divided by the product of the magnetic field constant μ_0 and c^2 (Tanabashi

et al., 2018, Table 1.1 or Sect. 7):

$$\varepsilon_0 = \frac{1}{\mu_0 \cdot c^2} \tag{3.1}$$

By definition, the magnetic field constant is equal to 4π multiplied by $10^{-7}\frac{N}{A^2}$:

$$\mu_0 = 4\pi \cdot 10^{-7}\frac{N}{A^2} \tag{3.2}$$

The above two Eqs. yield:

$$\varepsilon_0 = \frac{10^7}{4\pi \cdot c^2}\frac{N}{A^2} = 8.854\,187\,82 \cdot 10^{-12}\,\frac{\mathrm{F}}{\mathrm{m}} \tag{3.3}$$

Hereby, the unit Farad per meter can alternatively be expressed by Coulomb per Volt and per meter.

3.2 QST form charges within particles

In this section, we develop the concept of the formation of charge within particles. Thereby the particles as well as the charges are formed by QST.

The charge is not assumed here, it is derived. For it we analyze the constituents of elementary particles with electric charge. The mass of such particles is caused by the Higgs particle via the Higgs mechanism, see Tanabashi et al. (2018).

The Higgs particle has already been explained by the binding of three QST, each corresponding to a particular excitation of the vacuum (Carmesin, 2019c, Chap. 9). These excitation states of the vacuum have been derived by an analysis of the cosmic unfolding, and they are based on the light horizon, it is the horizon at which objects can just exhibit a causal influence upon us.

As a consequence, these three QST exhibit an internal dynamics inside the elementary particle. For comparison, another internal dynamics is already well known from atoms: In an atom

there are a nucleus and electrons, these exhibit an internal dynamics, and thereby photons can be emitted and absorbed. We will show in this chapter, that the internal dynamics of the three QST can emit quanta which represent the electric field. For it we summarize properties of these three QST first:

The masses of all particles with an electric charge are caused by the Higgs-particle. That particle is constituted by a bound triple of QST with the eigenvalues $n = 1$, $n = 2$ and $n = 3$, for an illustration see Fig. (2.13). Accordingly, we model each particle with an electric charge by a bound triple of QST with these eigenvalues $n = 1$, $n = 2$ and $n = 3$:

$$\Psi_{particle\ with\ electric\ charge} = \text{triple}(\Psi_{n=1}, \Psi_{n=2}, \Psi_{n=3}) \tag{3.4}$$

3.3 Circular frequencies of the constituents

In this section, we elaborate the circular frequencies of the three constituents of an elementary particle with an electric charge, see Eq. (3.4), Fig. (2.13) and Sect. 3.2). The circular frequency ω_1 of the constituent $\Psi_{n=1}$ is three times the circular frequency ω_0 of the corresponding ZPO $\Psi_{n=0}$, see e. g. (Carmesin, 2021d, THM 19):

$$\omega_1 = 3 \cdot \omega_0 = (2n + 1) \cdot \omega_0 \tag{3.5}$$

Similarly, the circular frequency ω_2 of $\Psi_{n=2}$ is five times ω_0:

$$\omega_2 = 5 \cdot \omega_0 = (2n + 1) \cdot \omega_0 \tag{3.6}$$

In the same manner, ω_3 of $\Psi_{n=3}$ is seven times ω_0:

$$\omega_3 = 7 \cdot \omega_0 = (2n + 1) \cdot \omega_0 \tag{3.7}$$

Proposition 1 Circular frequencies

A Higgs Boson as well as a particle that can form an electric charge are constituted by three QST as follows (Carmesin, 2021a, Chapters 7-9):

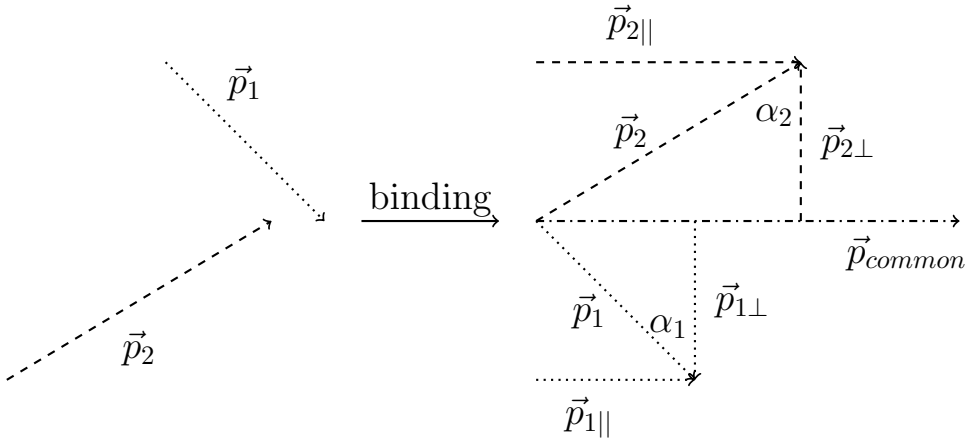

Figure 3.1: Momenta of two longitudinal QST before and after binding: After the binding, parallel components $\vec{p}_{1||}$ and $\vec{p}_{2||}$ remain unchanged. However, the orthogonal components $\vec{p}_{1\perp}$ and $\vec{p}_{2\perp}$ vary with time around the value $\vec{p}_{\perp} = 0$, as a consequence of the binding.

(1) These three QST are characterized by the following eigenvalues of the number operator: $n_1 = 1$, $n_2 = 2$ *and* $n_3 = 3$.

(2) The circular frequencies can be described by using the circular frequency ω_0 *of the ZPO as follows:*

$$\omega_j = (2n_j + 1) \cdot \omega_0 = \bar{n}_j \cdot \omega_0 \quad \text{with} \quad \bar{n}_j = 2n_j + 1 \tag{3.8}$$

3.4 Formation of a local mass

When the three QST of a charged elementary particle form a superposition and are bound to a triple, then their three momenta $\vec{p}_1$, $\vec{p}_2$ and $\vec{p}_3$ add up to a common momentum (Fig. 3.1):

$$\vec{p}_{\text{triple}} = \vec{p}_1 + \vec{p}_2 + \vec{p}_3 \tag{3.9}$$

Thereby, the velocity of the triple may be below c (Carmesin, 2021a, PROP 17):

$$\text{typically} \quad v < c \tag{3.10}$$

A velocity smaller than c is only possible for a nonzero own mass, according to special relativity. Correspondingly, the triple exhibits a common nonzero own mass m_c

$$m_c > 0 \tag{3.11}$$

In this manner the QST can form a common mass m_c[1].

3.5 Separation of parallel component

In this section, we analyze the possible gravitational interaction among the three QST that are bound in a particle Fig. (2.13). For that purpose and for each of the three QST, we analyze the component parallel to the propagation of m_c and a corresponding orthogonal component (Fig. 3.1).

3.5.1 Components of the momenta

The momentum $\vec{p}_j$ of each QST in section (3.2) can be regarded as a linear combination of the component $\vec{p}_{j||}$ parallel to $\vec{p}_{\text{triple}}$ and of the component $\vec{p}_{j\perp}$ orthogonal to the momentum of the triple $\vec{p}_{\text{triple}}$:

$$\vec{p}_j = \vec{p}_{j||} + \vec{p}_{j\perp} \tag{3.12}$$

3.5.2 Components of the wave functions

Before the binding, each QST propagates freely according to its momentum $\vec{p}_j$. So the QST is described by a plane wave as follows:

$$\Psi_j = \nu \cdot \exp\left(i\omega_j t - i\vec{r} \cdot \frac{\vec{p}_j}{\hbar}\right) \tag{3.13}$$

[1]Note that an observer at a distance of that triple might observe a different mass $m_{distance}$, as that observer measures the mass on the basis of the observed QST. In this section, we do not derive the mass that is observable at a large distance.

Hereby, ν represents a normalization factor, eventually in the framework of distributions. That function can be factorized:

$$\Psi_j = \nu \cdot \exp\left(i\omega_j t\right) \cdot \exp\left(-i\vec{r}_{||} \cdot \frac{\vec{p}_{j||}}{\hbar}\right) \cdot \exp\left(-i\vec{r}_{\perp} \cdot \frac{\vec{p}_{j\perp}}{\hbar}\right) \quad (3.14)$$

Thereby, the first exponential describes an oscillation. The second exponential represents the propagation in the direction of propagation of the common mass m_c:

$$\Psi_{j||} = \exp\left(-i\vec{r}_{||} \cdot \frac{\vec{p}_{j||}}{\hbar}\right) \quad (3.15)$$

Similarly, the third exponential describes the motion orthogonal to the direction of propagation of the common mass m_c.

$$\Psi_{j\perp} = \exp\left(-i\vec{r}_{\perp} \cdot \frac{\vec{p}_{j\perp}}{\hbar}\right) \quad (3.16)$$

Altogether, the wave function is factorized as follows:

$$\Psi_j = \nu \cdot \exp\left(i\omega_j t\right) \cdot \Psi_{j||} \cdot \Psi_{j\perp} \quad (3.17)$$

3.5.3 Wave function Ψ_j after the binding

After the binding of the three QST in section (3.2), $\Psi_{j||}$ remains unchanged, as the triple of the QST propagates freely. However, the perpendicular component $\Psi_{j\perp}$ is essentially changed by the binding of the three QST, as the QST are bound and cannot escape in the orthogonal direction. That effect is illustrated by the wiggly lines in Fig. (2.13).

3.5.4 Condition of the binding

In this section we show that the three QST can be bound even by a small mass m_c. At a distance r from the mass m_c, the escape velocity is as follows:

$$v_{esc} = \frac{2 \cdot G \cdot m_c}{r} \quad (3.18)$$

Waveguides: A waveguide (e. g. a glass fiber) binds light. For it, the waveguide is produced with different indices of refraction. Thereby, the inner region has the highest index of refraction (Taylor and Yariv, 1974, p. 1045):

$$n = \sqrt{\frac{\varepsilon_r}{\varepsilon_0}} \text{ and } n_{max} = \sqrt{\frac{\varepsilon_{r,max}}{\varepsilon_0}} \tag{3.19}$$

Hereby, ε_r is the relative electric permittivity (Jackson, 1975, Eq. 4.38). So the inner region has the smallest velocity of propagation:

$$c(\varepsilon_r) = \sqrt{\frac{1}{\varepsilon_0 \cdot \varepsilon_r \cdot \mu_0 \cdot \mu_r}} \text{ and } c_{min} = \sqrt{\frac{1}{\varepsilon_0 \cdot \varepsilon_{r,max} \cdot \mu_0 \cdot \mu_r}} \tag{3.20}$$

Gravitational lenses: A gravitational lens can be described by the index of refraction $n(\vec{r})$ at locations $\vec{r}$ in the region of the lens (Straumann, 2013, Sect. 5.8.1). Correspondingly, the dynamic mass or mass m_c acts as a gravitational lens. Thus it can be described by the index of refraction $n(\vec{r})$. So it can effectively act as a waveguide, provided that the vertical component of the wave vector is sufficiently small compared to the parallel component of the wave vector (Taylor and Yariv, 1974, p. 1045, Fig. 2).

Similarly, we estimate the formation of a bound mode of propagation or of an effective waveguide by analyzing, whether the perpendicular component of the velocity of propagation $v_{j\perp}$ is below the escape velocity.

Perpendicular component $v_{j\perp}$ below v_{esc}? We analyze a QST that propagates at c. We name its momentum p_j. We call its perpendicular component of the momentum $p_{j\perp}$. We denote its perpendicular component of the velocity by $v_{j\perp}$. According to

vector analysis, the following relation holds:

$$\frac{p_{j\perp}}{p_j} = \frac{v_{j\perp}}{c} \tag{3.21}$$

That equation is solved for $v_{j\perp}$ as follows:

$$v_{j\perp} = c \cdot \frac{p_{j\perp}}{p_j} = c \cdot \cos\alpha_j \tag{3.22}$$

Hereby, α_j is the angle enclosed by $\vec{p}_{j\perp}$ and $\vec{p}_j$ (Fig. 3.1).

The QST is bound, if the perpendicular component $v_{j\perp}$ is smaller than the escape velocity:

$$v_{j\perp} < v_{esc} \rightarrow \text{QST is bound} \tag{3.23}$$

The following statement is equivalent:

$$\cos\alpha_j < \frac{v_{esc}}{c} \rightarrow \text{QST is bound} \tag{3.24}$$

Time delay: When light or another object propagating at the velocity of light c passes a gravitational lens, then there occurs a time delay, whereby theory and observation are in precise accordance (Straumann, 2013, Sect. 4.5). Thus, the QST enclosed in a triple of QST exhibit a time delay. So the triple propagates slower than the velocity c. Consequently, the triple exhibits an own mass m_0 and the corresponding amount of inertia.

Proposition 2 Formation of inertia

The masses of elementary particles form by the binding of three QST in a triple of QST (Carmesin, 2021a, Chapters 7-9).

Thereby, the inertia forms as follows:

(1) As a consequence of the binding, these three QST form a propagating center of energy.

(2) That center of energy acts as a gravitational lens, so it can be described by a relatively high refractive index in the center.

(3) Accordingly, that center of energy acts as a waveguide that binds the three QST, whereby the gravitational lens causes a time delay (Straumann, 2013, Sect. 4.5).

(4) As a consequence of the time delay, a distant observer measures a propagation of the triple at a velocity below c. Thus that observer identifies an own mass m_0 of the triple and a corresponding inertia of the triple.

3.5.5 Wave function Ψ after the binding

In this section, we derive the wave function $\Psi_{||}$ of the mass m_c after the binding.

The charged elementary particle is formed by binding three QST with wave functions Ψ_1, Ψ_2 and Ψ_3. The wave function Ψ of the triple is the sum of the three wave functions:

$$\Psi = \Psi_1 + \Psi_2 + \Psi_3 \tag{3.25}$$

Each summand is composed of the above four factors (Eq. 3.17):

$$\Psi = \nu_1 \cdot e^{i\omega_1 t} \cdot \Psi_{1||} \Psi_{1\perp} + \nu_2 \cdot e^{i\omega_2 t} \cdot \Psi_{2||} \Psi_{2\perp} + \nu_3 \cdot e^{i\omega_3 t} \cdot \Psi_{3||} \Psi_{3\perp} \tag{3.26}$$

Each mode Ψ_j includes the respective circular frequency ω_j. So the state of the triple contains the original three circular frequencies. So the spectrum of the triple is expressed as follows:

$$\text{spectrum}(E_c) = \{\omega_1, \omega_2, \omega_3\} \tag{3.27}$$

3.6 Oscillation of orthogonal component

Each perpendicular component $\Psi_{j\perp}$ of the state Ψ of the triple basically oscillates at the respective circular frequency ω_j (Eq. 3.26):

$$\text{spectrum}(\Psi_{j\perp}) = \{\omega_j\} \tag{3.28}$$

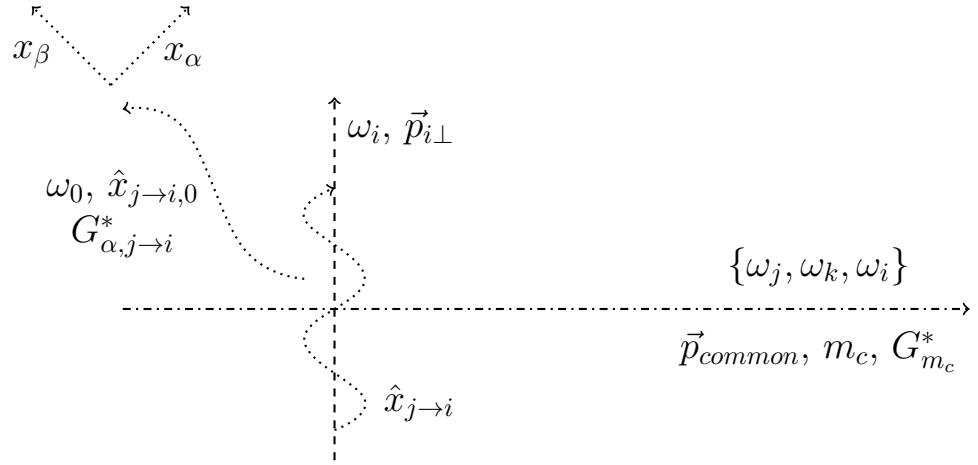

Figure 3.2: Forced oscillation (dotted) with amplitude $\hat{x}_{j\to i}$ and with circular frequency ω_j:
It is caused by the field $G^*_{m_c}$ oscillating at ω_j.
That oscillation emits QST at ω_0, with transverse fields $G^*_{\alpha,j\to i}$, orthogonal to the radial directions of propagation x_β.
Altogether, there occur six such forced oscillations with amplitudes $\hat{x}_{i\to j}$, $\hat{x}_{i\to k}$, $\hat{x}_{j\to i}$, $\hat{x}_{j\to k}$, $\hat{x}_{k\to i}$, $\hat{x}_{k\to j}$.

Proposition 3 Spectra in a triple of QST

In a triple of QST there occur the following spectra:

(1) The propagating center of energy E_c exhibits the three oscillations of the three QST:

$$\text{spectrum}(E_c) = \{\omega_1, \omega_2, \omega_3\} \tag{3.29}$$

(2) Each of the three QST of the triple exhibits its own circular frequency ω_j and a component $\Psi_{j\perp}$ orthogonal to the propagation of E_c, whereby $\Psi_{j\perp}$ has the circular frequency ω_j:

$$\text{spectrum}(\Psi_{j\perp}) = \{\omega_j\} \tag{3.30}$$

3.7 Forced oscillation

The three constituents in section (3.2) are bound together in an elementary particle. In this section, we analyze the internal dynamics exhibited by these three QST inside the particle, we mentioned that dynamics already in section (3.2).

As the three QST are longitudinal quantized waves with three different circular frequencies ω_1, ω_2 and ω_3, there occur six forced oscillations: ω_1 causes a forced oscillation at the QST with ω_2, and we name the amplitude of that oscillation $\hat{x}_{1\to2}$. In the same manner there occur forced oscillations with amplitudes $\hat{x}_{1\to3}$, $\hat{x}_{2\to1}$, $\hat{x}_{2\to3}$, $\hat{x}_{3\to1}$ and $\hat{x}_{3\to2}$.

One might imagine such a forced oscillation by an everyday life analogy: In a violin, or in any other bow instrument such as a contrabass or a viola, the bow causes an oscillation of the chord. Similarly, one longitudinal QST causes a forced oscillation at another longitudinal QST. Altogether, six such forced oscillations occur and form a small orchestra (in the analogy).

We will derive the physical properties of these forced oscillations. Moreover, we will show that these forced oscillations exhibit the properties of the electric field of an elementary charge in a very precise manner. Accordingly, the three QST exhibit the properties of an elementary charge in a very precise manner.

In this section, the forced oscillations among the constituents are elaborated, see Fig. (3.2).

3.7.1 Homogeneous DEQ of an elongation

A constituent with a circular frequency ω_i and a longitudinal normalized direction vector $\vec{e}_i$ can be described as a set of coupled harmonic oscillators, each of which obeys the following equation of motion of the acceleration of the elongation x_i:

$$\ddot{x}_i + \omega_i^2 \cdot x_i = 0 \tag{3.31}$$

Thereby, these oscillators exhibit the same circular frequency ω_i in each transverse direction, as there is no physical reason for an anisotropy. Correspondingly, the tensors factorize in the equation of motion of the QST (Carmesin, 2021d, Sect. 5.6.4). Accordingly, the transverse modes can exhibit a corresponding oscillation forced by another constituent.

3.7.2 Inhomogeneous DEQ of an elongation

Another constituent with a circular frequency ω_j and a longitudinal normalized direction vector $\vec{e}_j$ generates a gravitational field $\vec{G}^*_j$ as follows:

$$\vec{G}^*_j = \hat{G}^*_j \cdot \vec{e}_j \cdot \cos(\omega_j \cdot t + \phi) \tag{3.32}$$

Hereby, ϕ is a phase, $\hat{G}^*_j$ is the amplitude of the field. That amplitude is caused by the mass m_c, thus that amplitude is equal to the amplitude of the field $|\vec{G}^*_{m_c}|$ or $G^*_{m_c}$, for short:

$$\hat{G}^*_j = G^*_{m_c} = |\vec{G}^*_{m_c}| \tag{3.33}$$

The above field represents an additional acceleration of the constituent with the circular frequency ω_i. As a consequence, the constituent oscillating at ω_j causes a forced oscillation of the constituent marked by i, whereby the elongation $x_{j\to i}$ has a transverse direction. For that transverse direction, the homogeneous DEQ (3.31) is supplemented by the additional acceleration represented by the field. So the following inhomogeneous DEQ holds:

$$\ddot{x}_{j\to i} + \omega_i^2 \cdot x_{j\to i} = G^*_{m_c} \cdot \cos(\omega_j \cdot t) \tag{3.34}$$

3.7.3 Amplitude of the forced oscillation

According to the above inhomogeneous DEQ (3.34), there occurs a forced oscillation as follows (Landau and Lifschitz, 1976,

§ 22):

$$x_{j\to i} = \frac{G^*_{m_c}}{\omega_i^2 - \omega_j^2} \cdot \cos(\omega_j \cdot t) \tag{3.35}$$

Amplitudes of forced oscillations: Eq. (3.35) includes the amplitudes of forced oscillations:

$$\boxed{\hat{x}_{j\to i} = \frac{G^*_{m_c}}{\omega_i^2 - \omega_j^2}} \tag{3.36}$$

Eigenvalues n_j in forced oscillations: The circular frequency ω_j of a forced oscillation is a product of the circular frequency ω_0 of the respective ZPO and the factor $2n_j + 1$, whereby n_j is the eigenvalue of the number operator, see PROP (1):

$$\omega_j = \omega_0 \cdot (2n_j + 1) = \omega_0 \cdot \bar{n}_j \tag{3.37}$$

Consequently, the amplitudes of forced oscillations (Eq. 3.35) are as follows:

$$\hat{x}_{j\to i} = \frac{G^*_{m_c}}{\omega_0^2 \cdot |\bar{n}_i^2 - \bar{n}_j^2|} \tag{3.38}$$

In particular, the following fields can be derived: For the first eigenvalue $n_j = 1$ with $j = 1$, the other eigenvalues are $n_i = 2$ with $i = 2$ and $n_k = 3$ with $k = 3$. Thus the following factors $\bar{n}_j$, $\bar{n}_i$ and $\bar{n}_k$ are derived, see PROP (1):

$$\bar{n}_1 = 3; \quad \bar{n}_2 = 5; \quad \bar{n}_3 = 7 \tag{3.39}$$

Proposition 4 Forced oscillation in the triple

In a triple of QST, there occur the following forced oscillations:

(1) The center of energy E_c oscillates at circular frequencies ω_j with $j \in \{1, 2, 3\}$. Thereby, each of these oscillations ω_j causes a forced oscillation at a QST with $\omega_{i\neq j}$ in the triple. Hereby, the following amplitude is generated:

$$\hat{x}_{j\to i} = \frac{G^*_{m_c}}{\omega_i^2 - \omega_j^2} \tag{3.40}$$

(2) Correspondingly, there occur six forced oscillations in the triple, whereby the amplitudes are as follows:

$$\hat{x}_{1\to2}, \hat{x}_{1\to3}, \hat{x}_{2\to1}, \hat{x}_{2\to3}, \hat{x}_{3\to1}, \hat{x}_{3\to2} \tag{3.41}$$

3.8 Transverse effective field

In this section, we show that the forced oscillations cause a transverse field, see Fig. (3.2).

3.8.1 Quanta of spacetime forming the field

A mass m_c, that forms a gravitational field $G^*_{m_c}$, generates that field as follows (Carmesin, 2021d, Sect. 8.8 and THM 34). The mass emits (or absorbs) the QST that establish the dark energy. These are ZPO. These QST form additional space. That additional space generates a curvature of spacetime. That curvature of spacetime represents the generated field $G^*_{m_c}$.

Zero-point oscillations: Accordingly, QST that represent **zero-point oscillations** are emitted (or absorbed) here. So these QST have the circular frequency ω_0 of the ZPO. Moreover, these QST propagate (locally) unidirectional in a radial direction x_β, see Fig. (3.2). The field is oriented in a direction x_α, see Fig. (3.2). Thus the corresponding tensor is $\varepsilon_{\alpha,\alpha}$. Moreover, we apply the definition of the tensor $\varepsilon_{\alpha,\alpha}$. For it, we remind the corresponding field equation of the QST (Eq. 2.26):

$$c \cdot \dot{\varepsilon}_{\alpha,\alpha} = \pm G^*_{\alpha,j\to i} \tag{3.42}$$

Hereby, the directions of the nonzero tensor element and the field coincide and are both transverse to the direction of propagation (Fig. 3.2).

Moreover, we apply the definition of the tensor $\varepsilon_{\alpha,\alpha}$:

$$c \cdot \frac{\partial}{\partial t} \frac{\delta x_{\alpha,j\to i}}{dx_\alpha} = \pm G^*_{\alpha,j\to i} \tag{3.43}$$

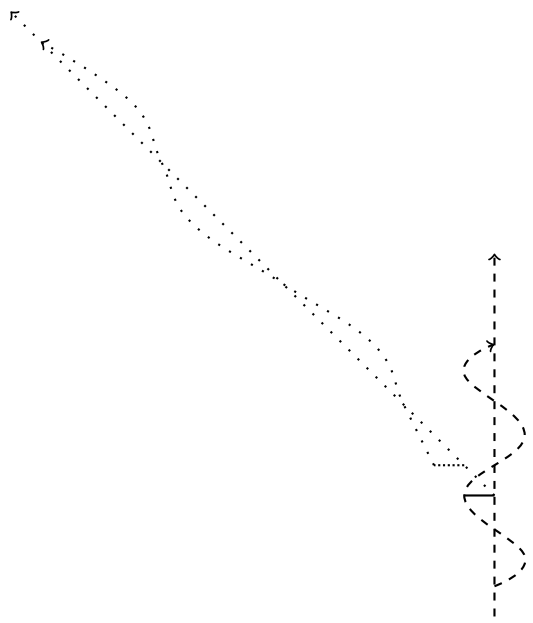

Figure 3.3: Forced oscillation (dashed) with amplitude $\hat{x}_{j\to i}$ (solid line) emits QST (loosely dotted) with amplitude $\hat{x}_{j\to i,0}$ (densely dotted). Thereby, the amplitudes are equal, $\hat{x}_{j\to i,0} = \hat{x}_{j\to i}$, similarly to the plucking of a chord of a guitar or of any other plucking instrument such as a cittern.

Energetically, these emitted ZPOs correspond to the five dimensional space, (Carmesin, 2021a, THMs 8, 9).

3.8.2 Principle of equal amplitudes

Emission of quanta: A forced oscillation with its amplitude $\hat{x}_{j\to i}$ emits quanta with their own amplitude $\hat{x}_{j\to i,0}$.

Own frequency of emitted quanta: The emitted quanta have their own frequency. It is different from the frequencies $\omega_{j\to i} = \omega_j$ of the emitting forced oscillations. Similarly, a photon emitted by a hydrogen atom has its own frequency, different from the frequencies of the electron or proton of the atom.

Independent propagation: The emitted quanta propagate independently. Accordingly, they are not stimulated permanently

like a forced oscillation. Instead, an emitted quantum is initially elongated, similarly as a chord of a guitar (or of any other plucking instrument) is elongated when it is plucked. Thereby the amplitudes of the plucking and of the chord are equal, see Fig. (3.3). Correspondingly, we expect $\hat{x}_{j\to i} = \hat{x}_{j\to i,0}$. Accordingly, we formulate the following principle.

Principle: A forced oscillation is characterized by its amplitude $\hat{x}_{j\to i}$, see Eq. (3.38). Analogously, an emitted QST is characterized by its own amplitude $\hat{x}_{j\to i,0}$. These two amplitudes are equal:

$$\boxed{\hat{x}_{j\to i} = \hat{x}_{j\to i,0}} \tag{3.44}$$

Definition 1 Principle of equal amplitudes

When a forced oscillation of a triple of QST with an amplitude $\hat{x}_{j\to i}$ emits a QST with an amplitude $\hat{x}_{j\to i,0}$, then the two amplitudes are equal:

$$\hat{x}_{j\to i} = \hat{x}_{j\to i,0} \tag{3.45}$$

3.8.3 Field $\hat{G}^*_{\alpha,j\to i}$ generated by transverse QST

At a location in space, an emitted QST represents an oscillator with the circular frequency ω_0 and the amplitude $\hat{x}_{j\to i,0}$. So the **elongation** $x_{\alpha,j\to i}$ (see Eq. 3.43) is as follows:

$$x_{\alpha,j\to i}(t) = \hat{x}_{j\to i,0} \cdot \cos(\omega_0 \cdot t) \tag{3.46}$$

That elongation is inserted into the field equation (see Eq. 3.43):

$$c \cdot \frac{\partial}{\partial t} \frac{\delta x_{\alpha,j\to i}(t)}{dx_\alpha} = \pm G^*_{\alpha,j\to i} \tag{3.47}$$

In the limit of small dx_α, the above fraction is the derivative:

$$\lim_{dx_\alpha \to 0} \frac{\delta x_{\alpha,j\to i}(t)}{dx_\alpha} = \frac{\partial}{\partial x_\alpha} x_{\alpha,j\to i}(t) \tag{3.48}$$

The application of the chain rule yields:

$$\frac{\partial}{\partial x_\alpha} x_{\alpha,j\to i}(t) = \frac{\partial t}{\partial x_\alpha} \cdot \frac{\partial}{\partial t} x_{\alpha,j\to i}(t) \tag{3.49}$$

Hereby, the first derivative in the above equation is equal to $\frac{1}{c}$ (Carmesin, 2021d, Sect. 5):

$$\frac{\partial}{\partial x_\alpha} x_{\alpha,j\to i}(t) = \frac{1}{c} \cdot \frac{\partial}{\partial t} x_{\alpha,j\to i}(t) \tag{3.50}$$

Using the above limit (see Eqs. 3.48, 3.50) to Eq. (3.50) provides the following field equation:

$$c \cdot \frac{\partial}{\partial t} \frac{1}{c} \cdot \frac{\partial}{\partial t} x_{\alpha,j\to i}(t) = \pm G^*_{\alpha,j\to i} \tag{3.51}$$

The factors with c in the above Eq. cancel. Applying Eq. (3.46) to the above Eq. yields the following field Eq.:

$$\frac{\partial}{\partial t} \cdot \frac{\partial}{\partial t} \hat{x}_{j\to i,0} \cdot \cos(\omega_0 \cdot t) = \pm G^*_{\alpha,j\to i} \tag{3.52}$$

Evaluation of the derivatives implies the field Eq. shown below:

$$\omega_0^2 \cdot \hat{x}_{j\to i,0} \cdot \cos(\omega_0 \cdot t) = \pm G^*_{\alpha,j\to i} \tag{3.53}$$

Insertion of the amplitude (Eq. 3.38) yields the following Eq.:

$$\omega_0^2 \cdot \frac{G^*_{m_c}}{\omega_0^2 \cdot |\bar{n}_i^2 - \bar{n}_j^2|} \cdot \cos(\omega_0 \cdot t) = \pm G^*_{\alpha,j\to i} \tag{3.54}$$

Simplification of the above term provides the field Eq. in the next line:

$$\frac{G^*_{m_c}}{|\bar{n}_i^2 - \bar{n}_j^2|} \cdot \cos(\omega_0 \cdot t) = \pm G^*_{\alpha,j\to i} \tag{3.55}$$

The corresponding amplitude $\hat{G}^*_{\alpha,j\to i}$ of the emitted field is as follows:

$$\boxed{\hat{G}^*_{\alpha,j\to i} = \frac{G^*_{m_c}}{|\bar{n}_i^2 - \bar{n}_j^2|} \quad \text{without process of emission}} \tag{3.56}$$

Thereby, the process of the emission has not yet been analyzed, it is investigated in section (3.9). Hereby, the field $G^*_{m_c}$ is caused by the mass m_c (Carmesin, 2021d, THMs 7 and 17):

$$\boxed{G^*_{m_c} = \frac{m_c \cdot G}{r^2}} \tag{3.57}$$

The field of all transverse QST emitted at a time is called as follows:

$$G^*_{emitted,\perp} = \text{amount of all transverse QST} \tag{3.58}$$

Hereby, the details are worked out below, see Eq. (3.70).

Proposition 5 QST emitted by forced oscillation

A forced oscillation with amplitude $\hat{x}_{j\to i}$ emits QST with the following amplitude:

$$\hat{G}^*_{\alpha,j\to i} = \frac{G^*_{m_c}}{|\bar{n}_i^2 - \bar{n}_j^2|} \quad \text{without process of emission} \tag{3.59}$$

Hereby, the field of m_c is as follows:

$$G^*_{m_c} = \frac{m_c \cdot G}{r^2} \tag{3.60}$$

3.9 Process of emission

During the process of emission, the emitting m_c loses energy, so the field $G^*_{m_c}$ is reduced in a proportional manner. That causes a reduced emission, in turn. In this section, we analyze and elaborate the effect of that reduction.

When a transverse QST with a field $\hat{G}^*_{\alpha,j\to i}$ is emitted, and when a fraction $q \in [0;1]$ of that QST has already been emitted, then the field $G^*_{m_c}$ is reduced by $\hat{G}^*_{\alpha,j\to i} \cdot q$. So the following field remains:

$$G^*_{m_c,rest} = G^*_{m_c} - \hat{G}^*_{\alpha,j\to i} \cdot q \tag{3.61}$$

In this case, the remaining field causes the emitted field, accordingly, Eq. (3.56) is generalized as follows:

$$\hat{G}^*_{\alpha,j\to i} = \frac{G^*_{m_c,rest}}{|\bar{n}_i^2 - \bar{n}_j^2|} \tag{3.62}$$

Inserting yields the next Eq.:

$$G^*_{m_c,rest} = G^*_{m_c} - \frac{G^*_{m_c,rest}}{|\bar{n}_i^2 - \bar{n}_j^2|} \cdot q \tag{3.63}$$

The solution of that Eq. is as follows:

$$G^*_{m_c,rest} = G^*_{m_c} \cdot \frac{1}{1 + q \cdot \frac{1}{|\bar{n}_i^2 - \bar{n}_j^2|}} \tag{3.64}$$

Integration: The average of the fraction in Eq. (3.64) is obtained by integration:

$$I_{j\to i} = \int_0^1 \frac{1}{1 + q \cdot \frac{1}{|\bar{n}_i^2 - \bar{n}_j^2|}} dq \tag{3.65}$$

The integral is evaluated analytically:

$$I_{j\to i} = |\bar{n}_i^2 - \bar{n}_j^2| \cdot \ln\left(1 + \frac{1}{|\bar{n}_i^2 - \bar{n}_j^2|}\right) \tag{3.66}$$

So the averaged field is as follows:

$$\langle G^*_{m_c,rest} \rangle = G^*_{m_c} \cdot I_{j\to i} \tag{3.67}$$

Application of the above Eq. and of Eq. (3.62) yields the field:

$$\boxed{\hat{G}^*_{\alpha,j\to i} = \langle \hat{G}^*_{\alpha,j\to i} \rangle = G^*_{m_c} \cdot \ln\left(1 + \frac{1}{|\bar{n}_i^2 - \bar{n}_j^2|}\right)} \tag{3.68}$$

Hereby, we denote $\langle \hat{G}^*_{\alpha,j\to i} \rangle$ by $\hat{G}^*_{\alpha,j\to i}$, for short.

Proposition 6 Process of emission

During the process, in which a forced oscillation with amplitude $\hat{x}_{j\to i}$ *emits a QST, the forced oscillation loses energy. That effect reduces the emitted amplitude as follows:*

(1) There occurs an averaged amplitude $\langle \hat{G}^*_{\alpha,j\to i}\rangle$*. It is also named* $\hat{G}^*_{\alpha,j\to i}$ *for short.*

(2) The averaged amplitude is as shown below:

$$\hat{G}^*_{\alpha,j\to i} = \langle \hat{G}^*_{\alpha,j\to i}\rangle = \frac{\langle G^*_{m_c,rest}\rangle}{|\bar{n}_i^2 - \bar{n}_j^2|} = G^*_{m_c}\cdot \ln\left(1+\frac{1}{|\bar{n}_i^2 - \bar{n}_j^2|}\right) \tag{3.69}$$

3.10 Emission and Absorption of quanta

The QST with eigenvalue $n_3 = 3$ and $\bar{n}_3 = 7$ has a negative sign (Carmesin, 2021a, Sect. 9.4). We remind that this is a consequence of the minimization of the energy of the triple (Carmesin, 2021a, Chap. 9).

So the field $G^*_{emitted,\perp}$ is derived as follows:

$$G^*_{emitted,\perp} = G^*_{m_c}\cdot \frac{}{\sqrt{\hat{G}^{*2}_{\alpha,1\to 2} + \hat{G}^{*2}_{\alpha,1\to 3} + \hat{G}^{*2}_{\alpha,2\to 1} + \hat{G}^{*2}_{\alpha,2\to 3} - \hat{G}^{*2}_{\alpha,3\to 1} - \hat{G}^{*2}_{\alpha,3\to 2}}} \tag{3.70}$$

Accordingly, the **scaled emitted transverse field** is represented by the following ratio, and we denote that ratio by $\kappa_{emitted,\perp}$:

$$\kappa_{emitted,\perp} = \frac{G^*_{emitted,\perp}}{G^*_{m_c}} \tag{3.71}$$

In order to evaluate the field, we apply Eq. (3.68):

$$\boxed{\kappa_{emitted,\perp} = 0.085\,736\,162} \tag{3.72}$$

3.10.1 Gravity and signs

The QST in the triple are emitted or absorbed (Carmesin, 2021a, Sect. 9.4). The flow of the QST of dark energy causes an additional volume. Thereby, that volume forms a curvature, and that curvature causes gravity (Carmesin, 2021d, Chap. 1). Hereby, the additionally formed volume and the resulting gravity are not influenced by the direction of the flowing QST. We remind that this can be understood either by the quadrupole symmetry of QST or by the fact that the QST of dark energy propagate in an isotropic manner and without canceling each other, see e. g. Carmesin (2021d). Consequently, the signs of the emission (see Eq. 3.70) do not influence the gravitational interaction of the triple.

Proposition 7 Transverse emitted field

(1) In a triple of QST with $n_j \in \{1,2,3\}$, there occur forced oscillations. These forced oscillations emit transverse QST with the following field:

$$G^*_{emitted,\perp} = \sqrt{\hat{G}^{*2}_{\alpha,1\to2} + \hat{G}^{*2}_{\alpha,1\to3} + \hat{G}^{*2}_{\alpha,2\to1} + \hat{G}^{*2}_{\alpha,2\to3} - \hat{G}^{*2}_{\alpha,3\to1} - \hat{G}^{*2}_{\alpha,3\to2}} \tag{3.73}$$

(2) Accordingly, the scaled emitted transverse field is as follows:

$$\kappa_{emitted,\perp} = \frac{G^*_{emitted,\perp}}{G^*_{m_c}} \tag{3.74}$$

(3) In the present case, we do not apply any corrections, and we obtain the following value of the scaled emitted transverse field:

$$\kappa_{emitted,\perp} = 0.085\,736\,162 \qquad \text{without corrections} \tag{3.75}$$

3.11 Interaction caused by $G^*_{emitted,\perp}$

In this section, we analyze the interaction caused by the transverse emitted field $G^*_{emitted,\perp}$. For it, we transform the elementary charge to the Planck units.

3.11.1 Elementary charge in Planck units

In this section, we transform the elementary charge e to Planck units. A charge q in SI units[2] is transformed to a charge $\tilde{q}$ in Planck units by multiplication by the factor $\frac{1}{\sqrt{4\pi\cdot\varepsilon_0\cdot\hbar\cdot c}}$, see table (8.3):

$$\tilde{q} = q \cdot \frac{1}{\sqrt{4\pi \cdot \varepsilon_0 \cdot \hbar \cdot c}} \tag{3.76}$$

In order to provide a value for comparisons, we apply the observed value of the elementary charge (Tanabashi et al., 2018, Table 1.1):

$$e_{obs} = 1.602\,176\,6208(98) \cdot 10^{-19}\,\mathrm{C} \tag{3.77}$$

In terms of Planck units, the above charge is as follows:

$$\tilde{e}_{obs} = 0.085\,424\,5431(6) \tag{3.78}$$

3.11.2 Comparison of $\kappa_{emitted,\perp}$ with elementary charge

In this section, we compare the scaled emitted transverse charge $\kappa_{emitted,\perp}$ (PROP 7(3)) with the elementary charge $\tilde{e}_{obs}$. Both quantities are essentially equal. The relative difference is as follows:

$$\Delta_{\kappa_{emitted,\perp},\tilde{e}_{obs}} = \frac{\kappa_{emitted,\perp} - \tilde{e}_{obs}}{\tilde{e}_{obs}} = 0.36\% \tag{3.79}$$

This finding indicates that $\kappa_{emitted,\perp}$ is the amount of the electric charge $\tilde{e}_{obs}$. In order to obtain a further confirmation of that result, we analyze the corresponding field in Planck units:

[2]Hereby, the charge q should be distinguished from the integration variable used above.

3.11.3 Gravitational field $\tilde{G}^*_{m_c}$

In this section, we derive the gravitational field $\tilde{G}^*_{m_c}$ of the considered triple of QST, in terms of Planck units. The gravitational field $\tilde{G}^*_{m_c}$ as a function of the distance $\tilde{r}$ is as follows, see table (8.3):

$$\tilde{G}^*_{m_c} = \frac{\tilde{m}_c}{\tilde{r}^2} \tag{3.80}$$

Scaled common mass $\tilde{m}_{c,near}$: If a distant observer measures the common mass $\tilde{m}_{c,distant}$, than the result is usually smaller than the value measured by a near observer $\tilde{m}_{c,near}$. This result is derived in section (4.6). The scaled common mass $\tilde{m}_{c,near}$ is equal to one, see section (4.6):

$$\tilde{m}_{c,near} = 1 \tag{3.81}$$

Correspondingly, $\tilde{m}_{c,near}$ is an important invariant. Accordingly, $\tilde{m}_{c,near}$ is analyzed within the chapter about symmetries and invariants (4) in section (4.6). We emphasize here that there is no cyclic argument, the topic $\tilde{m}_{c,near}$ merely fits better to the chapter (4) than to the present chapter.

Application of $\tilde{m}_{c,near}$: The emitted transverse field $\tilde{G}^*_{m_c}$ is generated at the triple. So it is caused by the near mass $\tilde{m}_{c,near}$. Thus we derive the following emitted transverse field:

$$\tilde{G}^*_{m_c} = \frac{\tilde{m}_{c,near}}{\tilde{r}^2} = \frac{1}{\tilde{r}^2} \tag{3.82}$$

3.11.4 Emitted transverse field $\tilde{G}^*_{emitted,\perp}$

In this section, we derive the emitted transverse field $\tilde{G}^*_{emitted,\perp}$, in terms of Planck units. For it, we apply Eq. (3.74):

$$\kappa_{emitted,\perp} = \frac{G^*_{emitted,\perp}}{G^*_{m_c}} \tag{3.83}$$

We expand the fraction by the factor that transforms $G^*_{m_c}$ to the corresponding term in Planck units $\tilde{G}^*_{m_c}$:

$$\kappa_{emitted,\perp} = \frac{\tilde{G}^*_{emitted,\perp}}{\tilde{G}^*_{m_c}} \tag{3.84}$$

We solve for $\tilde{G}^*_{emitted,\perp}$:

$$\tilde{G}^*_{emitted,\perp} = \kappa_{emitted,\perp} \cdot \tilde{G}^*_{m_c} \tag{3.85}$$

In order to derive the emitted transverse field $\tilde{G}^*_{emitted,\perp}$ as a function of the distance $\tilde{r}$, we apply Eq. (3.82) to the above equation:

$$\tilde{G}^*_{emitted,\perp} = \kappa_{emitted,\perp} \cdot \frac{1}{\tilde{r}^2} \tag{3.86}$$

3.11.5 Electric field $\tilde{\mathscr{E}}$ in Planck units

In this section, we summarize the electric field $\tilde{\mathscr{E}}$ of an elementary charge $\tilde{e}_{obs}$, in terms of Planck units, see table (8.3). In Planck units, an observed elementary charge $\tilde{e}_{obs}$ emits an observed electric field $\tilde{\mathscr{E}}$ as a function of the distance $\tilde{r}$ as follows:

$$\tilde{\mathscr{E}} = \frac{\tilde{e}_{obs}}{\tilde{r}^2} \tag{3.87}$$

3.11.6 Comparison of the fields $\tilde{G}^*_{emitted,\perp}$ and $\tilde{E}^*$

In this section, we compare the scaled emitted transverse field $\tilde{G}^*_{emitted,\perp}$, see Eq. (3.86),

$$\tilde{G}^*_{emitted,\perp} = \kappa_{emitted,\perp} \cdot \frac{1}{\tilde{r}^2}, \tag{3.88}$$

with the electric field $\tilde{\mathscr{E}}$, see Eq. (3.87):

$$\tilde{\mathscr{E}} = \frac{\tilde{e}_{obs}}{\tilde{r}^2} \tag{3.89}$$

For it we form the ratio:

$$\frac{\tilde{\mathscr{E}}}{\tilde{G}^*_{emitted,\perp}} = 1.0036 \tag{3.90}$$

We realize that both fields are essentially equal, whereby the relative difference is caused by the relative difference between the observed electric charge $\tilde{e}_{obs}$ and the scaled emitted transverse field $\kappa_{emitted,\perp}$, and it amounts to 0.36 %:

$$\Delta_{\tilde{\mathscr{E}},\tilde{G}^*_{emitted,\perp}} = \frac{\tilde{G}^*_{emitted,\perp} - \tilde{\mathscr{E}}}{\tilde{\mathscr{E}}} = 0.36\% \tag{3.91}$$

The above relative difference decreases to $5.4 \cdot 10^{-8}$, when simultaneously emitted transverse as well as screening and QED corrections QST are analyzed, see chapter (6).

Theorem 1 Elementary charge: emission of single QST

In a triple of QST with $n_j \in \{1, 2, 3\}$, there occur forced oscillations. These forced oscillations emit QST with a scaled transverse field $\kappa_{emitted,\perp}$. At an emission of single QST, the scaled emitted transverse field $\kappa_{emitted,\perp}$ has the following properties:

(1) The amount $\kappa_{emitted,\perp}$ is essentially equal to the scaled elementary charge:

$$\kappa_{emitted,\perp} = \tilde{e}_{obs} \cdot (1 + 0.36\%) \tag{3.92}$$

The remaining difference is below a corresponding error of measurement, when corrections are applied, see Chap. (6).

(2) The emitted transverse field $\tilde{G}^*_{emitted,\perp}$ is essentially equal to the electric field $\tilde{\mathscr{E}}$ of an elementary charge:

$$\tilde{G}^*_{emitted,\perp} = \frac{\kappa_{emitted,\perp}}{\tilde{r}^2} = \frac{\tilde{e}_{obs}}{\tilde{r}^2} \cdot (1 + 0.36\%) = \tilde{\mathscr{E}} \cdot (1 + 0.36\%) \tag{3.93}$$

The remaining difference is below a corresponding error of measurement, when corrections are applied, see Chap. (6).

(3) As a consequence, the elementary charge as well as the electric field are explained by quantum gravity. Consequently, the electric interaction is explained by quantum gravity.

3.11.7 Derivation in SI-units

In this section, we derive the result of THM (1) in the framework of SI units, as some readers might prefer these units.

For it, we test whether $G^*_{emitted,\perp}$ represents the electric field $\tilde{\mathscr{E}}$ of a particle with one elementary charge e.

In particular, we analyze the Coulomb force or the corresponding electric field $\tilde{\mathscr{E}}$. The respective coupling constant is $\frac{1}{4\pi\cdot\varepsilon_0}$. The gravitational coupling constant G is also named Newtonian coupling constant G_N (Tanabashi et al., 2018, Table 1.1), so that it is distinguished from other coupling constants. Similarly, we denote the coupling constant $\frac{1}{4\pi\cdot\varepsilon_0}$ by Coulomb coupling constant G_C:

$$G_C = \frac{1}{4\pi\cdot\varepsilon_0} \tag{3.94}$$

First, we remind the form of the electromagnetic field of a charge e at a distance r:

$$\tilde{\mathscr{E}} = G_C \cdot \frac{e}{r^2} \tag{3.95}$$

Secondly, we test the following hypothesis:

$$\text{hypothesis}: \quad \tilde{\mathscr{E}} = \frac{\sqrt{G_C}\cdot G^*_{emitted,\perp}}{\sqrt{G_N}\cdot\tilde{m}_c} \;\text{ with }\; \tilde{m}_c = 1 \tag{3.96}$$

Hereby, the condition $\tilde{m}_c = 1$ is derived below, see section (4.6). Thirdly, we insert Eqs. (3.95) and (3.71):

$$\text{hypothesis}: \quad G_C\cdot\frac{e}{r^2} = \frac{\sqrt{G_C}\cdot G^*_{m_c}\cdot\kappa_{emitted,\perp}}{\sqrt{G_N}\cdot\tilde{m}_c} \;\text{ with }\; \tilde{m}_c = 1 \tag{3.97}$$

Fourthly, we insert Eq. (3.57):

$$\text{hypothesis}: \quad G_C \cdot \frac{e}{r^2} = \frac{m_c \cdot G_N}{r^2} \cdot \frac{\sqrt{G_C} \cdot \kappa_{emitted,\perp}}{\sqrt{G_N}\tilde{m}_c} \quad \text{with} \quad \tilde{m}_c = 1 \tag{3.98}$$

Fifthly, we cancel $\sqrt{G_N}$, and we multiply by $r^2/\sqrt{G_C}$:

$$\text{hypothesis}: \quad \sqrt{G_C} \cdot e = m_c \cdot \frac{\sqrt{G_N} \cdot \kappa_{emitted,\perp}}{\tilde{m}_c} \quad \text{with} \quad \tilde{m}_c = 1 \tag{3.99}$$

Next, we apply the definition $m_c = M_P \cdot \tilde{m}_c$, see tab. (8.3):

$$\text{hypothesis}: \quad \sqrt{G_C} \cdot e = M_P \cdot \sqrt{G_N} \cdot \kappa_{emitted,\perp} \quad \text{with} \quad \tilde{m}_c = 1 \tag{3.100}$$

Seventhly, we apply the square, and we divide by $\hbar \cdot c$:

$$\text{hypothesis}: \quad \frac{G_C \cdot e^2}{\hbar \cdot c} = M_P^2 \cdot \frac{G_N}{\hbar \cdot c} \cdot \kappa^2_{emitted,\perp} \quad \text{with} \quad \tilde{m}_c = 1 \tag{3.101}$$

In the above Eq., we identify the fraction at the left hand side by α, see (Tanabashi et al., 2018, Table 1.1),

$$\alpha = \frac{G_C \cdot e^2}{\hbar \cdot c} \tag{3.102}$$

and we identify the fraction at the right hand side by $1/M_P^2$, see table (8.3). So the square $\kappa^2_{emitted,\perp}$ represents the theoretical value α_{theo}, provided by the new theory of quantum gravity:

$$\text{hypothesis}: \quad \alpha = \kappa^2_{emitted,\perp} = \alpha_{theo} \quad \text{with} \quad \tilde{m}_c = 1 \tag{3.103}$$

In order to evaluate α_{theo}, we apply Eq. (3.72):

$$\alpha_{theo} = \kappa^2_{emitted,\perp} = 7.350\,689\,541 \cdot 10^{-3} \tag{3.104}$$

For comparison, we use the measured value of the fine-structure constant (Tanabashi et al., 2018, Table 1.1):

$$\alpha_{obs} = 7.297\,352\,5664(17) \cdot 10^{-3} \tag{3.105}$$

The relative difference is as follows:

$$\Delta_\alpha = \frac{\kappa^2_{emitted,\perp} - \alpha_{obs}}{\alpha_{obs}} = 0.73\% \quad \text{without corrections} \tag{3.106}$$

Relatively precise confirmation of hypothesis: The hypothesis is in relatively precise accordance with observation. So the hypothesis is confirmed in a relatively precise manner.

Screening: The difference is already quite small, though we did not yet apply the phenomenon of screening of the elementary charge. Accordingly, in this chapter, we derive the value of the bare elementary charge e_{bare}, see Landau and Lifschitz (1982), Greiner and Reinhardt (1995).

Bare elementary charge: In order to derive the bare elementary charge, we solve Eq. (3.102) for e:

$$e = \sqrt{\frac{\alpha \cdot \hbar \cdot c}{G_C}} \tag{3.107}$$

The bare elementary charge is the value without screening. So it is derived by using the above value α_{theo}: Thus we derive:

$$e_{bare} = \sqrt{\frac{\alpha_{theo} \cdot \hbar \cdot c}{G_C}} \tag{3.108}$$

The evaluation provides the result:

$$e_{bare} = 1.608\,021\,197 \cdot 10^{-19}\,\mathrm{C} \tag{3.109}$$

The observed value of the screened elementary charge is shown next (Tanabashi et al., 2018, Table 1.1):

$$e_{obs} = 1.602\,176\,6208(98) \cdot 10^{-19}\,\mathrm{C} \tag{3.110}$$

The relative difference is as follows:

$$\Delta_{screening} = \frac{e_{bare} - e_{obs}}{e_{obs}} = 0.36\% \qquad \text{without corrections} \tag{3.111}$$

3.11.8 Interpretation

The new theory of quantum gravity (Carmesin, 2021d, Chap. 1-6) provides a mechanism for the formation of masses of charged elementary particles (Carmesin, 2021a, Chap. 7, 9). Moreover, our derivation in this chapter shows, how these elementary particles form electric charge and electric interactions. The relative difference between the bare elementary charge and the observed elementary charge is relatively small, namely 0.36 %. Screening and the simultaneous emission of QST are elaborated in terms of corrections in chapter (6), and these provide relative differences between theory and observation at the 10^{-8} scale. These relatively small deviations between theory and observation are interpreted as a clear evidence for the present theory.

So the same theory of quantum gravity explains the H_0-tension (Fig. 2.14) as well as the electric charge in a very precise manner. Thus quantum gravity unifies the phenomena of gravity and electricity in a fully elementary and beautiful manner.

Derived charge: Using the present theory, we explain what the charge is. For it we use Eq. (3.108), and we insert Eq. (3.103):

$$e_{bare} = \kappa_{emitted,\perp} \cdot \sqrt{\frac{\hbar \cdot c}{G_C}} \tag{3.112}$$

In the Gaussian system of units, the coupling G_C takes the value one (Jackson, 1975, p. 818). In that system, the ratio $\kappa_{emitted,\perp}$ represents a scaled version of the electric charge:

$$e_{bare} = \kappa_{emitted,\perp} \cdot \sqrt{\hbar \cdot c} \quad \text{in Gaussian units} \tag{3.113}$$

In Planck units (tab. 8.3), the scaled electric charge is as follows (Eq. 3.71):

$$\boxed{\tilde{e}_{bare} = \frac{e_{bare}}{\sqrt{\hbar \cdot c/G_C}} = \frac{e_{bare}}{q_P} = \kappa_{emitted,\perp} = \frac{G^*_{emitted,\perp}}{G^*_{m_c}}} \tag{3.114}$$

In Planck units, the bare charge is the ratio of the field $G^*_{emitted,\perp}$ caused by the internal dynamics of the three QST and the local gravitational field $G^*_{m_c}$ of the three QST.

Feynman's view (Feynman, 1985, p. 129) realized that the fine-structure constant essentially describes the amount of electromagnetic activity exhibited by the elementary charge: *'There is a most profound and beautiful question associated with the observed coupling constant, e_{cc}[3] − the amplitude for a real electron to emit or absorb a real photon. It is a simple number that has been experimentally determined to be close to 0.08542455. (My physicist friends won't recognize this number, because they like to remember it as the inverse of its square: about 137.03597 with an uncertainty of about 2 in the last decimal place. It has been a mystery ever since it was discovered more than fifty years ago, and all good theoretical physicists put this number up on their wall and worry about it.)*

Immediately you would like to know where this number for a coupling comes from: is it related to π or perhaps to the base of natural logarithms? Nobody knows. It's one of the greatest damn mysteries of physics: a magic number that comes to us with no understanding by humans. You might say the 'hand of God' wrote that number, and 'we don't know how He pushed His pencil.' We know what kind of a dance to do experimentally to measure this number very accurately, but we don't know what kind of dance to do on the computer to make this number come out − without putting it in secretly!'.

Indeed, I present a program that can run *on the computer to make this number come out − without putting it in secretly!*, see section (8.6). Moreover, I provide two corrections in chapter (6), one correction takes care of several QST emitted simultaneously, the other correction takes care of screening or corrections of quantum electrodynamics, QED.

[3] I added the subscript cc in order to mark a difference to the elementary charge e.

I think that Feynman's view shows precisely the essential relevance of the coupling constant α and of its explanation. In particular, the observed coupling constant, e_{cc}, suggested by Feynman, is now explained by the ratio $\kappa_{emitted,\perp}$ of the emitted field $G^*_{emitted,\perp}$ and the gravitational field $G^*_{m_c}$.

Moreover, Feynman points out at the next page in his book, that the number α alone is not yet very useful. Indeed, our present theory provides many insights, whereby the number α derived by our theory serves as a test of our theory. In particular, we elaborated a physical theory that provides the formation of electric charge, the propagation of electric interaction characterized by α, the corresponding symmetries, see next chapter and the formation of electrodynamics, see chapter (5). Altogether, our theory is useful and provides many insights.

Theorem 2 Elementary charge: emission of single QST in SI units

In a triple of QST with $n_j \in \{1,2,3\}$, there occur forced oscillations. These forced oscillations emit QST with a scaled field $\kappa_{emitted,\perp}$. At an emission of single QST, the scaled field $\kappa_{emitted,\perp}$ has the following properties (simultaneously emitted QST are described by THM (3):

(1) The emitted QST mediate an interaction with the following fine-structure constant:

$$\alpha_{theo} = \kappa^2_{emitted,\perp} = 7.350\,689\,541 \cdot 10^{-3} \tag{3.115}$$

The relative difference between the theoretical value and the observed value of the fine-structure constant

$$\alpha_{obs} = 7.297\,352\,5664(17) \cdot 10^{-3} \tag{3.116}$$

is as shown next:

$$\Delta_\alpha = \frac{\kappa^2_{emitted,\perp} - \alpha_{obs}}{\alpha_{obs}} = 0.73\% \quad \text{without corrections} \tag{3.117}$$

(2) The QST emitted by the triple of QST mediate an interaction with the observed fine-structure constant. Correspondingly, the QST emitted by the triple of QST provide the electric field and mediate the electric interaction.

(3) The triple of QST represents the following bare elementary charge:

$$e_{bare} = \sqrt{\frac{\alpha_{theo} \cdot \hbar \cdot c}{G_C}} \quad \text{with} \quad G_C = \frac{1}{4\pi\varepsilon_0} \tag{3.118}$$

The evaluation provides the result:

$$e_{bare} = 1.608\,021\,197 \cdot 10^{-19}\,\mathrm{C} \tag{3.119}$$

The observed value of the screened elementary charge (Tanabashi et al., 2018, Table 1.1)

$$e_{obs} = 1.602\,176\,6208(98) \cdot 10^{-19}\,\mathrm{C} \tag{3.120}$$

provides the relative difference as follows:

$$\Delta_{screening} = \frac{e_{bare} - e_{obs}}{e_{obs}} = 0.36\% \qquad \text{without corrections} \tag{3.121}$$

Chapter 4

Symmetries of Electric Charge

In this chapter, we analyze the symmetries inherent to the electric charge formed by QST. These theoretical symmetries are identical to the observed symmetries, see Tanabashi et al. (2018), and provide additional evidence for the new theory of quantum gravity.

4.1 $\frac{1}{r^2}$ law

The electric field is a mesoscopic description of the radial flow of quanta, see Fig. (3.2) and Eqs. (3.95, 3.96). So the absolute value of the electric field $\mathscr{E}$ is proportional $\frac{1}{r^2}$. thus the corresponding ratio is another invariant:

$$\mathscr{E} \cdot r^2 = G_C \cdot q = \text{Invariant} \tag{4.1}$$

4.2 Time inversion T

A reversion of the time evolution is described by the time reversal operator, see Tanabashi et al. (2018):

$$T \cdot \Delta t = -\Delta t \tag{4.2}$$

The charge formed by the QST emits quanta that constitute the electric field $\vec{\mathscr{E}}$, see Eqs. (3.95, 3.96). Thereby, the direction of

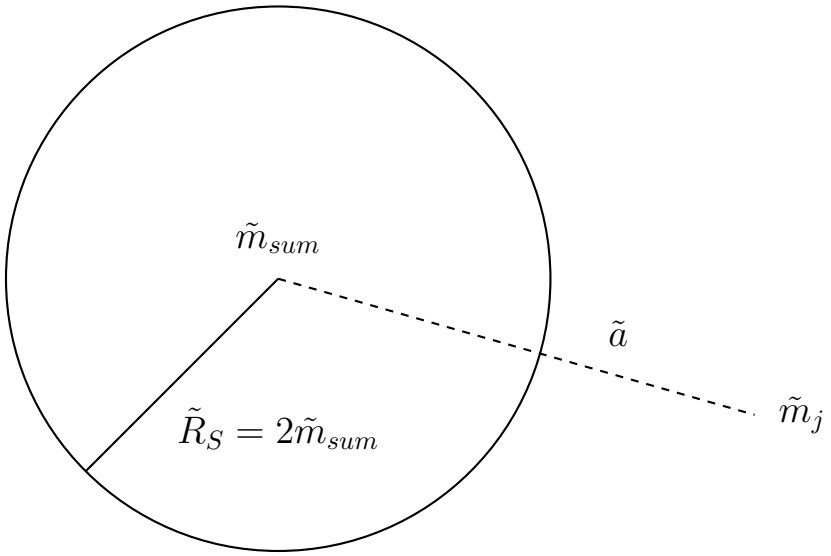

Figure 4.1: QST with dynamic mass $\tilde{m}_j$ is falling towards the other two QST with the dynamic mass $\tilde{m}_{sum}$.

the flow of these quanta determines the sign of the interaction (Carmesin, 2021a, Sect. 9.4). So the sign of the electric field is reversed by T:

$$T \cdot \vec{\mathscr{E}} = - \vec{\mathscr{E}} \tag{4.3}$$

4.3 Formation of negative charge $q = -e$

The fields generated by the three QST forming a charge can be inverted (Carmesin, 2021a, THM 9 and Sect. 9.4). As a consequence, for each charge q that the three QST form, there is another triple of QST that forms the charge $q' = -q$. That relation is usually expressed by the charge conjugation operator C, see Tanabashi et al. (2018)

$$C \cdot q = -q \tag{4.4}$$

4.4 CT invariance

In this section, we show that the application of C and T does not change the relation between the electric field $\vec{\mathscr{E}}$ and the

charge q (Eq. 3.95):

$$\vec{\mathscr{E}} = G_C \cdot \frac{q}{r^2} \cdot \frac{\vec{r}}{r} \tag{4.5}$$

We show this invariance by application of $C \cdot T$ to the above Eq.:

$$C \cdot T \cdot \ \vec{\mathscr{E}} = C \cdot T \cdot G_C \cdot \frac{q}{r^2} \cdot \frac{\vec{r}}{r} \tag{4.6}$$

We apply $T \cdot \ \vec{\mathscr{E}} = -\ \vec{\mathscr{E}}$ and $C \cdot q = -q$:

$$-\ \vec{\mathscr{E}} = G_C \cdot \frac{-q}{r^2} \cdot \frac{\vec{r}}{r} \tag{4.7}$$

We multiply by -1:

$$\vec{\mathscr{E}} = G_C \cdot \frac{q}{r^2} \cdot \frac{\vec{r}}{r} \tag{4.8}$$

This Eq. is the same as Eq. (4.5). So the relation between charge and field is invariant with respect to a $C \cdot T$ transformation.

4.5 Isotropy of the field

The electric field is a mesoscopic description of the radial flow of quanta, see Fig. (3.2) and Eqs. (3.95, 3.96). So the field is invariant with respect to rotations with the center at the charge.

4.6 Invariant mass $\tilde{m}_c = 1$

In this section, we analyze the formation of the dynamical mass $\tilde{m}_c$. For it, we summarize the conditions of that binding first.

4.6.1 Conditions of the process of binding

In this section, we summarize the conditions of the process of the binding.

Pair of QST: We analyze the binding of three QST in two steps. Firstly, two dynamic masses $\tilde{m}_{n1}$ and $\tilde{m}_{n2}$ bind to a dynamic mass $\tilde{m}_{n3}$. Then the pair with the dynamic mass $\tilde{m}_{n3}$ and the third QST with a dynamic mass $\tilde{m}_{n4}$ bind. So it is sufficient to analyze the binding of two dynamic masses.

Accordingly, we analyze the binding of dynamic masses $\tilde{m}_1$ and $\tilde{m}_2$, bound to a dynamic mass $\tilde{m}_3$.

Relativistic QST: The QST are relativistic. So the extension $\tilde{a}_j$ of a dynamic mass $\tilde{m}_j$ is as follows:

$$\tilde{a}_j = \frac{1}{2 \cdot \tilde{m}_j} = \frac{1}{2 \cdot \tilde{E}_j} \quad \text{for} \quad j \in \{1, 2, 3\} \tag{4.9}$$

Fact of binding: We showed already that the three QST bind, e. g. according to the waveguide mechanism, whenever the perpendicular component of the momentum is sufficiently small, see section 3.5.4. Accordingly, we use the fact of the binding, in the following.

Energy measured by a distant observer: As the energy $\tilde{E}_{j,dist}$ of the three QST is in the GeV scale, for the case of a distant observer, it is very small compared to the Planck scale:

$$\tilde{E}_{j,dist} << \frac{1}{2} \quad \text{for} \quad j \in \{1, 2, 3\} \tag{4.10}$$

Minimal extension: The extension $\tilde{a}_j$ cannot be smaller than a Planck length:

$$\tilde{a}_j \geq 1 \quad \text{for} \quad j \in \{1, 2, 3\} \tag{4.11}$$

Maximal energy: The scaled energy of a QST can at most be equal to one half, as the QST are relativistic, see Eqs. (4.9, 4.11):

$$\tilde{E}_j \leq \frac{1}{2} \quad \text{for} \quad j \in \{1, 2, 3\} \tag{4.12}$$

4.6.2 Process of falling towards another

During the process of the binding of two QST, they fall towards another. In particular, we consider the falling of $\tilde{E}_1$ in the gravitational field or environment of $\tilde{E}_2$.

Thereby the gravitational energy of $\tilde{E}_1$ decreases by a factor $\epsilon < 1$ (Carmesin, 2021d, PROP 4). According to the law of energy conservation, that decrease of energy is compensated by an increase of the energy $\tilde{E}_1$ by the inverse factor $1/\epsilon > 1$.

At the beginning, the initial energies $\tilde{E}_{j,ini}$ of the QST are the values that a distant observer can measure:

$$\tilde{E}_{j,ini} = \tilde{E}_{j,dist} \text{ for } j \in \{1,2\} \tag{4.13}$$

After the falling of $\tilde{E}_1$ in the field of $\tilde{E}_2$, until a distance R is achieved, the factor $\epsilon < 1$ takes the following value (Carmesin, 2021d, PROP 4):

$$\epsilon = \sqrt{1 - R_S/R} \tag{4.14}$$

Hereby, R_S is the Schwarzschild radius of $\tilde{E}_2$. We expand the fraction in the above equation by L_P:

$$\epsilon = \sqrt{1 - \tilde{R}_S/\tilde{R}} \tag{4.15}$$

By definition, the Schwarzschild radius is as follows:

$$R_S = \frac{2Gm}{c^2} \text{ or } \tilde{R}_S = 2\tilde{E}_2 \tag{4.16}$$

We apply this relation and Eq. (4.9) to Eq. (4.15):

$$\epsilon = \sqrt{1 - 2\tilde{E}_2 \cdot 2\tilde{E}_1} \tag{4.17}$$

So the energy $\tilde{E}_1$ is as follows:

$$\tilde{E}_1 = \frac{\tilde{E}_{1,dist}}{\epsilon} = \frac{\tilde{E}_{1,dist}}{\sqrt{1 - 2\tilde{E}_2 \cdot 2\tilde{E}_1}} \tag{4.18}$$

Own system of the binary system: We use the own system of the binary system of the two relativistic objects with the energies $\tilde{E}_1$ and $\tilde{E}_2$. Thus the sum of the momenta is zero. So the absolute values of the momenta $|\tilde{p}_1|$ and $|\tilde{p}_2|$ are equal. As these QST are relativistic, the corresponding energies and dynamical masses are equal:

$$|\tilde{p}_1| = \tilde{E}_1 = \tilde{E}_2 = |\tilde{p}_2| \tag{4.19}$$

Energy $\tilde{E}_1$ in the center of dynamic mass system: We apply Eq. (4.19) to Eq. (4.18):

$$\tilde{E}_1 = \frac{\tilde{E}_{1,dist}}{\sqrt{1 - 4\tilde{E}_1^2}} \tag{4.20}$$

We divide the above equation by $\tilde{E}_{1,dist}$:

$$\frac{\tilde{E}_1}{\tilde{E}_{1,dist}} = \frac{1}{\sqrt{1 - 4\tilde{E}_1^2}} \tag{4.21}$$

Graphical solution: In order to solve the above equation, we apply a graphical solution first. For it, we introduce two functions:

$$f(\tilde{E}_1) = \frac{\tilde{E}_1}{\tilde{E}_{1,dist}} \tag{4.22}$$

$$g(\tilde{E}_1) = \frac{1}{\sqrt{1 - 4\tilde{E}_1^2}} \tag{4.23}$$

We represent these functions graphically in Fig. (4.2). The figure shows that the physically relevant solution is as follows:

$$\tilde{E}_1 \approx 1/2 \;\text{ with }\; \tilde{E}_1 < 1/2 \tag{4.24}$$

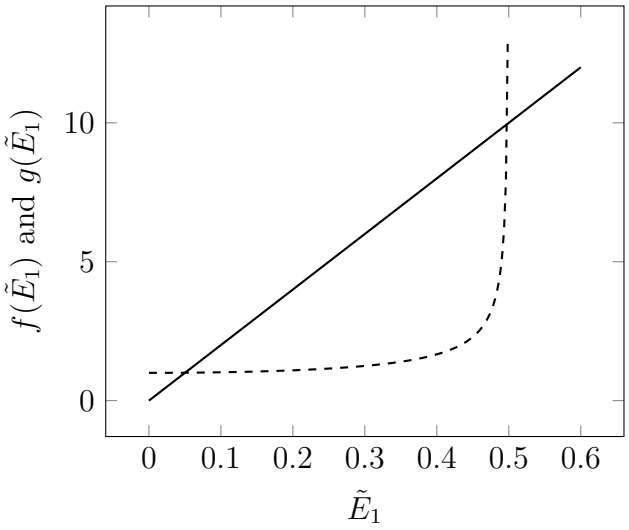

Figure 4.2: Intersections of functions $f(\tilde{E}_1)$ (solid line) and $g(\tilde{E}_1)$ (dashed). $g(\tilde{E}_1)$ exhibits a singularity at $\tilde{E}_1 = 1/2$. So the physically relevant intersection is at $\tilde{E}_1 \approx 1/2$, with $\tilde{E}_1 < 1/2$.

derived approximate solution: We apply Eq. (4.10) to the equation (4.21). So we derive

$$1 << \frac{\tilde{E}_1}{\tilde{E}_{1,dist}} = \frac{1}{\sqrt{1 - 4\tilde{E}_1^2}}, \tag{4.25}$$

or

$$1 << \frac{1}{\sqrt{1 - 4\tilde{E}_1^2}} \tag{4.26}$$

As the fraction in the above equation is very large compared to one, the denominator in that fraction is approximately zero:

$$0 \approx 1 - 4\tilde{E}_1^2 \tag{4.27}$$

We solve for the energy:

$$\tilde{E}_1 \approx \frac{1}{2} \tag{4.28}$$

Sum of energies $\tilde{E}_1 + \tilde{E}_1$: The sum of the scaled energies is approximately one:

$$\tilde{E}_{sum} = \tilde{E}_1 + \tilde{E}_2 \approx 1 \tag{4.29}$$

The mass $\tilde{E}_2$ can represent two bound QST. So the sum $\tilde{E}_{sum}$ can represent two or three bound QST. Thus the triple has a scaled common mass of approximately one:

$$\tilde{m}_c \approx 1 \tag{4.30}$$

Precision of the result: The approximation in Eq. (4.10) is very precise, as the typical masses of charged particles are as follows:

$$m_{j,dist} \leq 200GeV/c^2 = 3.57 \cdot 10^{-25}\,\text{kg} \tag{4.31}$$

For comparison, the Planck mass has the following value:

$$m_P = 2.176 \cdot 10^{-8}\,\text{kg} \tag{4.32}$$

So $\tilde{E}_{j,dist}$ is bound from above as follows:

$$\tilde{E}_{j,dist} = \tilde{m}_{j,dist} = \frac{m_{j,dist}}{m_P} \leq 1.64 \cdot 10^{-17} \tag{4.33}$$

So the expected relative error of $\tilde{m}_c$ is smaller than twice the root of the above bound:

$$\Delta_{rel,\tilde{m}_c} \leq 2\sqrt{1.64 \cdot 10^{-17}} = 8.1 \cdot 10^{-9} \tag{4.34}$$

So we derive:

$$\boxed{\tilde{m}_c = 1 + x \;\text{ with }\; x \in [-10^{-8}, 10^{-8}]} \tag{4.35}$$

4.7 Universality of the elementary charge

The mass of all particles with an electric charge is caused by the mass of the Higgs particle by the Higgs mechanism (Tanabashi et al., 2018, Sect. 11) or (Carmesin, 2021a, Sect. 9.3). So the

electric charge is formed by the three QST corresponding to the Higgs particle (Carmesin, 2021a, Chap. 9), as worked out in chapter (3). As a consequence, the elementary charge is the same in all charged particles.

$$\boxed{\tilde{q}_{elementary} = \tilde{e} \quad \text{for all particles}} \tag{4.36}$$

4.8 Conservation of charge

If the charge is conserved, the QST of these charge emit as many QST as they absorb. So there is no net production of five dimensional space. However, if the charge would not be conserved, then there would be a net production of five dimensional space. This is not stable after the dimensional transition to a dimension below five in the course of cosmic unfolding. Hence the charge is conserved since the dimension decreased below five. As a consequence, the continuity equation of electrodynamics holds (Landau and Lifschitz, 1971, § 29).

4.9 Superposition of fields

The fields in electrodynamics are a mesoscopic description of the QST emitted by a charge. These QST interact by gravity only, as they are not charged. So the interaction becomes essential only in the vicinity of the Planck scale. Thus the fields superimpose linearly, as long as the density is small compared to the Planck density (see table 8.3). So the principle of linear superposition is a very good approximation for the case of electromagnetic fields. As a consequence, the Maxwell equations can be derived, see chapter (5).

4.10 Energy conservation

The QST that are emitted from masses in the form of ZPOs are the basis of the expansion of the universe, see Carmesin

(2021d). Moreover, the ZPOs do not violate the principle of energy conservation, see Carmesin (2020b), Carmesin (2021d). So the formation of the electric field by QST does not violate the principle of conservation of energy.

4.11 Particles with zero charge

Elementary particles, the mass of which is caused by the Higgs particle, can exhibit zero charge. This is usually achieved by the cancellation of positive and negative charges. An example is the neutron, here the charges of one down quark and two up quarks cancel.

In principle, the charge zero can also be achieved, if the forced oscillations are hindered by a huge distance of the QST in the triple. For instance, the QST could propagate fully parallel, so that no transverse modes are excited at all.

The masses of the neutrinos are not caused by the Higgs particle, so the present mechanism does not apply, for details see Carmesin (2021a).

Chapter 5

From QST to Electrodynamics

In this chapter, we show how to derive the theory of **classical electrodynamics**, see e. g. Maxwell (1865), (Tanabashi et al., 2018, Sect. 7), Landau and Lifschitz (1971), and the theory of **quantum electrodynamics, QED**, see e. g. Landau and Lifschitz (1982), Feynman (1985), Greiner and Reinhardt (1995), Schwartz (2014), from the elementary charge, which is based on the quanta of spacetime, QST. Hereby, we use Gaussian coordinates in this chapter (Jackson, 1975, p. 818).

5.1 Basic questions

In this chapter we ask: What ingredients are essential for theories of electrodynamics? What essential ingredients of theories of electrodynamics are provided by the new theory of quantum gravity?

In order to derive the answers to these questions, we present and analyze derivations of these theories. In particular, we derive the theory of classical electrodynamics, and we show how to derive the theory of quantum electrodynamics.

5.2 From QST to classical Electrodynamics

The QST are the most elementary quanta, as they range from the Planck scale to the macroscopic scale, see e. g. Figs. (1.1,

2.12). At the mesoscopic level, these quanta form the elementary charge and the electric field $\vec{\mathscr{E}}$, see chapter (3). Accordingly, the classical theory of electrodynamics can be derived on the basis of the QST. This can be achieved as follows (hereby, we use the Gaussian system of units in this section, for a conversion see e. g. (Jackson, 1975, p. 818)):

5.2.1 Classical action of a particle with a mass m

In this section, we develop the action $S_{m,classical}$ of a particle with a mass m in classical mechanics:

In classical mechanics, the straight path from a point a to a point b is the path at which the integral

$$S_{m,classical} = \int_a^b m \cdot \frac{v^2}{2} ds \tag{5.1}$$

is minimal, while that integral is larger for all other paths from a to b. Accordingly, that integral provides a possible action, so that the lowest action corresponds to the physical path, according to the **principle of least action**. The constant $m/2$ in that integral is chosen so that the usual kinetic energy is derived from S_m (Landau and Lifschitz, 1976, § 4).

5.2.2 Action of a particle with a mass m in SRT

In this section, we develop the action S_m of a particle with a mass m in the theory of special relativity, SRT: For it, we express the squared line element ds^2 in the own frame of the particle:

$$ds^2 = c^2 dt_{own}^2 - dx_{own}^2 - dy_{own}^2 - dz_{own}^2 = c^2 dt_{own}^2 \tag{5.2}$$

Hereby, we used the fact that the elements $dr_{own,j}^2$ are zero in the own frame of the particle. Similarly, we express the squared line element ds^2 in the observer's frame:

$$ds^2 = c^2 dt_{obs}^2 - dx_{obs}^2 - dy_{obs}^2 - dz_{obs}^2 \tag{5.3}$$

Moreover, we remind the usual transformation, see e. g. Einstein (1905), Carmesin (2020b) or Carmesin (1996).

$$dt_{own} = dt_{obs} \cdot \sqrt{1 - \frac{v^2}{c^2}} \tag{5.4}$$

Using the above Eqs. (5.2, 5.3, 5.4), the action can be chosen so that the classical action is obtained in the limit v/c to zero (Landau and Lifschitz, 1971, § 8):

$$S_m = \int_a^b -m \cdot c^2 \cdot dt_{own} = \int_a^b -m \cdot c \cdot ds \tag{5.5}$$

Limit v/c to 0: At leading order in v/c, we derive:

$$dt_{own} \hat{=} dt_{obs} \cdot \left(1 - \frac{1}{2}\frac{v^2}{c^2}\right) \tag{5.6}$$

We apply that result to the action in Eq. (5.5):

$$S_m \hat{=} \left(\int_a^b -m \cdot c^2 + \int_a^b \frac{m}{2} v^2\right) \tag{5.7}$$

As only derivations of the action are relevant for the DEQs or the Lagrangian of the dynamics, we can omit the first integral in the above equation, and so we obtain the classical action:

$$S_m \hat{=} \int_a^b \frac{m}{2} v^2 = S_{m,classical} \tag{5.8}$$

5.2.3 Action of a charged particle in a field

In this section, we develop the action S_{mf} of a particle with a charge q or elementary charge e in a field. In SRT, that field is described by a four-potential A_i.

Moreover, in SRT, the action S_{mf} describing the interaction of the four-potential A_i with the events x^i of the particle should

be a corresponding Lorentz scalar. So the following form of the action S_{mf} arises (Landau and Lifschitz, 1971, Eq. 16.1):

$$S_{mf} = \int_a^b -\frac{e}{c} \cdot A_i \cdot dx_i \tag{5.9}$$

Hereby, we use the sum convention, and the constant c has been included so that the usual Maxwell equations arise.

5.2.4 Derivation of the matter-free Maxwell equations

In this section, we derive the Maxwell equation treating induction and the Maxwell equation stating the absence of magnetic monopoles.

Using the vector potential $\vec{A}$ and the potential Φ,

$$A^0 = \Phi \quad \text{and} \quad A^i = \vec{A}_i \quad \text{for} \quad 1 \leq i \leq 3, \tag{5.10}$$

the action $S_m + S_{mf}$ can be varied. Thereby the Langrangian

$$L = -mc^2 \cdot \sqrt{1 - \frac{v^2}{c^2}} + \frac{e}{c}\vec{A} \cdot \vec{v} - e \cdot \Phi \tag{5.11}$$

and the Hamiltonian can be derived (Landau and Lifschitz, 1971, Eq. 16.8):

$$H = \sqrt{m^2c^4 + c^2 \cdot \left(\vec{p} - \frac{e}{c}\vec{A}\right)^2} + e \cdot \Phi \tag{5.12}$$

The above Lagrangian can be applied in order to derive the electric force for the case of a static field

$$\vec{F}_{el} = e \cdot \vec{\mathscr{E}} \tag{5.13}$$

and the Lorentz force (Landau and Lifschitz, 1971, Eq. 17.6)

$$\vec{F}_L = \frac{e}{c} \cdot \vec{v} \times \vec{\mathscr{H}} \tag{5.14}$$

$$\frac{d\vec{p}}{dt} = e \cdot \vec{\mathscr{E}} + \frac{e}{c} \cdot \vec{v} \times \vec{\mathscr{H}} \tag{5.15}$$

Hereby, the curl of the vector potential $\vec{A}$,

$$\vec{\mathscr{H}} = \mathrm{curl}\vec{A}, \tag{5.16}$$

is the magnetic field $\vec{\mathscr{H}}$,

$$\vec{\mathscr{E}} = -\frac{1}{c}\frac{\partial \vec{A}}{\partial t} - \frac{\partial \Phi}{\partial \vec{r}} \tag{5.17}$$

is the electric field, and $\vec{v}$ is the velocity of the particle.

Using the above Eq. for $\vec{\mathscr{E}}$, applying the curl operator and inserting the above term for $\vec{\mathscr{H}}$ yields the Maxwell equation treating induction (Landau and Lifschitz, 1971, Eq. 26.1):

$$\mathrm{curl}\ \vec{\mathscr{E}} = -\frac{1}{c} \cdot \frac{\partial \vec{\mathscr{H}}}{\partial t} \tag{5.18}$$

If we apply the divergence to $\vec{\mathscr{H}}$ and use the definition (Eq. 5.16), then we obtain the Maxwell equation stating the absence of magnetic monopoles (Landau and Lifschitz, 1971, Eq. 26.2):

$$\mathrm{div}\,\vec{\mathscr{H}} = 0 \tag{5.19}$$

5.2.5 Conservation of charge

In order to derive the other two Maxwell equations, we introduce the four-dimensional current vector (Landau and Lifschitz, 1971, Eq. 28.2)

$$j^i = \rho \cdot \frac{dx^i}{dt} \tag{5.20}$$

Hereby, ρ is the charge density.

An essential ingredient is the conservation of charge, in particular, it provides the continuity equation:

$$\frac{\partial}{\partial t}\int \rho dV = 0 \tag{5.21}$$

5.2.6 Action of the field

In this S., we develop the action of the field tensor. Hereby, that tensor is defined as follows (Landau and Lifschitz, 1971, Eq. 26.5):

$$F_{ik} = \frac{\partial A_k}{\partial x^i} - \frac{\partial A_i}{\partial x^k} \tag{5.22}$$

Development of that action: The principle of linear superposition of the fields implies that the DEQ of the fields must be linear, thus the action must be quadratic, and hence the action is a quadratic Lorentz scalar, so it must have the following form (Landau and Lifschitz, 1971, Eq. 27.4, 27.5):

$$S_f = \frac{-1}{16\pi} \int F_{ik} \cdot F^{ik} dt \cdot dx dy dz = \frac{1}{8\pi} \int (\vec{E}^2 - \vec{H}^2) dt \cdot dV \tag{5.23}$$

5.2.7 Derivation of Maxwell equations with matter

Variation of the sum of the actions $S = S_m + S_{mf} + S_f$ (Landau and Lifschitz, 1971, § 30) yields the Maxwell equation treating the sources of the electric field

$$\text{div } \vec{\mathscr{E}} = 4\pi\rho, \tag{5.24}$$

and the Maxwell equation describing the generation of the magnetic field:

$$\text{curl} \vec{\mathscr{H}} = \frac{1}{c} \frac{\partial \vec{\mathscr{E}}}{\partial t} + \frac{4\pi}{c} \cdot \vec{j} \tag{5.25}$$

Altogether, these four Maxwell equations essentially constitute the theory of classical electrodynamics, see e. g. Landau and Lifschitz (1971), Jackson (1975).

5.2.8 Essential ingredients

In this section, we summarize the essential ingredients used in the above derivation of classical electrodynamics.

1. The elementary charge e has been used.
2. The conservation of charge has been applied.
3. The universality of the elementary charge e has been utilized.
4. The linear superposition of fields has been used.
5. The mass of elementary particles has been applied.
6. The principle of least action provides a formalism in order to develop DEQs from underlying symmetries.
7. SRT has been utilized, so that the invariance and universality of c is provided,
8. The action S_m has been developed, so that energy and momentum are conserved, so that isotropy and translation invariance in space and time are provided, see Noether (1918).
9. The action $S_{m,f}$ has been developed, so that the invariance and universality of c and e are provided, and so that SRT and the conventions inherent to the Maxwell equations in Gaussian units are obeyed.
10. The action S_f has been developed, so that the linear superposition of fields and the SRT are provided.

Hereby, the above items (1) to (4) have been derived in this book from the properties of the QST, see chapters (3, 4). Furthermore, the mass underlying elementary particles (item 5) has been derived from QST, see Carmesin (2021a). Moreover, in item (6), the SRT represents a mesoscopic description of space and time, whereby the microscopic description is provided by the QST, see Carmesin (2021d).

The other items represent the method of the derivation of Lagrangians or DEQs from underlying symmetries, whereby the additional symmetries are the isotropy of space and the translation invariance of space and time.

5.2.9 Essential result

The three QST forming a particle can generate an elementary charge. The elementary charge gives rise to a magnetic field, see e. g. Eqs. (5.11, 5.12, 5.16).

Altogether, there is a mechanism for the formation of electric charges on the basis of quantum gravity, whereas there is no such mechanism for the formation of magnetic monopoles on the basis of quantum gravity. So there are no magnetic monopoles formed by QST, instead, magnetism is formed as a consequence of the electric charge formed by QST.

5.3 From QST to QED

The theory of classical electrodynamics has been quantized, and thereby the theory of quantum electrodynamics, **QED** has been developed.

In this section, we summarize properties of that theory, and we compere these with the results of the present theory of the electron.

5.3.1 Propagation

Basically, an elementary particle propagates according to its wave equation (Landau and Lifschitz, 1982, Sect. II, III). More generally, there occur interactions with other particles, including the formation or annihilation of particles. These processes are named scattering.

5.3.2 Feynman diagrams

The scattering is described by Feynman diagrams (Landau and Lifschitz, 1982, Sect. VI, VII). Hereby, the scattering is based on the interaction, whereby the amplitude of that interaction is usually proportional to the coupling constant $e_{cc}^2 = \alpha$, see section (3.11.8). An example is the scattering amplitude M_{fi} from an initial state i to a final state f in the process of the scattering of electrons, whereby M_{fi} is proportional to the coupling constant $e_{cc}^2 = \alpha$ (Landau and Lifschitz, 1982, Eq. 73.11-73.17).

Hereby, e_{cc} is the elementary charge observed at a large distance. We did already derive the bare charge $\tilde{e}_{bare} = \kappa_{emitted,\perp}$, see Eq. (3.114). Accordingly, our theory underlies the theory of QED.

5.3.3 Perturbation theory

If an experiment is described, then an appropriate Feynman diagram can be developed. However, during the process described by the Feynman diagram, additional elementary particles can form and annihilate. Correspondingly, the Feynman diagram becomes more and more complicated. As all these processes might occur, there occurs an infinite sum of diagrams and respective processes.

So the question arises, whether that sum converges. Hereby, each complication corresponds to an additional interaction, providing an additional factor $e_{cc}^2 = \alpha$. thus the sum can only converge, if that coupling constant $e_{cc}^2 = \alpha$ is sufficiently small. In this manner, the QED works on the basis of a sufficiently small coupling constant $e_{cc}^2 = \alpha$. Thus the coupling constant $e_{cc}^2 = \alpha$ derived here is again a basis of the QED.

Technically, it is most transparent to organize the Feynman diagrams in powers of the coupling constant $e_{cc}^2 = \alpha$. In this manner, the QED additionally provides a perturbation theory (Landau and Lifschitz, 1982, Sect. VIII).

5.3.4 From quantum gravity to QED

In this section, we compare QED with quantum gravity.

1. QED can be derived from quantum gravity, as the elementary charge can be derived and explained by quantum gravity.

2. QED uses a mesoscopic or macroscopic concept of spacetime. Both can be derived and explained by quantum gravity.

3. QED uses charge and mass as a basis. The mass can be derived and explained by quantum gravity, see Carmesin (2021a).

4. While quantum gravity ranges from the Planck length L_P towards the light horizon R_{lh}, the concept of the Planck scale cannot be derived within QED, as gravity and the gravitational constant are essential in order to derive and explain the Planck scale.

Altogether, QED is a mesoscopic theory that can be derived from quantum gravity as follows: Firstly, we derive the elementary charge and the electromagnetic interaction from quantum gravity. Thereby, the electromagnetic interaction represents a mesoscopic theory.

Secondly, we quantize that mesoscopic electromagnetic interaction in order to derive quantum electrodynamics, at a mesoscopic level.

Chapter 6

Corrections

In the vicinity of a particle emitting an electromagnetic field, the energy of that field is high. As a consequence, particles can form and annihilate after a short time, in general, particles can form (Landau and Lifschitz, 1982, § 1). Such effects can be considered in terms of corrections, see e. g. (Landau and Lifschitz, 1982, § 118), (Greiner and Reinhardt, 1995, p. 370), (Wygas, 2013, p. 17-20). Moreover, several forced oscillations may emit quanta simultaneously. This effect can be treated in terms of a correction as well. Of course, we could have treated this effect already above. However, we preferred the separation of effects in order to achieve additional transparency concerning the various contributions to the elementary charge.

In this chapter, we derive the above described corrections that are essential for the formation of electric charge and electromagnetic interaction from the quanta of spacetime, QST.

6.1 Simultaneously emitted QST

In general, all emitted QST can occur simultaneously inside the triple of QST. In order to analyze that case, we apply Eq. (3.56):

$$\hat{G}^*_{\alpha,j\to i} = \frac{G^*_{m_c}}{|\bar{n}_i^2 - \bar{n}_j^2|} \tag{6.1}$$

Field of all QST: In the triple of QST, the field $G^*_{m_c}$ of m_c is superimposed by the emitted field $G^*_{emitted,\perp}$. Thereby, both fields $G^*_{m_c}$ and $G^*_{emitted,\perp}$ are emitted in an isotropic manner. Thus the fields are added directly:

$$\hat{G}^*_{sum} = G^*_{m_c} + G^*_{emitted,\perp} \tag{6.2}$$

Emission of a single QST: We remind the field of an emitted QST that is emitted in the absence of other emitted QST:

$$\hat{G}^*_{\alpha,j\to i,single} = G^*_{m_c} \cdot \frac{1}{|\bar{n}_i^2 - \bar{n}_j^2|} \tag{6.3}$$

Correspondingly, we obtain, see table (8.4):

$$\kappa_{\alpha,j\to i,single} = \frac{\hat{G}^*_{\alpha,j\to i,single}}{G^*_{m_c}} = \frac{1}{|\bar{n}_i^2 - \bar{n}_j^2|} \tag{6.4}$$

Energy density of single emitted QST: In the process of emission of quanta, the energy density and the probability densities are the essential quantities. Accordingly, we derive the energy density u of the emitted QST. For it we square the above equation, and we divide by $8\pi \cdot G$:

$$\hat{u}_{\alpha,j\to i,single} = \frac{\hat{G}^{*2}_{\alpha,j\to i,single}}{8\pi \cdot G} = \frac{G^{*2}_{m_c}}{8\pi \cdot G} \cdot \frac{1}{|\bar{n}_i^2 - \bar{n}_j^2|^2} \tag{6.5}$$

Energy density of emitted QST: In general, several QST are emitted simultaneously. As a consequence, the field $\hat{G}^*_{m_c}$ is replaced by the sum of fields $\hat{G}^*_{sum}$, in the above equation. So the right hand side of the above equation is replaced by the following term:

$$\frac{G^{*2}_{sum}}{8\pi \cdot G} \cdot \frac{1}{|\bar{n}_i^2 - \bar{n}_j^2|^2} \tag{6.6}$$

However, an emitted QST does not emit itself. Accordingly, the energy density of an emitted QST is subtracted from the above

energy density $\frac{G^{*2}_{sum}}{8\pi \cdot G}$:

$$\hat{u}_{\alpha,j\to i} = \frac{\hat{G}^{*2}_{\alpha,j\to i}}{8\pi \cdot G} = \frac{G^{*2}_{sum} - \hat{G}^{*2}_{\alpha,j\to i,single}}{8\pi \cdot G} \cdot \frac{1}{|\bar{n}_i^2 - \bar{n}_j^2|^2} \tag{6.7}$$

In order to simplify, we multiply the above equation by $8\pi \cdot G$, and we apply the root:

$$\hat{G}^{*}_{\alpha,j\to i} = \sqrt{G^{*2}_{sum} - \hat{G}^{*2}_{\alpha,j\to i,single}} \cdot \frac{1}{|\bar{n}_i^2 - \bar{n}_j^2|} \tag{6.8}$$

We insert Eq. (6.2):

$$\hat{G}^{*}_{\alpha,j\to i} = \sqrt{(G^{*}_{m_c} + G^{*}_{emitted,\perp})^2 - \hat{G}^{*2}_{\alpha,j\to i,single}} \cdot \frac{1}{|\bar{n}_i^2 - \bar{n}_j^2|} \tag{6.9}$$

In order to simplify that expression, we factorize $G^{*}_{m_c}$:

$$\boxed{\hat{G}^{*}_{\alpha,j\to i} = G^{*}_{m_c} \cdot \frac{\kappa_{sim.}}{|\bar{n}_i^2 - \bar{n}_j^2|}} \tag{6.10}$$

with simultaneously emitted QST

Hereby, $\kappa_{sim.}$ abbreviates the following root, whereby the subscript $sim.$ represents *simultaneously*:

$$\kappa_{sim.} = \sqrt{(1 + \kappa_{emitted,\perp})^2 - \kappa^2_{\alpha,j\to i,single}} \tag{6.11}$$

6.2 Process of emission with $\kappa_{sim.}$

The process of emission is similar to that analyzed in section (3.9). Accordingly, the field $G^{*}_{m_c}$ is reduced as a consequence of the emission as follows.

When a transverse QST with a field $\hat{G}^{*}_{\alpha,j\to i}$ is emitted, and when a fraction $q \in [0; 1]$ of that QST has already been emitted, then the field $G^{*}_{m_c}$ is reduced by $\hat{G}^{*}_{\alpha,j\to i} \cdot q$. So the following field remains:

$$G^{*}_{m_c,rest} = G^{*}_{m_c} - \hat{G}^{*}_{\alpha,j\to i} \cdot q \tag{6.12}$$

In this case, the remaining field causes the emitted field. Accordingly, Eq. (3.56) is generalized as follows:

$$\hat{G}^*_{\alpha,j\to i} = \frac{G^*_{m_c,rest}}{|\bar{n}_i^2 - \bar{n}_j^2|} \tag{6.13}$$

Next, we apply the principle of equal amplitudes to Eq. (6.12):

$$G^*_{m_c,rest} = G^*_{m_c} - \hat{G}^*_{\alpha,j\to i} \cdot q \tag{6.14}$$

Here, we apply Eq. (6.10), whereby we use the fact that $G^*_{m_c}$ is reduced to $G^*_{m_c,rest}$ everywhere in the triple. Hereby, simultaneously emitted QST are described by Eq. (6.10):

$$G^*_{m_c,rest} = G^*_{m_c} - G^*_{m_c,rest} \cdot \frac{\kappa_{sim.}}{|\bar{n}_i^2 - \bar{n}_j^2|} \cdot q \tag{6.15}$$

We solve that equation:

$$G^*_{m_c,rest} = G^*_{m_c} \cdot \frac{1}{1 + \frac{\kappa_{sim.}}{|\bar{n}_i^2 - \bar{n}_j^2|} \cdot q} \tag{6.16}$$

Next we derive the averaged value by integrating over all values $q \in [0, 1]$:

$$\langle G^*_{m_{rest}} \rangle = \int_0^1 G^*_{m_c} \cdot \frac{1}{1 + \frac{\kappa_{sim.}}{|\bar{n}_i^2 - \bar{n}_j^2|} \cdot q} dq \tag{6.17}$$

We evaluate that integral:

$$\langle G^*_{m_{rest}} \rangle = G^*_{m_c} \cdot \frac{|\bar{n}_i^2 - \bar{n}_j^2|}{\kappa_{sim.}} \cdot \ln\left(1 + \frac{\kappa_{sim.}}{|\bar{n}_i^2 - \bar{n}_j^2|}\right) \tag{6.18}$$

Next, we apply the average to Eq. (6.19):

$$\langle \hat{G}^*_{\alpha,j\to i} \rangle = \frac{\langle G^*_{m_c,rest} \rangle}{|\bar{n}_i^2 - \bar{n}_j^2|} \tag{6.19}$$

In the above equation, we insert Eq. (6.18):

$$\boxed{\langle \hat{G}^*_{\alpha,j\to i} \rangle = G^*_{m_c} \cdot \frac{1}{\kappa_{sim.}} \cdot \ln\left(1 + \frac{\kappa_{sim.}}{|\bar{n}_i^2 - \bar{n}_j^2|}\right) = \hat{G}^*_{\alpha,j\to i}} \tag{6.20}$$

Hereby, the average $\langle \hat{G}^*_{\alpha,j\to i} \rangle$ is also denoted by $\hat{G}^*_{\alpha,j\to i}$, for short.

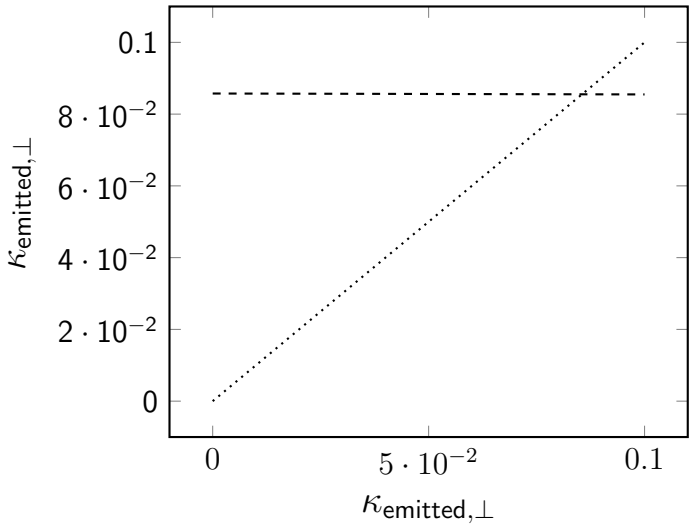

Figure 6.1: Graphic solution of fixed point equation: The scaled field $\kappa_{emitted,\perp}$ as a function of the $\kappa_{emitted,\perp}$, see Eq. (3.83, dashed). The point of intersection of function in Eq. (3.83, dashed) and the identical function (dotted) represents the fixed point or the solution.

6.2.1 Iteration for $\kappa_{emitted,\perp}$

In this section, we determine $\kappa_{emitted,\perp}$ by a fixed point iteration. In particular, we analyze the scaled emitted field $\kappa_{emitted,\perp}$ as shown in PROP (7),

$$\kappa_{emitted,\perp} = \frac{G^*_{emitted,\perp}}{G^*_{m_c}}(\kappa_{emitted,\perp}) \tag{6.21}$$

with

$$G^*_{emitted,\perp} = \sqrt{\hat{G}^{*2}_{\alpha,1\to2} + \hat{G}^{*2}_{\alpha,1\to3} + \hat{G}^{*2}_{\alpha,2\to1} + \hat{G}^{*2}_{\alpha,2\to3} - \hat{G}^{*2}_{\alpha,3\to1} - \hat{G}^{*2}_{\alpha,3\to2}} \tag{6.22}$$

as a function of $\kappa_{emitted,\perp}$. Hereby, the fields $\hat{G}^*_{\alpha,j\to i}$ are provided by Eqs. (6.20, 6.11, 6.4). In a graphic solution, the fixed point is the intersection of that function with the identical function, see Fig. (6.1). In the following, we derive the fixed point numerically.

For it, we introduce the following abbreviation:

$$\kappa_{1+\perp} = 1 + \kappa_{emitted,\perp} \tag{6.23}$$

Zeroth step: At the zeroth step, $\kappa_{1+\perp}$ takes the following initial value:

$$\kappa^{(0)}_{1+\perp} = 1 \tag{6.24}$$

Accordingly, the field takes the following value at the zeroth iteration step:

$$\frac{G^{*(0)}_{emitted,\perp}}{G^{*}_{m_c}} = \kappa^{(0)}_{emitted,\perp} = 0.085\,741\,142\,500 \tag{6.25}$$

First step: At the first iteration step, $\kappa_{\perp} = 1 + \kappa_{emitted,\perp}$ takes the following value:

$$\kappa^{(1)}_{1+\perp} = 1 + \kappa^{(0)}_{emitted,\perp} \tag{6.26}$$

Consequently, the field takes the following value at the first iteration step:

$$\frac{G^{*(1)}_{emitted,\perp}}{G^{*}_{m_c}} = \kappa^{(1)}_{emitted,\perp} = 0.085\,523\,059\,166 \tag{6.27}$$

Second step: At the 2^{nd} step, $1 + \kappa_{emitted,\perp}$ takes the following value:

$$\kappa^{(2)}_{1+\perp} = 1 + \kappa^{(1)}_{emitted,\perp} \tag{6.28}$$

Thus, the field takes the following value at the 2^{nd} step:

$$\kappa^{(2)}_{emitted,\perp} = 0.085\,523\,611\,918 \tag{6.29}$$

Third step: At the 3^{rd} step, $1 + \kappa_{emitted,\perp}$ is as follows:

$$\kappa^{(3)}_{1+\perp} = 1 + \kappa^{(2)}_{emitted,\perp} \tag{6.30}$$

Thus, the field takes the following value at the 3^{rd} step:

$$\kappa^{(3)}_{emitted,\perp} = 0.085\,523\,610\,517 \tag{6.31}$$

Fourth step: At the 4^{th} step, $1 + \kappa_{emitted,\perp}$ is as follows:

$$\kappa_{1+\perp}^{(4)} = 1 + \kappa_{emitted,\perp}^{(3)} \tag{6.32}$$

So, the field takes the following value:

$$\kappa_{emitted,\perp}^{(4)} = 0.085\,523\,610\,521 \tag{6.33}$$

Fifth step: At the 5^{th} step, $1 + \kappa_{emitted,\perp}$ is as follows:

$$\kappa_{1+\perp}^{(5)} = 1 + \kappa_{emitted,\perp}^{(4)} \tag{6.34}$$

So, the field takes the following value:

$$\kappa_{emitted,\perp}^{(5)} = 0.085\,523\,610\,521 \tag{6.35}$$

Fixed point: At the level of precision of 11 digits, the fixed point is achieved at the fourth iteration step:

$$\kappa_{emitted,\perp}^{fixed\ point} = 0.085\,523\,610\,521 \tag{6.36}$$

6.2.2 Bare elementary charge

In the SI system of units, the ratio $\kappa_{emitted,\perp}$ represents the bare elementary electric charge (Eq. 3.112):

$$e_{bare,sim.}^{fixed\ point} = \kappa_{emitted,\perp}^{fixed\ point} \cdot \sqrt{\frac{\hbar \cdot c}{G_C}} \tag{6.37}$$

The calculation yields:

$$e_{bare,sim.}^{fixed\ point} = 1.604\,034\,688\,868 \cdot 10^{-19}\,\mathrm{C} \tag{6.38}$$

The observed value of the screened elementary charge is shown next (Tanabashi et al., 2018, Table 1.1):

$$e_{obs} = 1.602\,176\,6208(98) \cdot 10^{-19}\,\mathrm{C} \tag{6.39}$$

The relative difference is as follows:

$$\Delta_{screening}^{fixed\ point} = \frac{e_{bare,sim.}^{fixed\ point} - e_{obs}}{e_{obs}} = 0.116\% \tag{6.40}$$

Theorem 3 Elementary charge: emission of QST

In a triple of QST with $n_j \in \{1, 2, 3\}$, there occur forced oscillations. These forced oscillations emit QST with a scaled field $\kappa_{emitted,sim.\perp}$ with the properties shown below. Hereby the subscript sim. indicates that the simultaneous emission of QST has been analyzed.

(1) The emitted QST mediate an interaction with the following fine-structure constant:

$$\alpha_{theo,sim.} = \kappa^2_{emitted,sim.\perp} = 7.314\,287\,957 \cdot 10^{-3} \tag{6.41}$$

The relative difference between the theoretical value and the observed value of the fine-structure constant

$$\alpha_{obs} = 7.297\,352\,5664(17) \cdot 10^{-3} \tag{6.42}$$

is as shown next:

$$\Delta_\alpha = \frac{\alpha_{theo,sim.} - \alpha_{obs}}{\alpha_{obs}} = 0.23\% \quad \text{without corrections} \tag{6.43}$$

(2) The QST emitted by the triple of QST mediate an interaction with the observed fine-structure constant. Correspondingly, the QST emitted by the triple of QST provide the electric field and mediate the electric interaction.

(3) The triple of QST represents the following bare elementary charge:

$$e^{fixed\ point}_{bare,sim.} = \kappa^{fixed\ point}_{emitted,\perp} \cdot \sqrt{\frac{\hbar \cdot c}{G_C}} \tag{6.44}$$

The evaluation provides the result:

$$e^{fixed\ point}_{bare,sim.} = 1.604\,034\,688\,868 \cdot 10^{-19}\,\mathrm{C} \tag{6.45}$$

The observed value of the screened elementary charge is shown next (Tanabashi et al., 2018, Table 1.1):

$$e_{obs} = 1.602\,176\,6208(98) \cdot 10^{-19}\,\mathrm{C} \tag{6.46}$$

The relative difference between the bare elementary charge and the screened elementary charge is as follows:

$$\Delta_{screening}^{fixed\ point} = \frac{e_{bare,sim.}^{fixed\ point} - e_{obs}}{e_{obs}} = 0.116\% \tag{6.47}$$

(4) The corresponding emitted scaled field is as follows:

$$\kappa_{emitted,\perp}^{fixed\ point} = 0.085\,523\,610\,521 \tag{6.48}$$

6.3 Quantum electrodynamics

Based on the above derivation of the bare elementary charge $e_{bare,sim.}^{fixed\ point}$, the theory of **quantum electrodynamics, QED**, see e. g. Schwinger (1948), Bialynicki-Birula and Bialynicki-Birula (1975), Feynman (1985), Wygas (2013), section (5.3), can be applied as a tool. Using that tool, phenomena such as screening can be analyzed. Thereby, the theoretical value e_{theo} of the observed electric charge can be derived from $e_{bare,sim.}^{fixed\ point}$ as follows:

6.3.1 Magnetic moment μ

Using the QED, the magnetic moment of the electron has been derived, see e. g. (Landau and Lifschitz, 1982, § 118), (Greiner and Reinhardt, 1995, p. 370), (Wygas, 2013, p. 17-20):

$$\mu = \frac{e \cdot \hbar}{2m_e \cdot c} \cdot \Sigma_{j=0}^{j=5}\ C_j \cdot \left(\frac{\alpha}{\pi}\right)^j \tag{6.49}$$

Hereby, the coefficients C_j are as follows (Wygas, 2013, p. 17-20):

$$\begin{pmatrix} C_0 \\ C_1 \\ C_2 \\ C_3 \\ C_4 \\ C_5 \end{pmatrix} = \begin{pmatrix} 1 \\ 0.5 \\ -0.328\,478\,965\,579\,193 \\ 1.181\,241\,456 \\ 1.9106(20) \\ 9.16(58) \end{pmatrix} \tag{6.50}$$

6.3.2 Derivation of e_{theo}

In this section, we apply the magnetic moment (Eq. 6.49) to the derivation of the value of the electric charge that is observed at a large distance, $e_{distant}$. That value includes the effect of screening.

In particular, Eq. (6.49) describes the magnetic moment that can be observed at a large distance:

$$\mu_{distant} = \frac{e_{distant} \cdot \hbar}{2m_e \cdot c} \cdot \Sigma_{j=0}^{j=5} \; C_j \cdot \left(\frac{\alpha}{\pi}\right)^j \tag{6.51}$$

Hereby, the additional summands to 1 in the above Eq. represent the corrections of the QED, such as screening. Correspondingly, the bare magnetic moment is as follows:

$$\mu_{bare} = \frac{e_{bare,sim.} \cdot \hbar}{2m_e \cdot c} \cdot (1 + 0) \tag{6.52}$$

Local property: The magnetic moment μ of the electron describes the mechanism of the formation of the magnetic field at the location of the electron. This magnetic field is not screened, as there are no magnetic monopoles, see chapter (5).

So the magnetic moment μ is the same for a local observer and for a distant observer:

$$\mu_{distant} = \mu_{bare} \tag{6.53}$$

We insert Eqs. (6.51, 6.51):

$$\frac{e_{distant} \cdot \hbar}{2m_e \cdot c} \cdot \Sigma_{j=0}^{j=5} \; C_j \cdot \left(\frac{\alpha}{\pi}\right)^j = \frac{e_{bare,sim.} \cdot \hbar}{2m_e \cdot c} \tag{6.54}$$

We solve for $e_{distant}$:

$$e_{distant} = \frac{e_{bare,sim.}^{fixed\ point}}{\Sigma_{j=0}^{j=5} \; C_j \cdot \left(\frac{\alpha}{\pi}\right)^j} \tag{6.55}$$

Hereby, the fine-structure constant α is determined from the charge as follows:

$$\alpha = e^2 \cdot \frac{G_C}{\hbar \cdot c} = e_{distant}^2 \cdot \frac{G_C}{\hbar \cdot c} \tag{6.56}$$

We identify that α is a function of $e_{distant}$ and vice versa. Accordingly, we derive the value of α by a fixed point iteration.

Proposition 8 Elementary charge at large distance

(1) The bare elementary charge $e_{bare,sim.}^{fixed\ point}$ *is effectively reduced by screening. So an observer at a large distance from an elementary charge observes the following elementary charge:*

$$e_{distant} = \frac{e_{bare,sim.}^{fixed\ point}}{\Sigma_{j=0}^{j=5}\ C_j \cdot \left(\frac{\alpha}{\pi}\right)^j} \tag{6.57}$$

(2) As the bare elementary charge $e_{bare,sim.}^{fixed\ point}$ *is equal to*

$$e_{bare,sim.}^{fixed\ point} = \sqrt{\frac{\hbar \cdot c}{G_C}} \cdot \kappa_{emitted,\perp}^{fixed\ point}, \tag{6.58}$$

we can introduce the distant value $\kappa_{emitted,\perp,distant}$ *of the scaled emitted field,*

$$\kappa_{emitted,\perp,distant} = \frac{e_{distant}}{\sqrt{\frac{\hbar \cdot c}{G_C}}}, \tag{6.59}$$

divide Eq. (6.57) by $\sqrt{\frac{\hbar \cdot c}{G_C}}$ *and derive*

$$\kappa_{emitted,\perp,distant} = \frac{\kappa_{emitted,\perp}^{fixed\ point}}{\Sigma_{j=0}^{j=5}\ C_j \cdot \left(\frac{\alpha}{\pi}\right)^j} \tag{6.60}$$

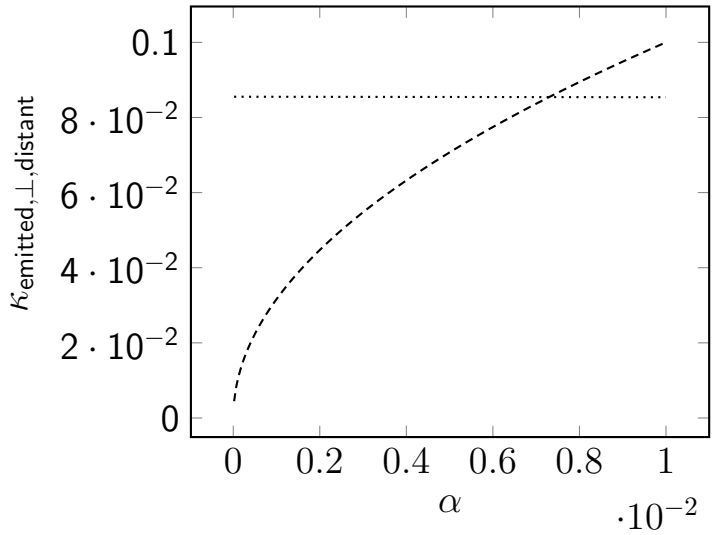

Figure 6.2: Graphic solution: The scaled field $\kappa_{emitted,\perp,distant}$ as a function of the fine-structure constant α. The point of intersection of two functions Eqs. (6.60, dotted) and (6.61, dashed) represents the theoretical value.

6.3.3 Iteration for $\kappa_{emitted,\perp,distant}$

In this section, we determine $\kappa_{emitted,\perp,distant}$ by a fixed point iteration. In particular, we solve two functions of α simultaneously, Eq. (6.60) as well as:

$$\kappa_{emitted,\perp,distant} = \sqrt{\alpha} \tag{6.61}$$

A graphic solution is shown in Fig. (6.2), while a numerical solution is presented below.

Zeroth step: At the zeroth step, $\kappa_{emitted,\perp,distant}$ takes the value obtained without using the sum in Eq. (6.60). It is the result described in THM (3):

$$\kappa^{(0)}_{emitted,\perp,distant} = \kappa^{fixed\ point}_{emitted,\perp} = 0.085\,523\,610\,521 \tag{6.62}$$

Accordingly, the fine-structure constant α is the square of the emitted field $\kappa^{(0)}_{emitted,\perp,distant}$ at the zeroth iteration step:

$$\alpha^{(0)} = 7.314\,287\,956\,548 \cdot 10^{-3} \tag{6.63}$$

First step: Using $\alpha^{(0)}$, we determine $\kappa^{(1)}_{emitted,\perp,distant}$ as follows:

$$\kappa^{(1)}_{emitted,\perp,distant} = \frac{\kappa^{(0)}_{emitted,\perp,distant}}{\Sigma^{j=5}_{j=0}\ C_j \cdot \left(\frac{\alpha^{(0)}}{\pi}\right)^j} = 0.085\,424\,318\,461 \quad (6.64)$$

Consequently, α takes the following value at the first step:

$$\alpha^{(1)} = 7.297\,314\,184\,492 \cdot 10^{-3} \quad (6.65)$$

Second step: At the 2^{nd} step, we evaluate:

$$\kappa^{(2)}_{emitted,\perp,distant} = \frac{\kappa^{(0)}_{emitted,\perp,distant}}{\Sigma^{j=5}_{j=0}\ C_j \cdot \left(\frac{\alpha^{(1)}}{\pi}\right)^j} = 0.085\,424\,548\,268 \quad (6.66)$$

So α takes the following value at the 2^{nd} step:

$$\alpha^{(2)} = 7.297\,353\,446\,864 \cdot 10^{-3} \quad (6.67)$$

Third step: At the 3^{rd} step, $\kappa_{emitted,\perp,distant}$ is as follows:

$$\kappa^{(3)}_{emitted,\perp,distant} = \frac{\kappa^{(0)}_{emitted,\perp,distant}}{\Sigma^{j=5}_{j=0}\ C_j \cdot \left(\frac{\alpha^{(2)}}{\pi}\right)^j} = 0.085\,424\,547\,737 \quad (6.68)$$

Thus, α takes the following value at the 3^{rd} step:

$$\alpha^{(3)} = 7.297\,353\,356\,045 \cdot 10^{-3} \quad (6.69)$$

Fourth step: At the 4^{th} step, we obtain:

$$\kappa^{(4)}_{emitted,\perp,distant} = \frac{\kappa^{(0)}_{emitted,\perp,distant}}{\Sigma^{j=5}_{j=0}\ C_j \cdot \left(\frac{\alpha^{(3)}}{\pi}\right)^j} = 0.085\,424\,547\,738 \quad (6.70)$$

So, α takes the following value:

$$\alpha^{(4)} = 7.297\,353\,356\,255 \cdot 10^{-3} \quad (6.71)$$

Fifth step: At the 5^{th} step, we evaluate:

$$\kappa^{(5)}_{emitted,\perp,distant} = \frac{\kappa^{(0)}_{emitted,\perp,distant}}{\Sigma_{j=0}^{j=5}\ C_j \cdot \left(\frac{\alpha^{(4)}}{\pi}\right)^j} = 0.085\,424\,547\,738 \quad (6.72)$$

So, α takes the following value:

$$\alpha^{(5)} = 7.297\,353\,357\,255 \cdot 10^{-3} \quad (6.73)$$

Fixed point: At step five, we obtain the same results as in step four, at the chosen level of accuracy of 11 digits. At this fixed point, we obtain the following results:

$$\boxed{\kappa^{(5)}_{emitted,\perp,distant} = \kappa^{fixed\ point}_{emitted,\perp,distant} = 0.085\,424\,547\,738} \quad (6.74)$$

The corresponding charge is as follows:

$$\boxed{e^{fixed\ point}_{distant} = 1.602\,176\,720\,829 \cdot 10^{-19}\ \mathrm{C} = e_{theo}} \quad (6.75)$$

6.4 Comparison with observed charges

In this section, we compare the derived elementary charge with observations of that charge. Hereby, we emphasize that our present theory is able to analyze the **elementary charge** in a separated manner, whereas classical electrodynamics and quantum electrodynamics inherently describe charge and mass in combination. Accordingly, charges of particular particles are considered. Usually, the **electron e^- and positron e^+ are especially representative for** e, the elementary charge.

6.4.1 Deviation of electron and positron charge

The relative difference of the charges of the electron and the positron is as follows (Tanabashi et al., 2018, p. 36):

$$\Delta_{e^+,e^-,rel.} = \frac{q_{e^+} + q_{e^-}}{e_{obs}} < 4 \cdot 10^{-8} \quad (6.76)$$

So the representative particles e^- and e^+ may exhibit the above relative charge deviation of $4 \cdot 10^{-8}$.

6.4.2 Deviation of charge conjugation

The relative deviation from charge conjugation invariance represents possible deviations of observed charges that should take the value of the elementary charge and the observed charges. These relative and possibly statistical deviations range from $3.1 \cdot 10^{-8}$ to $2.4 \cdot 10^{-3}$ (Tanabashi et al., 2018, p. 114-115):

$$\Delta_{q^+,q^-,rel.} \in [3.1 \cdot 10^{-8}, 2.4 \cdot 10^{-3}] \tag{6.77}$$

6.4.3 Deviation of observation of electron mass

The relative error of measurement or observation of the mass of the electron may be essential for a comparison of the elementary charge with the charge of the electron. This is the case, as there are possible deviations between charges of elementary particles that are assumed to be equal in the SMEP.

The relevance of the mass is increased, as the measurements of the charge of a particle include screening, and this is conceptually described in the framework of the theory of QED. In that theory, results are obtained by using the mass and the charge in common expressions. So the difference between bare charge and observed charge includes a relative error of the order of magnitude of the mass of the electron. That error is evaluated next: The observed value of the mass of the electron is shown next (Tanabashi et al., 2018, Table 1.1):

$$m_{e,obs} = 0.510\,998\,9461(31)\,\frac{\mathrm{MeV}}{\mathrm{c}^2} \tag{6.78}$$

The relative error of measurement or observation of that mass is as follows:

$$\Delta_{obs.\ m_e,rel.} = \frac{3.1 \cdot 10^{-8}\ \frac{\mathrm{MeV}}{\mathrm{c}^2}}{m_{e,obs}} = 6.1 \cdot 10^{-8} \tag{6.79}$$

6.4.4 Deviation of observation of electron charge

The observed value of the screened elementary charge is shown next (Tanabashi et al., 2018, Table 1.1):

$$q_{e^-} = 1.602\,176\,6208(98) \cdot 10^{-19}\,\mathrm{C} \tag{6.80}$$

The relative difference is as follows:

$$\boxed{\Delta_{rel.,e_{theo},q_{e^-}} = \frac{e_{theo} - q_{e^-}}{q_{e^-}} = 5.4 \cdot 10^{-8}} \tag{6.81}$$

6.4.5 Interpretation

A possible comparison of the theoretical elementary charge e_{theo} and the charge of the electron should include both errors of measurement, $\Delta_{obs.\ m_e,rel.}$ and $\Delta_{q^+,q^-,rel.}$. These add up as follows:

$$\Delta_{obs.\ sum,rel.} = \Delta_{obs.\ m_e,rel.} + \Delta_{q^+,q^-,rel.} = 6.71 \cdot 10^{-8} \tag{6.82}$$

That sum of the relative errors of measurement or observation is larger than the relative difference between theory and observation:

$$\Delta_{rel.\ obs.\ e+m_e} = 6.71 \cdot 10^{-8} > 5.4 \cdot 10^{-8} = \Delta_{rel.,theo,obs\ e} \tag{6.83}$$

In this sense, the difference between theory and experiment is smaller than the error of measurement. This view is additionally supported by the other deviations summarized above. So the theory is in precise accordance with observation.

Theorem 4 Elementary charge formed by QST

In a triple of QST with $n_j \in \{1, 2, 3\}$, there occur forced oscillations. These forced oscillations emit QST with a scaled field $\kappa_{emitted,\perp,distant}$ with the properties shown below. Hereby the subscript distant indicates that the value observed by a distant observer has been evaluated.

(1) The emitted QST mediate an interaction with the following fine-structure constant:

$$\alpha_{theo,distant} = \kappa^2_{emitted,distant\perp} = 7.297\,353\,356\,255 \cdot 10^{-3} \quad (6.84)$$

(2) The QST emitted by the triple of QST mediate an interaction with the observed fine-structure constant. Correspondingly, the QST emitted by the triple of QST provide the electric field and mediate the electric interaction.

(3) The considered triple of QST represents the following elementary charge:

$$e^{fixed\ point}_{distant} = 1.602\,176\,720\,829 \cdot 10^{-19}\,\mathrm{C} = e_{theo} \quad (6.85)$$

(4) The considered triple of QST represents the following scaled emitted field:

$$\kappa^{fixed\ point}_{emitted,\perp,distant} = 0.085\,424\,547\,738 \quad (6.86)$$

(5) For the prototypical case of the electron, the observed value of the screened elementary charge is shown next (Tanabashi et al., 2018, Table 1.1):

$$e_{obs} = 1.602\,176\,6208(98) \cdot 10^{-19}\,\mathrm{C} \quad (6.87)$$

The relative difference between the theoretical elementary charge and the observed elementary charge of the electron is as follows:

$$\Delta_{rel.,theo,obs\ e} = 5.4 \cdot 10^{-8} \quad (6.88)$$

(6) In order to compare our theoretical value of the elementary charge with the relative error of measurement of the electric charge of the electron, we add the relative errors of measurement of the charge and of the mass, as both influence the observed value:

$$\Delta_{rel.\ obs.\ e+m_e} = 6.71 \cdot 10^{-8} \quad (6.89)$$

(7) The relative difference between our theoretical value of the elementary charge and the observed value of the electric charge of the electron (Eq. 6.88) is smaller than the respective error of measurement (Eq. 6.89). In this sense our theoretical value of the elementary charge is in precise accordance with observation.

Chapter 7

Discussion

In this chapter, we systematically discuss our theory and results. For it we apply the **five categories of explanatory power** (Ylikoski and Kourikoski, 2010, S. 4.1 - 4.5).

(1) Non-sensitivity: The theory should not be very sensitive to changes in the background condition, (Ylikoski and Kourikoski, 2010, section 4.1). We achieve this by our application of the new theory of quantum gravity that we tested in the field of cosmology, whereby we apply that theory to the field of elementary particles. In other words, the present theory is robust.

(2) Precision: Our results are in precise accordance with observation, as the difference to observation is smaller than the error of observation, see THM (4). Moreover, our theory explains the H_0 tension in a precise manner (Fig 2.14), derives the cosmological parameters (Tab. 7.1) as well as the masses of neutrinos and the mass of the Higgs boson (Tab. 7.2), all in precise accordance with observation.

These results include a precise description of the dark energy and the vacuum: Firstly, the cosmological parameters include Ω_Λ, which describes the dark energy. Secondly, the dark energy is a mixture of corresponding QST, so it is a polychromatic vacuum, whereby the time evolution of the mixture cor-

responds to the time evolution of H_0, in precise accordance with observation, see Carmesin (2021c). Thirdly, the dark energy establishes the vacuum, which is precisely described in Carmesin (2021a). Fourthly, the excitation states of that vacuum include the masses of elementary particles, in precise accordance with observation, see Carmesin (2021a), whereby the internal dynamics of these elementary particles explains the elementary charge, the basis of the electromagnetic interaction.

(3) Factual accuracy: The theory at a given level of abstraction should exhibit a relatively small number of idealizations or falsehoods, (Ylikoski and Kourikoski, 2010, section 4.3). In our theory we overcome several common idealizations:

(3a) Instead of presuming three dimensional space, we derive the present-day stability of three dimensional space. Furthermore, we derive gravitational instabilities that caused higher dimensional space in the very early universe, see e. g. Carmesin (2021d) or Fig. 2.12).

(3b) Instead of presuming that the increase of the universe is based on an increase of volume only, we derive the dimensional phase transitions and their contribution to the increase of space, Carmesin (2021d) or Fig. 2.12).

(3c) Instead of presuming that general relativity, GR, could be a local theory, we derived the nonlocality of GR and the solution of the EPR paradox as a consequence, see e. g. (Carmesin, 2021d, THM. 5 and COR. 2).

(3d) Instead of presuming that the electromagnetic interaction could be a fundamental theory, we derive the electromagnetic interaction from quantum gravity.

(3e) Instead of presuming that the elementary charge could be a constant of nature that can only by obtained by measurement, we derive the elementary charge from quantum gravity.

(4) Integration: Our new theory of quantum gravity ranges from the Big Bang until today and beyond, it ranges from the Planck scale towards the light horizon, the horizon of objects that have causal influence upon us. That huge range is not set arbitrarily, instead it has been achieved by analyzing and integrating various fields of physics:

(4a) We integrate GR and quantum physics.

(4b) We integrate or unify the local dynamics described by the Schwarzschild metric and the global dynamics of space, see e. g. (Carmesin, 2021d, CHAP. 1).

(4c) Using these concepts,

we analyzed the stability of space as a function of density,

we discovered a series of gravitational instabilities,

we discovered a corresponding series of phase transitions that occurred in the early universe,

thereby, we discovered the structure of the vacuum,

hereby, we discovered the vacuum's possible excitation modes.

(4d) Based on these discoveries, we basically integrate or unify various fields of physics:

We integrate the standard model of cosmology, SMC, and the standard model of elementary particles, SMEP. In particular, we integrate the electromagnetic interaction and gravity.

(4e) We solve a variety of basic problems of physics, see S. (7.3).

(4f) We derive several predictions, see section (7.3).

(5) Cognitive salience: It should be relatively easy to understand a theory, and in particular a theory should apply concepts that are already known, see (Ylikoski and Kourikoski, 2010, section 4.5). Accordingly, the cognitive salience of our theory is especially large for the following reasons:

(5a) Our theory essentially applies the well known concepts of GR, quantum physics, elementary particles, phase transitions and the geometry of space.

(5b) Moreover, our theory reveals how to unify these concepts, and so our theory makes aware connections among these concepts. Thus, the understanding of these concepts becomes easier, without using any simplification and with providing novel results.

7.1 Comparison with observation

In this S., we present theoretical values x_{theo}, corresponding observed values x_{obs} and respective relative errors, see table (7.1):

$$\Delta_{theo-obs}x = \frac{x_{theo} - x_{obs}}{x_{obs}} \cdot 100\% \tag{7.1}$$

Hereby, we analyze absolute values only.

7.1.1 Condition of derivation

Thereby we derived all theoretical values by using quantum gravity, the corresponding universal constants G, c, k_B and h, see Tanabashi et al. (2018), as well as the Hubble parameter H_0 at $z = 1090$ as a reference for the present-day time after the Big Bang, see Planck-Collaboration (2020). In particular, we do not apply any other numerical input, such as fit parameters or boundary values, for instance.

7.1.2 Cosmological and density parameters

Based on our theory, we derived all cosmological parameters, except the independent time after the Big Bang.

quantity	x_{theo}	x_{obs}	$\lvert\Delta_{theo-obs}x\rvert$
Ω_Λ	0.68265	$0.6847 \pm 1.1\%$	0.3%
$\Omega_{K,av.}$	0	$0.0007 \pm 171\%$	100%
Ω_M	0.31726	$0.3153 \pm 1.1\%$	0.6%
$10^5 \cdot \Omega_\gamma$	5.35	$5.335 \pm 5.68\%$	0.26%
$10^5 \cdot \Omega_\nu$	3.9556	$3.8742 \pm 9.7\%$	2.1%
$10^5 \cdot \Omega_r$	9.306	$9.265 \pm 3.1\%$	0.44%
σ_8	0.8044	$0.8057 \pm 1\%$	0.16%

Table 7.1: Using H_0, we derived all cosmological parameters. Here we applied $\Omega_\Lambda + \Omega_M + \Omega_r = 1$, for details see Carmesin (2021a).

Our comparison in Table (7.1) shows: The relative difference of our theoretical values and the corresponding observed values is smaller than the error of measurement. So our results are in precise accordance with observation. For details see Carmesin (2021a) or glossary.

7.1.3 Masses and the elementary charge

The masses of the elementary particles of the SMEP can be divided into two groups:

(1) masses of neutrinos

(2) masses of the Higgs boson and masses caused by the Higgs boson, including masses of quarks, $W^{+,0,-}$ bosons, electrons, muons and tauons.

(3) the remaining elementary particles of the SMEP are the photons and gluons, these have zero mass.

Accordingly, we derived the masses of neutrinos in terms of the density parameter Ω_ν. Moreover, we derived the mass of the

Higgs boson, $m_{H,full,theo} = E_{H,full,theo}/c^2$.

We derived the elementary charge from quantum gravity, see THM (4).

quantity	x_{theo}	x_{obs}	$\Delta_{theo-obs}x$	reference
$10^5 \cdot \Omega_\nu$	3.9556	$3.8742 \pm 9.7\%$	$\pm 2.1\%$	THM* 7
m_H in $\frac{\text{GeV}}{\text{c}^2}$	125.541	$125.18 \pm 1.1\%$	$\pm 0.29\%$	THM* 8,9
$\tilde{e}$	0.085 424 548	0.085 424 543	$5.4 \cdot 10^{-8}$	THM 3

Table 7.2: Using H_0 and the universal constants G, c and h, we derived the masses that represent or cause all masses of the SMEP, see (Carmesin, 2021a, THM* 7-9). Using the above three universal constants, we derived the elementary charge.

Our comparison in Table (7.2) shows: The relative difference of our theoretical values and the respective observed values is smaller than the error of measurement. Thus our theory is in precise accordance with observation. This holds for all masses that represent or cause all masses of the SMEP as well as for the elementary charge.

7.2 Predictions

In this section we apply the basic solution of the hierarchy problem in order to predict novel elementary particles. In a dimension D the ZPE of the longitudinal mode is as follows:

$$ZPE_{LONG,D} = \frac{E_P}{2}/2^{\frac{D_{hori}-D}{D}} = 6.1049 \cdot 10^{18}\,\text{GeV}/2^{\frac{D_{hori}-D}{D}} \quad (7.2)$$

Here we used $D_{hori} = 301$. The corresponding object consists of the three lowest excitation modes with $n = 1$, $n = 2$ and $n = 3$:

$$E_{object,D} = \Sigma_{n=1}^{n=3}(2n+1)ZPE_{LONG,D} = 15 \cdot ZPE_{LONG,D} \quad (7.3)$$

Four dimensional QST: In $D = 4$ the predicted object has the energy $E_{object,D=4} = 4.077\,\text{MeV}$ and is very unstable.

7.2.1 Observation of dimensional phase transition?

A stochastic gravitational wave background, GWB, has been observed, and it is interpreted as a relic of phase transitions in the early universe. Thereby a transition temperature with the corresponding energy in the following interval has been found, see e. g. (Ratzinger and Schwaller, 2021, p. 5) or (Arzoumanian et al., 2021, Fig. 1):

$$E_{GWB,obs} \in [1; 10]\,\text{MeV} \tag{7.4}$$

This observation can be interpreted as follows: At the last dimensional phase transition of the cosmic unfolding, the above four dimensional elementary particles or QST with $E_{object,D=4} = 4.077\,\text{MeV}$ unfolded to an object with energies below one eV, see theorem, and thereby the object emitted its energy in the form of gravitational waves.

7.2.2 Deviation of the field of an elementary particle

The elementary charge is the same in each charged elementary particle, $\tilde{e} = \kappa_\perp$, see THM. (1).

However, an elementary particle with its particular mass $m_{particle,dist}$ and with the elementary charge $\tilde{e} = \kappa_\perp$ generates an electric field that depends slightly on the mass $m_{particle,dist}$, see section (4.6). It might be possible to measure this effect in the future.

7.2.3 Bare elementary charge

We derived a value for the bare elementary charge, see THM (3). It might be possible to measure this effect in the future.

7.2.4 No magnetic monopoles

We showed how the QST within elementary particles can form electric charge and electromagnetic interaction. Thereby, the electric charge is primarily formed, see chapters (3, 6), whereas the magnetic interaction is formed as a consequence, see chapter (5). According to this structure of formation of interactions, we predict that there are no magnetic monopoles in nature.

7.3 Solved problems

We summarize solved problems in order to make transparent how our theory integrates various fields and can be used to solve problems:

problem of rapid enlargement of distances, see Guth (1981), solved since 2017, see e. g. Carmesin (2017b), Carmesin (2021b)

horizon problem, see Guth (1981), solved since 2017, see e. g. Carmesin (2017b), Schöneberg and Carmesin (2021)

'inflaton' hypothesis and reheating problem, see Guth (1981) and Nanopoulos et al. (1983), Broy (2016), solved since 2017, see e. g. Carmesin (2017b), Carmesin (2020a)

dark matter problem, see Zwicky (1933), Sanders (2010), solved since 2018, see Carmesin (2018g), Carmesin (2019c)

dark energy problem, see Josset et al. (2017), solved since 2018, see e. g. Carmesin (2018f), Carmesin (2021d)

H_0 tension, see Riess et al. (2019), solved since 2018, see for instance Carmesin (2018f), Carmesin (2021d)

σ_8 tension, see Tröster et al. (2020), solved in Carmesin (2021d)

fine-tuning problem, see e. g. Landsman (2016), partially solved since 2019, see Carmesin (2019c), and for the case of all cosmological constants, see section (7.1.2

flatness problem, see Guth (1981), solved since 2020, see e. g. Carmesin (2020b), Carmesin (2021d)

zero energy hypothesis, see Tryon (1973), solved 2020, see e. g. Carmesin (2020b)

graviton hypothesis, see e. g. Blokhintsev and Galperin (1934), solved in Carmesin (2021d)

EPR paradox and nonlocality, see Einstein et al. (1935), solved in Carmesin (2021d)

problem of deriving macroscopic expansion of space from microscopic gravity, solved in Carmesin (2020b), Carmesin (2021d)

hierarchy problem of particle physics, see Shaposhnikov and Shkerin (2018), solved here

mass problem of the Higgs boson and the neutrinos, see Aad et al. (2012), Chatrchyan et al. (2012) Peskin (2015), Tanabashi et al. (2018), solved in Carmesin (2021a)

interaction problem of the nature of an interaction that can be repulsive as well as attractive, solved here in the framework of an effective interaction energy

By deriving the elementary charge e from quantum gravity, we showed that this charge e is not a fundamental constant of nature.

Using quantum gravity, we derived the elementary charge e, including multiples $q = n \cdot e$. Then we applied a usual derivation of electromagnetism from the concept of charge q or e. In this manner we showed that the electromagnetic interaction is not a fundamental interaction of nature.

By deriving the electromagnetic interaction from the elementary charge e or charge q, which are based on quantum gravity, we showed that the magnetic force is a relativistic consequence of the electric charge. Accordingly, within the discovered structure

of the formation of the electromagnetic interaction, there are no magnetic monopoles.

Several fundamental problems are solved for the first time in the present book. For it we use our theory. These problems include the fine-tuning problem of the elementary charge e (is e a fundamental constant of nature?), the problem of fundamental interactions (is the electromagnetic interaction fundamental?), the problem of possibility of magnetic monopoles (are there magnetic monopoles?).

We emphasize that our above solutions of problems achieve precise accordance with observation. Hereby, we do not use any fit parameter, instead we use quantum gravity and the universal constants G, c, k_B and h only. Moreover, our theory is well-founded, see e. g. Carmesin (2021d).

7.4 Interpretation

In this section, we use our derivations in order to develop interpretations.

7.4.1 Basic physical structures

In this section, we identify basic or fundamental physical structures. We derived the electromagnetic interaction based on quantum gravity. Hereby, the elementary charge is formed by three QST. Accordingly, quantum gravity is a fundamental physical structure, whereas the elementary charge is a derived and composed physical entity. Consequently, the electromagnetic interaction is a derived physical structure. Correspondingly, the universal constants of quantum gravity are fundamental, namely G, c and h. In contrast, the universal constants of electromagnetism are derived, namely e, α and ε_0.

The Boltzmann constant k_B enables the calculation of physical quantities such as the energy or the entropy from statistical

quantities such as the number of states. Correspondingly, k_B is a basic constant used for the application of statistics and combinatorics to physics.

7.4.2 Basics of space, time, particles and interactions

In this section, we summarize basic structures in physics. In essence, these structures can be summarized by space, time, particles and interactions, see e. g. Tanabashi et al. (2018) and Planck-Collaboration (2020).

We use our results about mass, see Carmesin (2021a), and about the electromagnetic interaction. Presumably, the weak interaction can be described by quantum gravity as well, as the electromagnetic and weak interaction have been unified already, see e. g. Weinberg (1967), Tanabashi et al. (2018). Moreover, one might expect that the strong interaction can be explained by quantum gravity, as the structure of the fields of the corresponding theory of quantum chromodynamics is similar to the fields of electromagnetism (Tanabashi et al., 2018, S. 9.1).

Accordingly, the ultimate basic structure is formed by space and time.

7.4.2.1 Quantum field theories

Present-day physicists often use a **quantum field theory, QFT** as a basic tool, see e. g. Schwartz (2014). An example is the QED, see C. (5). In this book, we confirmed that QED is a useful tool in order to calculate corrections that are caused at a large distance of an elementary particle and at low density, see C. (6).

As a matter of fact, each field theory and each QFT requires a continuous space or spacetime as a prerequisite. However, we derived that space exhibits gravitational instabilities at high density, see e. g. Fig. (2.12). Accordingly, space undergoes discontinuous phase transitions at the corresponding critical den-

sities. Thus the required continuous space or spacetime is not provided in nature. Consequently, the QFTs are applicable only in a restricted range.

7.4.2.2 The present new theory of quantum gravity

The present new theory of quantum gravity describes quanta of space time, QST. Their properties are characterized with help of a Hilbert space. As a consequence, no space or spacetime is required in this theory. Accordingly, the QST describe the continuous as well as the discontinuous time evolution of space. Thereby, the QST describe the time evolution of the universe including all cosmological constants (except one independent constant describing the present-day time after the Big Bang).

As a further result, the QST describe the full spectrum of states and excitation states of the vacuum. As an additional and essential result, the QST describe the formation of mass, see Carmesin (2021a). These masses exhibit an internal dynamics, and this dynamics describes the formation of the elementary charge and the electromagnetic interaction.

Hereby, all results are achieved in precise accordance with observation and without any fit parameter. Thereby, the new theory of quantum gravity has been developed or derived in a well-founded manner.

7.4.2.3 Field $\vec{G}^*_\perp$ corresponding to $q = e/3$

In quarks, the charge $q = e/3$ has been observed, see Tanabashi et al. (2018). In this section, we show how the field $\vec{G}^*_\perp$ corresponding to such a charge $q = e/3$ can form.

In chapter (3), we derived the formation of an elementary charge e by three QST. In general, these three QST can form a single quantum in terms of a *linear superposition.*

Common mass m_c: In that case, the mass of the superposition is equal to one third of the mass m_c of the three QST. We derive

this fact by an investigation of the orthonormal eigenstates of the energy operator $\hat{E}$:

$$\hat{E}\Psi_j = E_j \cdot \Psi_j \tag{7.5}$$

For the case of the normalized linear combination $\Psi = \frac{1}{\sqrt{3}}(\Psi_1 + \Psi_2 + \Psi_3)$, we investigate the expectation value of the energy:

$$\langle E \rangle = \langle \Psi | \hat{E}\Psi \rangle = \frac{1}{3} \cdot \langle \Psi_1 + \Psi_2 + \Psi_3 | \hat{E}(\Psi_1 + \Psi_2 + \Psi_3) \rangle \tag{7.6}$$

We evaluate the operator:

$$\langle E \rangle = \frac{1}{3} \cdot \langle \Psi_1 + \Psi_2 + \Psi_3 | (E_1\Psi_1 + E_2\Psi_2 + E_3\Psi_3) \rangle \tag{7.7}$$

Using the orthogonality of the eigenstates, we derive:

$$\langle E \rangle = \frac{1}{3} \cdot \Sigma_{j=1}^{3} E_j \cdot \langle \Psi_j | \Psi_j \rangle \tag{7.8}$$

As the eigenstates are normalized, we obtain:

$$\langle E \rangle = \frac{1}{3} \cdot \Sigma_{j=1}^{3} E_j \tag{7.9}$$

So the energy of the linear combination is one third of the sum of the energies. Consequently, the dynamic mass of the linear combination is one third of the sum of the dynamic masses. In particular, for the case of a non-relativistic state, the mass of the linear combination is one third of the sum of the masses, $\tilde{m}_c = 1/3$.

Charge q resulting from $\tilde{m}_c = 1/3$: As a consequence, the formed field is equal to one third of the field $\vec{G}_{\perp}^{*}$ formed by the three QST. Consequently, the electric field corresponds to a charge $q = e/3$, see Eq. (3.96). Of course, the theoretical charge $\kappa_{\perp}$ is still equal to one elementary charge $\tilde{e}$. However, as a distant observer can only measure the field, a distant observer gets the impression that there would be a charge $q = e/3$.

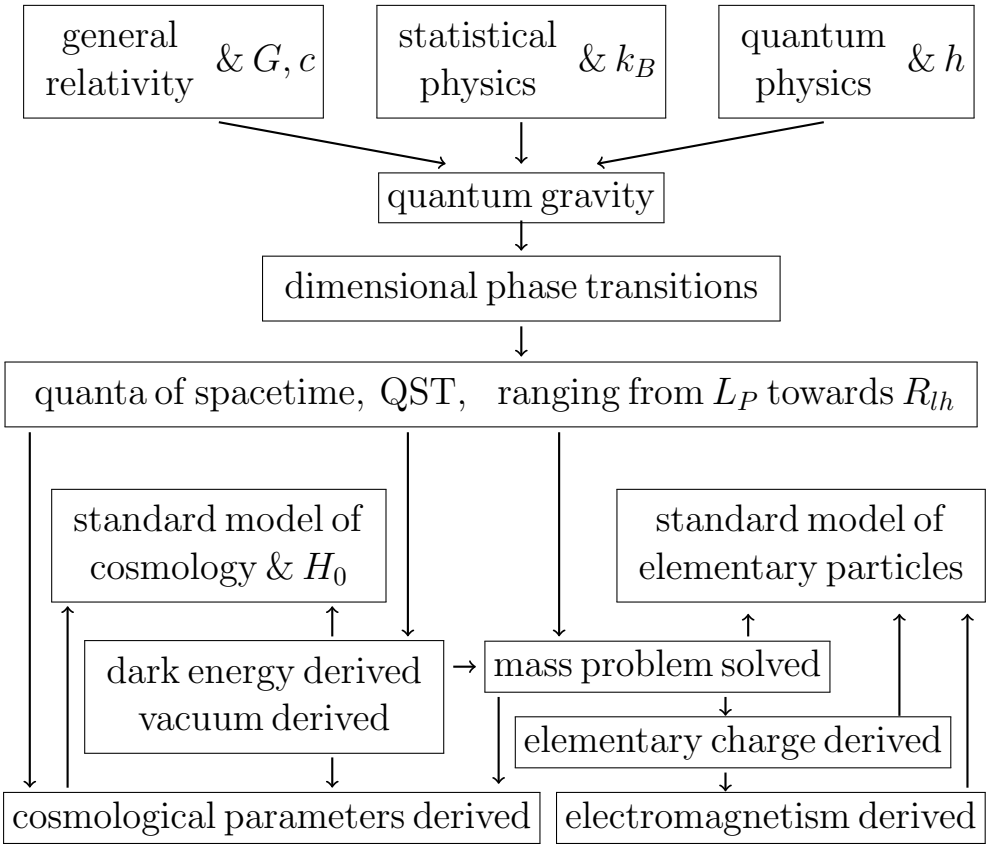

Figure 7.1: Paths from basic theories to derivations, explanations and calculations: These derivations reflect the structure of physics and have been published e. g. since Carmesin (2017b) towards Carmesin (2021a).

7.4.2.4 Outlook

There are many interesting questions that could be analyzed on the basis of the present theory in the future, examples are as follows: Is it possible to derive more interactions and symmetries in elementary particle physics, see e. g. Tanabashi et al. (2018), on the basis of quantum gravity? Is it possible to explain open questions of structure formation and particle formation by using quantum gravity? How can the dimensional phase transitions in the early universe be observed directly and used technically, see Sect. (7.2.1)?

7.5 Unification of SMC and SMEP

The standard models of cosmology, SMC, and of elementary particles, SMEP, have been unified as follows, see Fig. (7.1): Based on the three basic concepts, GR, SP (statistical physics) and QP, QG has been developed. Therefrom, QST and dimensional phase transitions including cosmic unfolding have been derived, see e. g. Carmesin (2017b), Carmesin (2019c), Carmesin (2021d).

Using these results, we derived the dark energy, all essential cosmological parameters, the basic masses, the elementary charge as well as the electromagnetic interaction. Altogether, we derived our results from the basic theories only. As numerical input, we used the universal constants G, c, k_B and h as well as the time reference H_0 only. In this manner, we achieved precise accordance with observation.

7.5.1 Public documentation and discussion

The theory in Fig. (7.1) has been published since Carmesin (2017b), and it has been discussed at many conferences. This process is described as follows:

Reviewed papers: Several results have been published in peer reviewed papers, see[1].

Conferences: Many results have been presented at conferences, see[2].

[1]Peer reviewed papers: Carmesin (2016), Carmesin (2018a), Carmesin (2018c),Carmesin (2018d),Carmesin (2018b), Helmcke et al. (2018), Sprenger and Carmesin (2018), Carmesin (2019b), Carmesin (2020a), Carmesin and Carmesin (2020), Heeren et al. (2020), Schöneberg and Carmesin (2020), Carmesin (2021b), Carmesin (2021e), Schöneberg and Carmesin (2021), Lieber and Carmesin (2021), Sawitzki and Carmesin (2021)

[2]Presentations at conferences: Carmesin (2017a), Carmesin and Carmesin (2018a),Carmesin and Carmesin (2018b), Helmcke et al. (2018), Sprenger and Carmesin (2018), Carmesin and Brüning (2018), Carmesin (2019d), Carmesin (2019a), Brüning et al. (2019), Rademacker et al. (2019), Carmesin (2019f), Brüning and Carmesin (2019),

Books: Four books have been published, see[3]. Additionally, a book series has been started, and therein, five books have already been published, see[4].

Internet: Many results are available at my page at Research gate:
http://www.researchgate.net/profile/ Hans_Otto_Carmesin
Some results are available at my homepage:
hans-otto.carmesin.org

7.5.2 An essential insight by quantum gravity

Quantum gravity reveals that there occurred an enormous sequence of phase transitions in the early universe: a cosmic unfolding of space, ranging from the Planck scale to the millimeter scale, see Fig. (2.12). The corresponding quantum states cause all masses of elementary particles, and they form neutrinos, Higgs bosons, the quanta of dark energy as well as many novel elementary particles, ranging from the Planck mass to the neutrino mass scale. Moreover, these quanta form the elementary charge and the electromagnetic interaction.

Carmesin (2020a), Carmesin and Carmesin (2020), Heeren et al. (2020), Schöneberg and Carmesin (2020), Carmesin (2021b), Carmesin (2021e), Schöneberg and Carmesin (2021), Lieber and Carmesin (2021), Sawitzki and Carmesin (2021)

[3]Books: Carmesin (2017b), Carmesin (2018g), Carmesin (2018f), Carmesin (2018e)

[4]Book series since 2019: Carmesin (2019c), Carmesin (2020c), Carmesin (2020b), Carmesin (2021d), Carmesin (2021a)

Chapter 8

Appendix

8.1 Universal constants

In this section we present universal constants. Hereby, ε_0 is not a fundamental constant, as it can be derived from fundamental constants.

quantity	observed value	reference
G	$6.674\,08(31) \cdot 10^{-11}\ \frac{\mathrm{m}^3}{\mathrm{kg}\cdot\mathrm{s}^2}$	Tanabashi et al. (2018)
c	$299\,792\,458\ \frac{\mathrm{m}}{\mathrm{s}}$, exact	Tanabashi et al. (2018)
h	$6.626\,070\,15\ \cdot 10^{-34}$ Js, exact	Newell et al. (2018)
k_B	$1.380\,649\ \cdot 10^{-23}\ \frac{\mathrm{J}}{\mathrm{K}}$, exact	Newell et al. (2018)
ε_0	$8.854\,187\,817\ \cdot 10^{-12}\ \frac{\mathrm{F}}{\mathrm{m}}$	Tanabashi et al. (2018)

Table 8.1: Universal constants ((Newell et al., 2018, table 3), (Tanabashi et al., 2018, table 1.1)).

8.2 Observed values

quantity	observed value	reference
H_0 in $\frac{\text{km}}{\text{s·Mpc}}$	67.36 ± 0.54 (0.8 %)	[CMB]
Ω_Λ	0.6847 ± 0.0073 (1.1 %)	[CMB]
Ω_K	0.0007 ± 0.0019	[CMB]
z_{eq}	$3402 \pm 26(0.76\%)$	[CMB]
Ω_M	$0.3153 \pm 0.0073(2.3\%)$	[CMB]
Ω_r	$9.265^{+0.288}_{-0.283} \cdot 10^{-5}$ (3.1 %)	[CMB]
σ_8	$0.8057 \pm 0.008(1\%)$	[CMB]
ρ_{cr,t_0} in $\frac{kg}{m^3}$	$8.660^{+0.137}_{-0.137} \cdot 10^{-27}$ (1.6 %)	[CMB]
$\tilde{\rho}_{cr,t_0}$	$7.037 \cdot 10^{-123}$	[CMB]
$\tilde{\rho}_{v,t_0}$	$4.8181 \cdot 10^{-123}$	[CMB]
Ω_b	0.0493 ± 0.00032	[CMB]
Ω_c	0.2645 ± 0.0048	[CMB]
R_{lh}	$4.1412 \cdot 10^{26}$ m	[C2019]
T_{CMB}	$2.7255(6)(0.02\%)$ K	[T2018]
Ω_{CMB}	5.4501	[C2021]
Ω_ν	$3.8742 \cdot 10^{-5}(9.7\%)$	[C2021]
$\tilde{e}$	0.085 424 548	[T2018]
α	$7.297\,352\,5664(17) \cdot 10^{-3}$	[T2018]

Table 8.2: Observations: [CMB] marks data based on the CMB ((Planck-Collaboration, 2020, table 2)), in particular based on the modes TT, TE, EE, the low energy and lensing. Quantities with a tilde are presented in natural units alias Planck units (see subsection 8.3). Hereby 1 Mpc = $3.0856776 \cdot 10^{19}$ km. [C2019] is based on an evaluation in Carmesin (2019c). [C2021] is based on an evaluation in Carmesin (2021a). [T2018] is based on Tanabashi et al. (2018).

8.3 Natural units

Planck (1899) introduced Planck units. We mark quantities in natural units by a tilde, see Tab. 8.3 or Carmesin (2019c).

physical entity	Symbol	Term	in SI-Units
Planck length	L_P	$\sqrt{\frac{\hbar G}{c^3}}$	$1.616 \cdot 10^{-35}$ m
Planck time	t_P	$\frac{L_P}{c}$	$5.391 \cdot 10^{-44}$ s
Planck energy	E_P	$\sqrt{\frac{\hbar \cdot c^5}{G}}$	$1.956 \cdot 10^{9}$ J
Planck mass	M_P	$\sqrt{\frac{\hbar \cdot c}{G}}$	$2.176 \cdot 10^{-8}$ kg
Planck volume	$V_{D,P}$	L_P^D	
Planck volume, ball	$\bar{V}_{D,P}$	$V_D \cdot L_P^D$	
Planck density	ρ_P	$\frac{c^5}{G^2\hbar}$	$5.155 \cdot 10^{96}$ $\frac{\text{kg}}{\text{m}^3}$
Planck density, ball	$\bar{\rho}_P$	$\frac{3c^5}{4\pi G^2\hbar}$	$1.2307 \cdot 10^{96}$ $\frac{\text{kg}}{\text{m}^3}$
Planck density, ball	$\bar{\rho}_{D,P}$	$\frac{M_P}{\bar{V}_{D,P}}$	
Planck temperature	T_P	$T_P = \frac{E_P}{k_B}$	
scaled volume	$\tilde{V}_D$	$\frac{V_D}{\bar{V}_{D,P}}$	
scaled energy	$\tilde{E}$	E_P	$E = \tilde{E} \cdot E_P$
scaled density	$\tilde{\rho}_D$	$\frac{\tilde{M}}{\tilde{r}^D} = \frac{\tilde{E}}{\tilde{r}^D}$	$\rho_D = \tilde{\rho}_D \cdot \bar{\rho}_{D,P}$
scaled length	$\tilde{x}$	L_P	$x = \tilde{x} \cdot L_P$
Planck charge	q_P	$\sqrt{4\pi\varepsilon_0 \cdot \hbar \cdot c}$	$11{,}71\, e$
scaled charge	$\tilde{q}$	$\tilde{q} = \frac{q}{q_P}$	

Table 8.3: Planck - units.

8.4 Fields and scaled fields

In this section we present the various types of fields.

quantity	relation	field of ...
$G^*_{m_c}$	Eq. 3.57	triple
$\vec{G}^*_j$	Eq. 3.32	triple
$G^*_{\alpha,j\to i}$	Eqs. 3.56, 3.68, 6.10	emission
$G^*_{emitted,\perp}$	Eq. 3.70	QST emitted by triple
$G^*_{m_c,rest}$	Eq. 3.61	process of emission
$\kappa_{any\ type}$	$\kappa_{any\ type} = \frac{G^*_{any\ type}}{G^*_{m_c}}$	scaled form
$\kappa_{1+\perp}$	Eq. 6.23	$\kappa_{1+\perp} = 1 + \kappa_\perp$
$\kappa_{sim.}$	Eq. 6.11	simultaneous forced osc.

Table 8.4: Fields and scaled fields.

8.5 Glossary

Words marked bold face can usually be found in the glossary.

Abbreviation: S. (section), C. (chapter), DEF. (definition), PROP. (proposition), THM. (theorem).

amplitude of matter fluctuations, σ_8: (C. 1)

Big Bang: Start of time evolution of visible space

causal horizon: light horizon

cdm, cold dark matter: See Fig. (1.1), Carmesin (2018e) or Carmesin (2019c).

CMB, Cosmic Microwave Background: Radiation emitted at $z \approx 1090$. (Tab. 8.2)

classical electrodynamics: C. (5)

complete time evolution of spacetime: Evolution of the light horizon $R_{lh}(t)$ ranging from the Planck - length L_P to the actual light horizon $R_{lh}(t_0)$

cosmic unfolding: It causes the **extremely rapid distance enlargement in the early universe**

cosmological constant: Λ corresponds to the dark energy with its density ρ_Λ (Tab. 8.2).

coupling constant of electrodynamics: S. (1.1.1), C. (3)

curvature parameter: the curvature parameter k describes the global curvature of space, see e. g. Carmesin (2021d)

dark energy: Energy of the cosmological density of the vacuum ρ_Λ (Tab. 8.2).

density, critical: ρ_{cr,t_0} or ρ_{cr} (Tab. 8.2 or e. g. Carmesin (2021d))

density, critical, at a dimensional transition: $\tilde{\rho}_{D,c}$

density parameter: $\Omega_j = \rho_j / \rho_{cr,t_0}$ (Tab. 8.2)

density, vacuum: $\rho_\Lambda = \Omega_\Lambda \cdot \rho_{cr,t_0}$ (Tab. 8.2)

dimensional distance enlargement factor: A factor $Z_{D+s \to D}$ occurs at a dimensional phase transition from a dimension $D+s$ to a dimension D and describes the corresponding increase of distances (Fig. 2.12).

dimension of the space: (C. 2)

dimensional horizon D_{max} or $D_{horizon}$: It is the maximal dimension that the space within the actual light horizon can have achieved in the past. Thereby the following transformations of space are essential: the isotropic scale and the enlargement

of distance caused by a $\rightarrow$ dimensional transition. (S. 2.5.2).

dimensional phase transition: Change of spatial dimension D (S. 2.5.2).

dimensional unfolding: Change of spatial dimension D (S. 2.5.2).

dynamical mass: $M = \frac{E}{c^2}$

elementary charge: S. (1.1.1)

expansion of space: Expansion since the Big Bang at constant dimension D (S. 2.5.2).

extremely rapid distance enlargement in the early universe: Guth (1981) conjectured that factor, the factor has been explained by dimensional transitions in this book and by Carmesin (2017b), Carmesin (2019c)

flat, flatness, flatness problem: Space without curvature is flat (S. 7.3).

forced oscillation: C. (3)

frame: Each observation apparatus is localized in spacetime. That localization establishes a frame.

gravitational field: G^* (C. 1)

GR: General relativity (C. 1)

horizon: Global limit of visibility (C. 1)

Hubble - parameter: $H = \frac{\dot{a}}{a}$ (C. 1)

Hubble - constant: $H_0 = H(t_0)$ Hubble parameter at t_0

incomplete: A theory that does not describe the physically known objects or properties is incomplete

light horizon, actual: $R_{lh} = 4.142 \cdot 10^{26}\,\mathrm{m}$ (Tab. 8.2)

modes of modification: C. (2)

natural units: Planck - units (Tab. 8.3)

pbh, primordial black holes: See Fig. (1.1) and Carmesin (2020b).

Planck scale: At that scale there occurs the **length limit** and the **density limit** in nature. Accordingly, natural units or Planck units have been introduced (Tab. 8.3).

polychromatic vacuum: It includes several wavelengths of the quanta of space, see e. g. Carmesin (2018f), Carmesin (2018e), Carmesin (2019c) or Carmesin (2021d)

principle of lowest action: C. (5)

principle of equal amplitudes: C. (3)

quantum electrodynamics, QED: C. (5)

QG, quantum gravity: Combination of gravitation and quantum physics (C. 2 or Carmesin (2019c))

QP, quantum physics: Quantum physics, see C. 1

QST, quantum of spacetime, or quantum of vacuum: Representations are quantized RGWs, quantized spacetime scalar, quantized spacetime tensor (C. 2)

rapid enlargement of distances: (Fig. 2.5)

rate gravity four-vector, RGV: C. (2)

rate gravity scalar, RGS: C. (2)

RGW, rate gravity wave: Carmesin (2021d) or C. (2)

rate of the formation of vacuum: (S. 2.5.2)

rate tensor, generalized: C. (2)

redshift: Relative increase of the wavelength $z = \frac{\Delta\lambda}{\lambda}$ (C. 2)

SP, statistical physics: (C. 7)

scaled emitted transverse field: C. (3)

Schwarzschild radius R_S: At this radius the escape velocity is equal to c

SMC, Standard Model of Cosmology: (C. 1)

SMEP, Standard Model of Elementary Particles: (C. 1)

spacetime: Combination of space and time (C. 1

SRT, special relativity theory: (C. 1)

standard deviation at a sphere with radius R: σ_R

standard deviation at a sphere with radius R_8: $\sigma_8 = \sigma_{R_8}$ It is also called amplitude of matter fluctuations or amplitude of matter fluctuations.

time evolution of the vacuum: C. (1, 2)

transverse emitted field: C. (3)

unfolding, dimensional: Space unfolds when the dimension decreases (S. 2.5.2)

universal constants: (Tab. 8.1)

vacuum: The vacuum has a volume, a density and the velocity c. (C. 1, S. 2.5.2 or Carmesin (2021d))

ZPE: Zero-point energy of omnipresent zero-point oscillations (C. 1, 2, S. 2.5.2)

ZPO: Zero-point oscillations are omnipresent quantum states corresponding to a ground state (C. 1, 2, S. 2.5.2)

```
/**
Calculation of scaled emitted field kap_emitted_perp and of alpha
The theory is a part of the following book Carmesin (2021),
list of Literature see below
Program Code in Java: Hans-Otto Carmesin,  October 2nd 2021
*/
import java.io.FileReader;import java.io.FileWriter;import java.io.IOException;
import java.util.Scanner;import java.io.*;import java.lang.Math;
//
public class alpha_20211011 {
  public static void main(String args[]) throws IOException {
    System.out.println("Start ");
    //
    // 1) initialization of variables
    int i = 0;  int j = 0;  // subscripts of QST
    double z=1.; // variable
    double kap_emitted_perp = 0.; // scaled emitted field
    double alpha = 0.; // fine-structure constant
    double [] n2=new double[10]; // eigenvalue of number operator
    double [] nb=new double[10]; // 2*n2+1
    double [][] kap_alpha=new double[10][10];//particular scaled emitted field
    //
    // 2) eigenvalues  n_j of QST
      while ( j < 4) {
      n2[j] = j; nb[j] = 2*j+1;
      j = j + 1;}
    //
    // 3) scaled emitted fields
       j = 1;
       while ( j < 4) { i = 1;
          while ( i < 4) { z=1.;
          if ( (i-j)*(i-j) >0.5) {
           kap_alpha[i][j]=Math.log(1+1./Math.abs(nb[i]*nb[i]-nb[j]*nb[j]));
           if (i==3) z=-1.;
           kap_emitted_perp=kap_emitted_perp+z*kap_alpha[i][j]*kap_alpha[i][j];
          } // end of if
```

Figure 8.1: Program for the calculation of $\kappa_{emitted,\perp}$ and α, in the simplest version. Upper part.

8.6 Program

Acknowledgement

I thank Matthias Carmesin for helpful discussions. I thank Paul Sawitzki, Philipp Schöneberg, Jörn Kankelfitz, Dennis Feldmann and Jonas Lieber for interesting discussions. I am especially grateful to I. Carmesin for many helpful discussions.

```
36          } // end of if
37          i=i+1;}
38        j = j + 1;}
39      kap_emitted_perp = Math.pow(kap_emitted_perp, 0.5);
40      // Output
41      try   {
42      BufferedWriter out =  new BufferedWriter(
43      new FileWriter("Output_alpha_20211002.txt"));
44      out.write("*****  Output of program alpha_20211002:  *****"); out.newLine();
45      out.write("Simplest v.: without simultaneously emitted QST"); out.newLine();
46      out.write("Simplest v.: also without screening or any QED-corrections");
47      out.newLine ();
48      alpha = kap_emitted_perp*kap_emitted_perp;
49      out.write("kap_emitted_perp = " + kap_emitted_perp + ", alpha = " + alpha);
50      out.newLine ();
51      out.write("*****  End of output of program alpha_20211002:  *****");
52      out.close();
53      }
54      catch (IOException err) {
55      System.out.println("IOFehler");
56      }
57      System.out.println("the end");
58    } // end of main
59 }
60 /**
61 Literature:
62 Carmesin, Hans-Otto (October 2021):
63 The Elementary Charge Explained by Quantum Gravity.
64 Berlin, Verlag Dr. Köster.
65
66 *****  Output of program alpha_20211002:  *****
67 Simplest version: without simultaneously emitted QST,
68 without screening or any QED-corrections
69 kap_emitted_perp = 0.08573616238654197,   alpha = 0.007350689540771494
70 *****  End of output of program alpha_20211002:  *****
71 */
```

Figure 8.2: Program for the calculation of $\kappa_{emitted,\perp}$ and α, in the simplest version. Lower part.

Bibliography

Aad, G., ATLAS-Collaboration, et al. (2012). Observation of a new particle in the search for the Standard Model Higgs boson with the ATLAS detector at the LHC. *Phys. Lett. B*, 716:1.

Abbott, T. M. C. et al. (2020). Dark energy survey year 1 results: Cosmological contraints from galaxy clustering and weak lensing. *Phys. Rev. D*, 102:1–34.

Addison, G. E., Watts, D. J., Bennett, C. L., Halperin, M., Hinshaw, G., and Weiland, J. L. (2018). Elucidating ΛCDM: Impact of Baryon Acoustic Oscillation Measurements on the Hubble Constant Discrepancy. *ApJ*, 853:1–12.

Archimedes (1897). *The Sand-Reckoner, In: The Works of Archimedes (230 BC), translated by T. L. Heath in 1897.* Cambridge University Press, Cambridge.

Arzoumanian, Z. et al. (2021). Searching For Gravitational Waves From Cosmological Phase Transitions with the NANOGrav 12.5-Year Dataset. *arXiv*, 2104.13930v1:1–13.

Bethge, K. and Schröder, Ulrich, E. (1991). *Elementarteilchen und ihre Wechselwirkungen.* Wissenschaftliche Buchgesellschaft, Darmstadt, 2 edition.

Bialynicki-Birula, I. and Bialynicki-Birula, Z. (1975). *Quantum Electrodynamics.* Pergamon Press, Oxford, 1 edition.

Birrer, S. et al. (2020). TDCOSMO: IV. Hierarchical time-delay cosmography - joint inference of the Hubble constant and galaxy density profiles. *Astronomy and Astrophysics*, 643:1–40.

Blakeslee, J. P. et al. (2021). The Hubble Constant from Infrared Surface Brightness Fluctuation Distances. *The Astrophysical Journal*, 911(65):1–12.

Blokhintsev, D. I. and Galperin, F. M. (1934). Neutrino hypothesis and conservation of energy. *Pod Znamenem Marxisma*, 6:147–157.

Böhringer, H., Chon, G., Bristow, M., and Collins, C. A. (2015). The extended ROSAT-ESO Flux-Limited X-Ray Galaxy Cluster Survey (REFLEX II). *Astronomy and Astrophysics*, 574(A26):1–8.

Boltzmann, L. (1877). Über die Beziehung zwischen dem zweiten Hauptsatz der mechanischen Wärmetheorie und der Wahrscheinlichkeitsrechnung respektive den Sätzen über das Wärmegleichgewicht. *Sitzungsberichte der königlichen Akademie der Wissenschften zu Wien*, 76:428.

Brahe, T. (1588). *De mundi aetherei recentioribus phaenomenis*. Brahe, Uraniborg.

Broy, B. J. (2016). *Inflation and effective Shift Symmetries*. PhD thesis, University Hamburg, Hamburg.

Brüning, P. and Carmesin, H.-O. (2019). The Elementary Oscillation of Dark Energy. *Verhandl. DPG (VI)*, 54(3):30.

Brüning, P., Carmesin, H.-O., and Helmcke, B. J. (2019). Numerical Investigation of the Emergence of Dark Energy and the Time Evolution of the Hubble Constant. *Verhandl. DPG (VI)*, 54(3):30.

Carmesin, H.-O. (1996). *Grundideen der Relativitätstheorie*. Verlag Dr. Köster, Berlin.

Carmesin, H.-O. (2016). Mit dem Zwillingsparadoxon zur speziellen und allgemeinen Relativitätstheorie. *PhyDid B Internetzeitschrift*.

Carmesin, H.-O. (2017a). Quantum Gravity: Discoveries about the Early Universe Including Big Bang, Big Bounce and a Critical Discussion of these. German Astronomical Society Conference at University Göttingen.

Carmesin, H.-O. (2017b). *Vom Big Bang bis heute mit Gravitation: Model for the Dynamics of Space*. Verlag Dr. Köster, Berlin.

Carmesin, H.-O. (2018a). A Model for the Dynamics of Space - Expedition to the Early Universe. *PhyDid B, FU Berlin, hal-02077596*, pages 1–9.

Carmesin, H.-O. (2018b). Eine Theorie des Gravitationswellensignals ausschließlich mit Schulmitteln - verallgemeinerbar auf elektromagnetische Sender, Wellenlehre und Schwarzschild - Metrik. In Friege, G. and Scholz, R., editors, *Blubb - Gravitationswellen - schwarze Löcher*, pages 21–38. Westermann, Braunschweig.

Carmesin, H.-O. (2018c). Einstein in der Schule (Teil 1) Unterrichtskonzepte zur allgemeinen Relativitätstheorie. *Astronomie und Raumfahrt im Unterricht*, 55(3/4):55–59.

Carmesin, H.-O. (2018d). Einstein in der Schule (Teil 2) Unterrichtskonzepte zur allgemeinen Relativitätstheorie. *Astronomie und Raumfahrt im Unterricht*, 55(6):33–36.

Carmesin, H.-O. (2018e). *Entstehung der Raumzeit durch Quantengravitation - Theory for the Emergence of Space,*

Dark Matter, Dark Energy and Space-Time. Verlag Dr. Köster, Berlin.

Carmesin, H.-O. (2018f). *Entstehung dunkler Energie durch Quantengravitation - Universal Model for the Dynamics of Space, Dark Matter and Dark Energy.* Verlag Dr. Köster, Berlin.

Carmesin, H.-O. (2018g). *Entstehung dunkler Materie durch Gravitation - Model for the Dynamics of Space and the Emergence of Dark Matter.* Verlag Dr. Köster, Berlin.

Carmesin, H.-O. (2019a). A Novel Equivalence Principle for Quantum Gravity. *Verhandl. DPG (VI)*, 54(3):42.

Carmesin, H.-O. (2019b). A Novel Equivalence Principle for Quantum Gravity. *PhyDid B - Didaktik der Physik - Beiträge zur DPG - Frühjahrstagung - Aachen - Germany - hal-02511998*, pages 1–9.

Carmesin, H.-O. (2019c). Die Grundschwingungen des Universums - The Cosmic Unification - With 8 Fundamental Solutions based on G, c and h. In Carmesin, H.-O., editor, *Universe: Unified from Microcosm to Macrocosm - Volume 1.* Verlag Dr. Köster, Berlin.

Carmesin, H.-O. (2019d). Equivalence Principle of Quantum Gravity. *Verhandl. DPG (VI)*, 54(2):74.

Carmesin, H.-O. (2019e). Kontroverse Konstante. *Physik Journal*, 18(7):14.

Carmesin, H.-O. (2019f). The Elementary Particle of Dark Matter. *Verhandl. DPG (VI)*, 54(3):42.

Carmesin, H.-O. (2020a). Explanation of the Rapid Enlargement of Distances in the Early Universe. *PhyDid B*, pages 9–17.

Carmesin, H.-O. (2020b). The Universe Developing from Zero-Point Energy: Discovered by Making Photos, Experiments and Calculations. In Carmesin, H.-O., editor, *Universe: Unified from Microcosm to Macrocosm - Volume 3*. Verlag Dr. Köster, Berlin.

Carmesin, H.-O. (2020c). Wir entdecken die Geschichte des Universums mit eigenen Fotos und Experimenten. In Carmesin, H.-O., editor, *Universe: Unified from Microcosm to Macrocosm - Volume 2*. Verlag Dr. Köster, Berlin.

Carmesin, H.-O. (2021a). Cosmological and Elementary Particles Explained by Quantum Gravity. In Carmesin, H.-O., editor, *Universe: Unified from Microcosm to Macrocosm - Volume 5*. Verlag Dr. Köster, Berlin.

Carmesin, H.-O. (2021b). Lernende erkunden die Raumzeit. *Der Mathematik Unterricht*, 2.:47–56.

Carmesin, H.-O. (2021c). Physical Explanation of the H_0-Tension. *International Journal of Engineering and Science Invention*, 10(8,II):34–38.

Carmesin, H.-O. (2021d). Quanta of Spacetime Explain Observations, Dark Energy, Graviton and Nonlocality. In Carmesin, H.-O., editor, *Universe: Unified from Microcosm to Macrocosm - Volume 4*. Verlag Dr. Köster, Berlin.

Carmesin, H.-O. (2021e). The Origin of the Energy. *PhyDid B, FU Berlin*, pages 29–34.

Carmesin, H.-O. and Brüning, P. (2018). A Monte Carlo Simulation of Cosmic Inflation. *Verhandl. DPG*, page DD27(3).

Carmesin, H.-O. and Carmesin, M. (2018a). Explanation of Cosmic Inflation by Gravitation. *Verhandl. DPG*, page GR16(7).

Carmesin, H.-O. and Carmesin, M. (2018b). Explanation of Cosmic Inflation by Quantum Gravity. *Verhandl. DPG*, page EP14(5).

Carmesin, H.-O., Emse, A., Piehler, M., Pröhl, I. K., Salzmann, W., and Witte, L. (2021). *Universum Physik Sekundarstufe II Nordrhein-Westfalen Einführungsphase*. Cornelsen Verlag, Berlin.

Carmesin, M. and Carmesin, H.-O. (2020). Quantenmechanische Analyse von Massen in ihrem eigenen Gravitationspotenzial. *PhyDid B, FU Berlin*, pages 19–27.

Cavendish, H. (1798). Experiments to determine the density of the earth. *Phil. Trans. R. Soc. Lond.*, 88:469–516.

Chatrchyan, S., CMS-Collaboration, et al. (2012). Observation of a new boson at a mass of 125 GeV with the CMS experiment at the LHC. *Phys. Lett. B*, 716:30.

Coulomb, C.-A. (1785). Construction et usage d'une balance electrique etc. *Histoire de l'Academie des sciences avec les memoires de mathematique et de physique*, 1788:569–577.

Dalton, J. (1808). *A New System of Chemical Philosophy Part I*. Bickerstaff, London.

Dupuy, A. et al. (2019). Partitioning the universe into gravitational basins using the cosmic vector field. *MNRAS*, 489:L1–L6.

Einstein, A. (1905). Zur Elektrodynamik bewegter Körper. *Annalen der Physik*, 17:891–921.

Einstein, A. (1915). Die Feldgleichungen der Gravitation. *Sitzungsberichte der Königlich Preußischen Akademie der Wissenschaften*, pages 844–847.

Einstein, A. (1917). Kosmologische Betrachtungen zur allgemeinen Relativitätstheorie. *Sitzungsberichte der Königlich Preußischen Akademie der Wissenschaften*, pages 142–152.

Einstein, A., Podolski, B., and Rosen, N. (1935). Can quantum-mechanical description of physical reality be considered complete? *Phys. Rev.*, 47:777–780.

Escamilla-Rivera, C. and Najera, A. (2021). Dynamical Dark Energy Models in the Light of Gravitational-Wave Transient Catalogues. *arXiv*, 2103.02097v1:1–25.

Faraday, M. (1852). On the physical character of the lines of magnetic force. *The London, Edinburgh and Dublin Philosophical Magazine and Journal of Science, Taylor and Francis*, 4(3):401–428.

Feynman, R. P. (1985). *QED - The Strange Theory of Light and Matter*. Princeton University Press, Princton.

Goodstein, D. (1997). The Big Crunch. *EOS, Transactions, American Geophysical Union*, 78:329–334.

Greiner, W. and Reinhardt, J. (1995). *Theoretische Physik 7: Quantenfeldtheorie*. Verlag Harri Deutsch, Frankfurt am Main, 2. edition.

Guth, A. H. (1981). Inflationary universe: A possible solution to the horizon and flatness problems. *Physical Review D*, 23:347–356.

Heeren, L., Sawitzki, P., and Carmesin, H.-O. (2020). Comprehensive Derivation of a Density Limit of the Evolution of Space. *PhyDid B, FU Berlin*, pages 39–42.

Helmcke, B. J., Carmesin, H.-O., Sprenger, L., and Brüning, P. (2018). Three methods for the observation of the Big Bang with our school telescope. *PhyDid B*, pages 55–60.

Hubble, E. (1929). A relation between distance and radial velocity among extra-galactic nebulae. *Proc. of National Acad. of Sciences*, 15:168–173.

Jackson, J. D. (1975). *Classicla Electrodynamics*. John Wiley, New York.

Josset, T., Perez, A., and Sudarsky, D. (2017). Dark energy as the weight of violating energy conservation. *PRL*, 118:021102233–243.

Kepler, J. (1619). Harmonice Mundi - Linz - Libri Verlag. In Caspar, M., editor, *Gesammelte Werke - 1940*, volume 6, pages 1–563. Clarendon Press, Oxford.

Kepler, J. (1627). *Tabulae Rudolphinae*. Jonae Saurii, Ulm.

Kobel, M., Bilow, U., Lindenau, P., and Schorn, B. (2017). *Teilchenphysik*. Joachim Herz Stiftung, Hamburg.

Landau, L. and Lifschitz, J. (1965). *Course of Theoretical Physics III - Quantum Mechanics*. Pergamon Press, Oxford, 2. revised edition.

Landau, L. and Lifschitz, J. (1971). *Course of Theoretical Physics II - The Calssical Theory of Fields*. Pergamon Press, Oxford, 3. edition.

Landau, L. and Lifschitz, J. (1975). *Course of Theoretical Physics VII - Theory of Elasticity*. Pergamon Press, Oxford, 2. edition.

Landau, L. and Lifschitz, J. (1976). *Course of Theoretical Physics I - Mechanics*. Pergamon Press, Oxford, 3. edition.

Landau, L. and Lifschitz, J. (1982). *Course of Theoretical Physics IV - Quantum Electrodynamics*. Pergamon Press, Oxford, 2. edition.

Landsman, K. (2016). The fine-tuning argument: Exploring the improbability of our existence. In Landsman, K. and van Wolde, E., editors, *The Challenge of Chance*. Springer, Berlin.

Lee, J. M. (1997). *Riemannian Manifolds: An Introduction to Curvature*. Springer Verlag, New York.

Lieber, J. and Carmesin, H.-O. (2021). Dynamics in the Early Universe. *PhyDid B, FU Berlin*, pages 49–52.

Maxwell, J. C. (1865). A dynamical theory of the electromagnetic field. *Philosophical Transactions of the Royal Society of London*, 155:459–512.

Millikan, R. A. (1911). The Isolation of an Ion, a Precision Measurement of its Charge, and the Correction of Stokes's Law. *Physica Review*, 32:349–397.

Moore, T. A. (2013). *A General Relativity Workbook*. University Science Books, Mill Valley, CA.

Nanopoulos, D., Olive, K. A., and Srednicki, M. (1983). After primordial inflation. *Physics Letters B*, 127:30–34.

Newell, D. B. et al. (2018). The CODATA 2017 values of h, e, k, and N_A for the revision of the SI. *Metrologia*, 55:L13–L16.

Newton, I. (1686). *Newton's Principia - first American Edition - English 1729*. Daniel Adee, New York.

Noether, E. (1918). Invariante Variationsprobleme. *Nachrichten der Königlichen Gesellschaft der Wissenschaften zu Göttingen, Math-phys. Klasse*, pages 235–257.

Oersted, H. C. (1820). Experimente circa effectum conflictus electrici in acum magneticam. *Publisher Oerstedt at University of Copenhagen*, pages 1–5.

Oldershaw, Robert, L. (1998). Democritus - scientific wizard of the 5th century bc. *Speculations in Science and Technology*, 21:37–44.

Pesce, D. W. et al. (2020). The Megamaser Cosmology Project: XIII. Combined Hubble Constant Constraints. *Astrophysical Journal Letters*, 891:L1.

Peskin, Michael, E. (2015). On the Trail of the Higgs Boson. *Annalen der Physik*, 528:20–34.

Philcox, O. H. E., Ivanov, Mikhail, M., Simonovic, M., and Zaldarriaga, M. (2020). Combining Full-Shape and BAO Analyses of Galaxy Power Spectra: A 1.6% CMB-Independent Constraint on H_0. *Journal of Cosmology and Astroparticle Physics*, 2020:1–42.

Planck, M. (1899). Über irreversible Strahlungsvorgänge. *Verlag der Königlich Preußischen Akademie der Wissenschaften*, pages 440–480.

Planck, M. (1900). On the theory of the energy distribution law of the normal spectrum. *Verhandl. Dtsch. Phys. G.*, 2:237.

Planck, M. (1911). Eine neue Strahlungshypothese. *Verh. d. DPG*, 13:138–148.

Planck-Collaboration (2020). Planck 2018 results. VI. Cosmological parameters. *Astronomy and Astrophysics*, pages 1–73.

Popper, K. (1974). *Objektive Erkenntnis*. Hoffmann und Campe, Hamburg, 2. edition.

Rademacker, O., Brüning, P., and Carmesin, H.-O. (2019). Formation of Gosset Lattices of Dark Matter. *Verhandl. DPG (VI)*, 54(3):30.

Ratzinger, W. and Schwaller, P. (2021). Whispers from the dark side: Confronting light new physics with NANOGrav data. *SciPost Phys.*, 10:1–11.

Riess, A. G., Casertano, S., Yuan, W., Macri, L., and Scolnic, D. (2019). Large Magellanic Cloud Cepheid Standards Provide a 1 % Foundation for the Determination of the Hubble Constant and Stronger Evidence for Physics beyond Lambda-CDM. *The Astrophysical Journal ApJ*, 876:1–13.

Riess, A. G. et al. (2021). Cosmic Distances Calibrated at 1 % Precision with Gaia EDR3 Parallaxes and Hubble Space Telescope Photometry of 75 Milky Way Cepheids Confirm Tension with ΛCDM. *The Astrophysical Journal Letters*, 908:L6:1 – 11.

Ruben, D.-H. (1990). *Explaining Explanation*. Routledge, London.

Sanders, Robert, H. (2010). *The Dark Matter Problem*. Cambridge University Press, Cambridge.

Sawitzki, P. and Carmesin, H.-O. (2021). Dimensional transitions in a Bose gas. *PhyDid B, FU Berlin*, pages 53–59.

Schöneberg, P. and Carmesin, H.-O. (2020). Solution of a Density Problem in the Early Universe. *PhyDid B, FU Berlin*, pages 43–46.

Schöneberg, P. and Carmesin, H.-O. (2021). Solution of the horizon problem. *PhyDid B, FU Berlin*, pages 61–64.

Schwartz, M. D. (2014). *Quantum Field Theory and the Standard Model*. Cambridge University Press, Cambridge.

Schwinger, J. (1948). On Quantum-Electrodynamics and the Magnetic Moment of the Electron. *Phys. Rev.*, 73:416–418.

Shaposhnikov, M. and Shkerin, A. (2018). Gravity, scale invariance and the hierarchy problem. *J. HEP*, 10:1–42.

Sommerfeld, A. (1978). *Mechanik der deformierbaren Medien*. Verlag Harri Deutsch, Frankfurt, 6. edition.

Sprenger, L. and Carmesin, H.-O. (2018). A Computer Simulation of Cosmic Inflation. *PhyDid B*, pages 61–64.

Stephani, H. (1980). *Allgemeine Relativitätstheorie*. VEB Deutscher Verlag der Wissenschaften, Berlin, 2. edition.

Straumann, N. (2013). *General Relativity* . Springer, Dordrecht - Heidelberg - New York - London, 2. edition.

Suzuki, N. et al. (2011). The Hubble Space Telescope Cluster Supernova Survey: V. Improving the Dark Energy Constraints above z $>$ 1 and Building an Early-Type-Hosted Supernova Sample. *ApJ*, 746:85.

Tanabashi, M., Particle-Data-Group, et al. (2018). Review of particle physics. *Phys. Rev. D*, 98:1–1898.

Taylor, Henry, F. and Yariv, A. (1974). Guided wave optics. *Proceedings of the IEEE*, 62(8):1044–1060.

Tröster, T. et al. (2020). Cosmology from large-scale structure. *Astronomy and Astrophysics*, 633:1–9.

Tryon, Edward, P. (1973). Is the universe a vacuum fluctuation? *Nature*, 246:396–397.

Tsoucalas, G., Laios, K., Karamanou, M., and Androutsos, G. (2013). The atomic theory of Leucippus and its impact on medicine before Hippocrates. *Hellenic Journal of Nuclear Medicine*, 16:68–69.

Tully, B. R., Courtoise, H., Hoffmann, Y., and Pomerede, D. (2014). The Laniakea supercluster of galaxies. *Nature*, 513(7516):71–74.

van der Waals, J. D. (1873). *Over de Continuiteit van den gas- en vloeistoftoestand*. Sijthoff, Leiden.

Weinberg, S. (1967). A model of leptons. *Phys. Rev. Lett.*, 19:1264–1266.

Wirtz, C. (1922). Radialbewegung der Gasnebel. *Astronomische Nachrichten*, 215:281–286.

Wußing, H. and Brentjes, S. (1987). *Geschichte der Naturwissenschaften*. Aulis-Deubner, Köln, 2. edition.

Wygas, m. M. (2013). *Methoden zur Berechnung des anomalen magnetischen Moments in der QED: Perspektive des anomalen magnetischen Moments des Elektrons - Bachelor Thesis*. PhD thesis, University Bielefeld, Bielefeld Germany.

Ylikoski, P. and Kourikoski, J. (2010). Dissecting explanatory power. *Philosophical Studies*, 148:201–219.

Zwicky, F. (1933). Die Rotverschiebung von extragalaktischen Nebeln. *Helvetica Physica Acta*, 6:110–127.